WASHINGTON STATE UNIVERSITY

World Class. Face to Face.

Technology Research and Extension for Improved Management of Manures and Agricultural Residues


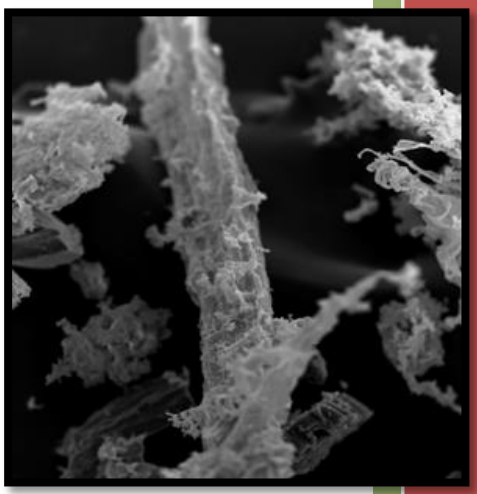


2013–15

Biennium

Technology Research and Extension for Improved Management of Manure and Agricultural Residues

A Project Report
for the

Washington State University
Agricultural Research Center

and the

Washington State Department of Agriculture

This Project was Supported by
Biomass Research Funds

Applied Bioenergy Research, also known as Appendix A research

In the 2007–09 biennium the Washington State Legislature funded a joint Washington State University (WSU) and Washington State Department of Agriculture (WSDA) program targeting applied bioenergy research. The funds were requested by WSU and WSDA to undertake near-term, applied research needed to successfully implement the Energy Freedom program and bioenergy initiatives enacted in 2006. Examples of projects to be funded were listed in ***Appendix A,*** which was attached to the funding request.

Since 2007, WSU's Agricultural Research Center and WSDA have collaborated on this research effort. The ***Appendix A*** funds have been directed to research projects coordinated by the WSU Department of Crops and Soils, as the Biofuels Cropping Systems project, and to research projects coordinated by the WSU Department of Biological Systems Engineering, in the area of energy conversion from agricultural wastes.

In the 2013-15 biennium, researchers from Washington State University Department of Biological Systems Engineering continued research on anaerobic digestion and other types of energy conversion from agricultural wastes with support from ***Appendix A*** funds. This report describes their projects and findings. In many cases, researchers have been able to successfully leverage these funds in support of additional funding provided by the Washington State Department of Ecology, as well as extramural funding competitively awarded by the National Science Foundation and the U.S. Department of Agriculture's National Institute of Food and Agriculture. These complementary funding sources have allowed for greater accomplishments and impact than would be possible through ***Appendix A*** funding alone.

For more information about the Applied Bioenergy Research project, contact:

James W. Moyer
Associate Dean for Research,
College of Agricultural, Human, and Natural Resource Sciences
Director of the Agricultural Research Center
PO Box 646240
Pullman, WA 99164-6240

Mary Beth Lang
Bioenergy and Special Projects Coordinator
Washington State Department of Agriculture
PO Box 42560
Olympia, WA 98504-2560

Technology Research and Extension for Improved Management of Manure and Agricultural Residues

By

Shulin Chen, Craig Frear, Manuel Garcia-Perez, Chad Kruger, Ali Abghari, Ping Ai, Nehal I. Abu-Lail, Greg Astill, Ian Dallmeyer, Markus Flury, Ann-Marie Fortuna, Allan Gao, Jesus Garcia-Nunez, Rishi Ghoghare, James B. Harsh, Hamid Iqbal, Jim Jensen, Nick Kennedy, Jingwei Ma, Shannon Mitchell, Matt Smith, Waled Suliman, Dianlong Wang, Georgine Yorgey, Liang Yu, Quanbao Zhao, Shuai Zhang, and Tao Zhu

Compiled and edited by
Sonia A. Hall

Department of Biological Systems Engineering
and the
Center for Sustaining Agriculture and Natural Resources
Washington State University

Table of Contents

List of Figures and Tables

Figures

Tables

List of Abbreviations

AD	Anaerobic Digestion
ARC	Agricultural Research Council
CH_4	Methane
CNG	Compressed Natural Gas
CO_2	Carbon Dioxide
CSANR	Center for Sustaining Agriculture and Natural Resources
EPA	Environmental Protection Agency
FAME	Fatty Acid Methyl Esters
GHG	Greenhouse Gas
H_2S	Hydrogen Sulfide
LCFA	Long Chain Fatty Acid
N	Nitrogen
N_2O	Nitrous Oxide
NGO	Non-Governmental Organization
NH_3	Ammonia
NR	Nutrient Recovery
NRCS	Natural Resources Conservation Service
OSAA	Ozone and Soaking in Aqueous Ammonia
P	Phosphorus
PSA	Pressure Swing Adsorption
SAA	Soaking in Aqueous Ammonia
TAN	Total Ammonia Nitrogen
TS	Total Solids
US	United States
USDA	United States Department of Agriculture
USGS	United States Geological Survey
VS	Volatile Solids
WA	Washington State
WSDA	Washington State Department of Agriculture
WSU	Washington State University

Acknowledgements

The authors of this report would like to thank the following people for their contribution to these studies:

- Alex Dunsmoor for laboratory work.
- Steve Dvorak and Kevin Lowry and colleagues at DVO Incorporated for design, engineering, and monitoring and data collection.
- Dr. Tom Bierma and Dr. Guang Jin at Illinois State University for their teamwork, concepts, and data.
- Steve Dvorak (again) and Tommy Kesler at DVO Incorporated, who also participated as full partners in the teamwork, concepts and design with ISU and WSU.
- Sonia A. Hall for her time, effort, and skill in compiling and editing this report.

Executive Summary

Directed by the State Legislature, the Agricultural Research Center at Washington State University has been collaborating with the Washington Department of Agriculture in conducting applied research that has near-term potential to commercialize biofuel and bioenergy production from renewable agricultural biomass grown in Washington. This collaboration has concentrated on two major initiatives: new biomass feedstock production—primarily oilseeds—and utilization of existing biomass feedstock—predominantly livestock and poultry manures, as well as other agricultural residues. Since its establishment in 2007, this latter initiative has resulted in new information and technologies that promote adoption of anaerobic digestion for dairy applications, in support of two major program goals:

- To conduct applied research focused on developing enabling technologies to convert existing agricultural residues, animal manure, and other feedstock to renewable energy, and
- To create economic development and job opportunities in rural areas and add new revenues to Washington farms.

Applied anaerobic digestion research has primarily—though not exclusively—focused on technologies that complement core anaerobic digestion technologies (Figure ES-1). In this context, anaerobic digesters are best seen as the core technology of a *biorefinery*, a facility that integrates biomass conversion processes—in this case, anaerobic digestion—with other components to produce a multitude of different value-added products including fuels, power, and chemicals from biomass. The strategy has thus focused on three core objectives:

- Improving economics through optimizing system design.
- Improving economics by producing higher-value co-products.
- Enhancing the environmental benefits provided by anaerobic digesters, particularly in the area of nutrient removal.

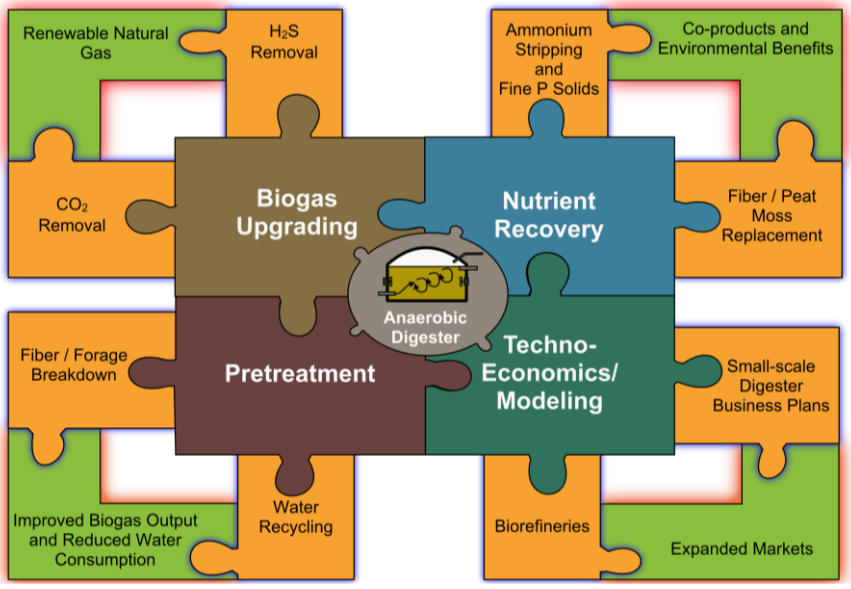

Figure ES-1. Applied anaerobic digestion research at Washington State University.

Washington State University researchers have focused on such opportunities as improving biogas upgrading to produce higher value renewable natural gas, stripping nutrients from anaerobic digester effluent, pretreatment efforts that improve the output of anaerobic digestion, and modeling efforts that support decision-making about various technology options. Each of these efforts aims to improve the environmental footprint and the economics of facilities processing dairy manure and other organic residues, thereby providing improved business opportunities to dairy farmers and other project developers, improving adoption rates of anaerobic digestion in the Pacific Northwest, and positioning the region as a national leader in the anaerobic digestion industry.

This report summarizes the major results and conclusions of eight specific research, development, and extension projects conducted during the 2013–15 biennial budget cycle, building on last biennium's results. These projects included sharing past research results to promote the commercialization of anaerobic digestion technologies (Chapter 1), developing and refining nutrient recovery technologies and their applications (Chapter 2), evaluating potential solutions to obstacles impeding the scale-up of existing technologies (Chapter 3), developing and refining technologies to produce value-added products from organic residues (Chapters 4, 5, 6, and 7), and evaluating the economics of alternative technologies (Chapter 8).

Industry support and extension

Improvements in the processing of dairy manure in Washington will only be made if advanced technologies are adopted and applied. Multiple extension and outreach activities were carried out during this biennium to encourage and facilitate such adoption. These activities included:

- A major field day event held at two dairy farms in Northwest Washington, showcasing applied research and demonstrations of anaerobic digestion.
- Presentations at multiple national and regional conferences where the extension team shared the results of anaerobic digestion, pyrolysis, and nutrient recovery-related research to extension, engineering, industry, regulatory, and educational professionals.
- Technical support to nine stakeholder groups ranging from federal agencies—for example, through the Nutrient Technology Challenge and the Biogas Opportunities Roadmap—to state agencies—such as the Washington State Departments of Agriculture, Ecology, and Commerce—to non-profit entities—including Sustainable Conservation, in California.
- Training of young professionals who are beginning their professional careers across three continents.
- An anaerobic digestion curriculum for training anaerobic digestion technicians.
- Publication of six formal extension publications.

An estimated 12,000 scientists, producers, industry specialists, regulators, policy-makers, and other interested parties across the country were reached. These activities led to increased awareness of biorefinery technologies, tools, resources, and successful experiences. Such awareness and resources are critical to the advancement and adoption of technologies and processes in Washington State that create energy from livestock manure and other organic residues.

Nutrient recovery technologies for dairy application

An existing approach to managing manure is to apply effluents from treated manure to agricultural lands. However, this can result in over-application of nutrients, which in turn can result in runoff of excess nitrogen and phosphorous into rivers and other water bodies, or leaching of these nutrients into groundwater. Dr. Garcia-Perez, his research group and collaborators explored nutrient recovery technologies for dairy manure management purposes, particularly the development of engineered biochars as soil amendments to meet multiple objectives: capturing excess nutrients and pathogenic microorganisms, increasing carbon sequestration, and improving the water holding capacity of sandy soils. They found that, though the engineered biochar had a noticeable capacity for adsorbing phosphorous from the liquid effluent from anaerobic digestion, adding biochar to compost did not reduce the leaching of nitrogen and phosphorous under experimental conditions. However, they did find that the amount of carbon dioxide released from biochar-amended sandy soils was always less than that of the soil alone. Similarly, the addition of biochar was generally found to be beneficial to the hydro-physical properties of sandy soil, improving its water holding capacity, which might contribute to increased crop yields.

A key lesson from the team's research was the importance of the biochar production conditions and secondary treatments on the biochar's ability to meet the stated objectives when used as a soil amendment. Both pyrolysis temperature and initial feedstock contributed to the physical, chemical, and surface area properties of the resulting biochar, which in turn determined its behavior when mixed with sandy soils. It is a challenge to produce a biochar with both high surface area—which led to higher water holding capacity—and high density of oxygenated functional groups on the surface—important for nutrient adsorption. These studies have therefore:

a) Confirmed the potential for using engineered biochars to address certain dairy manure management challenges, such as the transport of pathogenic bacteria in the soil and the emission of carbon dioxide, and
b) Emphasized the need for further applied research to determine how to optimize biochar's potential to capture nutrients and improve water holding capacity when used as a soil amendment.

Gypsum as a replacement for hazardous sulfuric acid

An important limitation of existing nutrient recovery technologies is the cost and hazard associated with the sulfuric acid used to recover ammonium sulfate in a process used for recovering nitrogen from anaerobically digested dairy manure. Dr. Frear and colleagues explored approaches to using gypsum as a replacement for sulfuric acid. Results from their experiments suggest that reacting gypsum slurry with ammonia and carbon dioxide gases can achieve desired levels of saturated ammonium sulfate. In addition, results from collaborators at Illinois State University and additional experimentation with zero inputs of carbon dioxide suggested that a preferred process is one that utilizes higher concentrations of carbon dioxide, as this was essential in helping increase the gypsum's solubility by liberating calcium ions from the gypsum. While concerns arose about increased clogging risk as a result of ammonium bicarbonate

production within these experiments, which were conducted at 20°C, the ammonia stripping process can also produce ammonia and carbon dioxide at temperatures as high as 50°C. At this temperature, the ammonium bicarbonate will disassociate, reducing concerns about clogging.

Although the reaction with gypsum was shown to be technically viable, industry partners who helped evaluate a scaled-up version of this process are concerned with the high capital and operating costs the process would incur, as well as with the lengthy reaction time when compared to the use of sulfuric acid. Commercialization is therefore on hold pending an economic analysis, and comparison with other means of producing ammonium sulfate.

Expansion and scale-up of hydrogen sulfide scrubbing technologies

Biogas produced during anaerobic digestion can only be marketed for high value uses such as compressed natural gas if it has a high level of purity. Dr. Frear's research group and industry partners carried out key studies to inform the scale-up of a previously developed selective hydrogen sulfide scrubbing concept, and to expand the concept to sequential scrubbing of carbon dioxide, thereby addressing the two main contaminants of raw biogas. An innovative commercial-scale, two-stage bubble column reactor was tested, and results showed that the reactor was able to remove greater than 95% of the hydrogen sulfide contained within raw biogas from a dairy anaerobic digester by adjusting column height, bubble size, and pressure. In addition to removing hydrogen sulfide, some carbon dioxide was also removed, leading to a system that (a) strips and recovers ammonia gas from the manure, (b) scrubs the raw digester gas of nearly all hydrogen sulfide, and (c) removes some carbon dioxide and thereby increases the methane concentration. In addition, lab-scale tests of a four-stage sequential biogas purification and regeneration process suggest that such a process is feasible. Results also showed that post-purification aeration could return effluent to an alkaline condition (regeneration step), thus allowing for continual biogas purification to remove additional carbon dioxide that could not be removed during the initial biogas purification step. Future tests at commercial scales are needed for this expansion to carbon dioxide scrubbing.

The economic potential of the system is considerable. The relative simplicity of this system makes it an ideal biogas purification process for digesters located on dairy operations. However, the length of reaction, the reliance on suitable ammonia stripping effluent, and the relatively high potential for methane loss are aspects that may need to be addressed in future efforts in order for successful commercialization to be achieved.

Pretreatment technologies to enhance methane production

One important challenge faced by anaerobic digestion facilities looking to use agricultural byproducts such as crop residues or manure fiber to produce high-value biogas is the low digestibility of these residues. Many large-scale biogas plants that use such materials as feedstock have low efficiency and need to retain the residues in the digester for long periods

because of this difficulty in degradation. Dr. Chen's research group therefore examined technologies to pretreat manure fiber and crop residues, so as to enhance the production of methane when the pretreated materials enter the anaerobic digester. After comprehensively investigating two pretreatments, they found that the combination of both pretreatments—ozone *and* soaking in aqueous ammonia—led to significantly greater biogas production when compared to only using ozone or only soaking in aqueous ammonia. They also found that the recommended pretreatment times for manure fiber differed noticeably from those for crop straw.

It is possible to design an ozone and soaking in aqueous ammonia pretreatment process for agricultural residues—crop straw or manure fiber—that leads to improved efficiency and increased methane production during anaerobic digestion. Great emphasis should be placed on optimizing the combined pretreatment parameters according to the characteristics of the material used as feedstock, as different feedstocks respond differently to these pretreatments, and parameters that optimize biogas production with one feedstock may not do the same with another.

Microbial biofertilizers

In a future where harvest and use of agricultural residues by biorefineries becomes prevalent, the constant removal of biomass from the field year after year could result in the loss of organic carbon from the soil, as well as the loss of nitrogen and phosphorous necessary for crop growth. Microbial biofertilizers incorporate an array of nitrogen-fixing and phosphate-solubilizing organisms, and their production—basically, microbial growth—requires a source of energy. Adding such biofertilizers to fields could present a partial solution to the problem of residue removal. Dr. Chen's research group evaluated the use of crop straw to produce sugars as a source of energy for a biofertilizer species of bacteria. They found that, when pretreated with ozone and soaking in aqueous ammonia, the crop straw could release 87% of available sugars when treated with hydrolyzing enzymes, and that these sugars could effectively be used as a source of energy for *Azotobacter vinelandii*, a biofertilizer bacteria species.

If the *A. vinelandii* cell mass and associated nitrogen content are effective at improving soil health parameters when applied as a biofertilizer to the soil, the team's preliminary economic analysis suggests that farmers could derive significant fertilizer cost-savings while improving soil quality, thereby having an alternative to removing the wheat straw from the field for biogas production.

Lipid production using wheat straw

Conventional biodiesel derived from plant oils or animal fats cannot be produced in large enough volumes to meet growing fuel demand, and—particularly in the case of plant oils—also raises concerns about competition with food supplies. Microbial lipids could provide an alternative next-generation renewable energy source. Dr. Chen's team explored the use of wheat straw—an agricultural residue widely available in Washington State—for the production of microbial lipids. They tested three different wheat straw treatments and evaluated the growth and lipid production of three different oleaginous yeasts grown using the pretreated wheat straw as a food

source. As in the previous biofertilizer study, they found that treating wheat straw with ozone and soaking in aqueous ammonia before enzymatic hydrolysis led to the release of the most sugars. However, once these sugar solutions were optimized for fermentation by the different yeast species, straw treated by soaking in aqueous ammonia alone supported 3- to 5-fold greater lipid production than straw also treated with ozone. Among the yeast species the team evaluated, *Cryptococcus curvatus* was the most effective at producing lipids when grown on sugars obtained from wheat straw, with those lipids accounting for up to 42% of the yeast's dry cell weight. There are additional advantages to using *Cryptococcus curvatus,* including their long-chain polyunsaturated fatty acid content.

Further research in needed to evaluate how to scale-up lipid production using wheat straw, and to quantify its economic feasibility. However, these results suggest there is potential for industrial-scale microbial lipid production based on agricultural residues, offering an additional alternative for the production of high value-added products from organic residues.

Techno-economic feasibility of anaerobic digestion alternatives

While anaerobic digestion technology has multiple benefits, it has not been widely adopted in the United States. Reasons for this limited adoption could include economics, lack of information regarding the financial feasibility of digestion, or both. Dr. Chen's team explored the possibility that the key to techno-economic feasibility lies in marketing additional, high value-added products obtained through multiple integrated processes. The team developed a comprehensive techno-economic model that integrates the pretreatment of feedstocks, anaerobic digestion to produce biogas, followed by purification and nutrient recovery to obtain higher value-added products from these processes. Their model computed rigorous mass and energy balances for each operation unit in a conceptual, integrated system. The model was then used to develop and evaluate a novel ammonia recycling technology that improves upon currently commercialized AIRTRAP technology, using the recovered ammonia to purify the biogas produced, and pretreat the crop residues and manure fibers that go into the anaerobic digestion process. Results showed that the proposed novel technology is technically feasible and can provide multiple benefits, such as efficient and effective biogas purification, on-site ammonia that can be used to pretreat feedstock and increase biogas productivity, ammonium sulfate fertilizer, and clean drinking water for livestock. These benefits would also lead to lower ammonia concentration in the resulting effluent, improving manure management.

The team also used the model to evaluate the integrated processes by comparing modeled situations using different feedstocks as inputs. Their results showed that, at a plant capacity of 7,500 dry ton $year^{-1}$, the use of food scraps as feedstock had the potential to deliver profits, due to (a) their higher biogas yield compared to other feedstocks, and (b) the receipt of tipping fees that come with receiving those food scaps. Crop residues showed greater potential for biogas production than did animal manure when co-digested with food scraps. The profitability of the anaerobic digestion of crop residues, however, was dependent on low cost and highly efficient pretreatments being integrated into the process. Results also showed that profitability increased

when the plant's capacity was scaled up, suggesting that the operation of large-scale anaerobic digestion systems would have the advantage of being more economically profitable.

As next steps, experiments should be conducted to refine these lessons and to promote scale-up in a way that optimizes profits, and (separately) for the commercialization of the additional high value-added products. This study's results, however, suggest that commercial scale integration of pretreated feedstocks, anaerobic digestion to produce biogas, and purification and nutrient recovery to obtain higher value-added products from these processes can be both technically feasible and profitable.

Conclusion

Together, these eight projects contribute to Washington State's potential to commercialize energy and co-product production from renewable agricultural biomass. In addition, this research informs new industries, which have the potential to create economic development and job opportunities in rural areas, and add new revenues for Washington farmers.

1. Commercialization, Industry Support, and Extension

Chad Kruger, Craig Frear, Georgine Yorgey, Nick Kennedy, Shannon Mitchell, Jim Jensen, Jingwei Ma, Quanbao Zhao, and Greg Astill

1.1 Outreach and extension activities

The applied nature of the research funded by Appendix A, particularly those projects that directly target new and improved technologies, will only lead to improvements in livestock and poultry manure management if these technologies are adopted and applied by commercial producers, processors and industry. Outreach and extension are therefore critical to achieving the program's objectives.

Mr. Chad Kruger (Director, Center for Sustaining Agriculture and Natural Resources [CSANR]), Dr. Craig Frear (Assistant Professor, Department of Biological Systems Engineering), and Ms. Georgine Yorgey (Associate in Research, CSANR), with support from several other individuals, were responsible for the delivery of outreach and extension for the biennium. This delivery was in the form of conference presentations, technical support to multiple stakeholders, the training of future professionals in the field, development of formal extension publications, and development of other durable extension products.

1.1.1 Anaerobic Digestion Field Day

Using combined funding from Appendix A and a Natural Resources Conservation Service's (NRCS) Conservation Innovation Grant, the extension team organized a major field-day event during this biennium, held in Lynden, Washington, on July 10, 2013. The field day, held at Vander Haak Dairy and Edaleen Dairy, with an optional tour of Maberry Farms in the afternoon, featured a summary of the applied research and technology demonstrations that have been developed over the last decade in pursuit of an anaerobic digestion (AD) system vision for on-farm manure and organics management. The day included 14 presentations by Washington State University (WSU) research and extension personnel (Craig Frear, Chad Kruger, Tim Ewing, Chris Benedict), and industry partners (e.g. Kyle Juergens, Andgar Corp; Eric Powell; Dan Evans, Promus Energy; Steve Vander Haak, Vander Haak Dairy; Rob Costello, Bellingham Technical College; Matt Maberry, Maberry Farms). The field day had approximately 108 attendees, with a target audience including farmers, government agency and regulatory representatives, community and political leaders, AD entrepreneurs, project developers and technology providers, community members, undergraduate and graduate students, and Carbon Masters.

1.1.2 Conference Presentations

Using funding from Appendix A, along with additional, complementary funds from the Washington Department of Ecology's Waste To Fuels Technology Partnership, the U.S.

Department of Agriculture (USDA) National Institute of Food and Agriculture (Award No. 2012-6800219814), the Washington Department of Commerce, and others where appropriate, the extension team made numerous presentations during the biennium related to anaerobic digestion, pyrolysis, and nutrient recovery, both regionally and nationally. Categorized by primary audience, these presentations were:

Extension and other agricultural support professionals

In 2015, the team made a total of 13 presentations at the "Waste to Worth" conference, a national manure management conference attended by extension professionals across the country. "Waste to Worth" was hosted in Seattle, WA from March 30 to April 2, 2015. Presentations included:

- University and anaerobic digestion industry partnerships: Lab testing (Mitchell)
- The dairy manure bio-refinery (Yorgey)
- Renewable natural gas: Biogas cleaning and upgrading 101 (Frear)
- Renewable natural gas: Economics (Kruger)
- Antibiotic degradation during anaerobic digestion and effects of antibiotics on biogas (Mitchell)
- Co-digestion: A primer on substrates and project considerations (Frear)
- Digested solids: forms, markets, and trends (Jensen)
- Panel discussion: Expanding markets for manure treatment technologies (Frear, invited panelist)
- A primer on available and emerging N, P and salt recovery: Performance and cost (Ma)
- Anaerobic digestion projects: Environmental credits 101 (Astill)
- Farm-based anaerobic digestion: Wastewater and nutrient considerations (Yorgey)
- Poultry digestion: Emerging farm-based opportunity (C. Frear, Q. Zhao, and S. Dvorak)
- Tours of two farm-based anaerobic digesters and nutrient recovery systems in Whatcom County (Frear, lead tour presenter, follow-up newspaper article).

Engineering professionals

The team presented results at the ASABE Annual International Meeting in Kansas City, MO in 2013, and in New Orleans, LA, in 2015, as well as at the Algae Biomass Summit and the Institute of Biological Engineering (2014):

- Ma, J., Yu, L., Zhao, Q., Chen, S., and Frear, C. (2015) Kinetic and microbial community analysis for enhanced food waste hydrolysis: an investigation on pH.
- Zeb, I., Ma, J., Zhao, Q., Yu, L., Frear, C. (2015) Recycling AD effluent as dilution water for AD process: effects of TAN and salinity.
- Frear, C., Zhao, Q., Ma, J., Zhao, Q. (2013) Anaerobic Digestion of Whole and Lipid-Extracted Algal Biomass from Four Industrial Strains--Determination of Important Methane and Nutrient Information, ASABE National Conference (2013), Kansas City, MO, July 22-25, 2013
- Ma, J., Zhao, Q., Frear, C., Laurens, L., Jarvis, E., and Nagle, N. (2014) Anaerobic digestion of whole and lipid-extracted algal biomass. Algae Biomass Summit, San Diego, CA.
- Ma, J., Zhao, Q., Frear, C., Laurens, L., Jarvis, E., and Nagle, N. (2014) The effect of calcium on the kinetics of methane production and LCFA degradation from algal biomass. Algae Biomass Summit, San Diego, CA.

- Ullman, J.L., Baar, E.L., Mitchell, S.M., Frear, C. (2014) Manure and bio-solid management practices to remove antibiotics and limit the promotion of antibiotic-resistance, Institute of Biological Engineering Annual Conference, Lexington, KY, March 6-8. IBE 2014 Conference Proceedings, p 35-36.
- Ma, J., Yu, L., Zhao, Q., Frear, C., and Chen, S. (2013) Enhance volatile fatty acid (VFA) and bio-methane productivity by pretreatment of lawn grass, ASABE National Conference (2013), Kansas City, MO, July 22-25, 2013
- Mitchell, SM, Ullman, J., Teel, AL., Watts, RJ, and Frear, C. (2013) Ampicillin, florfenicol, sulfamethazine and tylosin effect on biogas production and their degradation efficiency during anaerobic digestion, ASABE National Conference (2013), Kansas City, MO, July 22-25, 2013

Government and non-profit audiences

The team gave multiple presentations on anaerobic digestion-related topics at different events and conferences organized by federal agencies, including the Environmental Protection Agency (EPA), the USDA, the U.S. Geological Survey (USGS) and NRCS:

- Frear, C., Ma, J., Zhao, Q. (2014) Nutrient recovery technologies on CAFOs and implications to reactive nitrogen management, presentation to the EPA/USDA/USGS Working Group on Management Strategies for Reactive Nitrogen and Co-Pollutants, Washington DC, June 24-26, 2014.
- Frear, C. (2014) Review of emerging nutrient recovery technologies, EPA Region 9 Webinar, February 5, 2014
- Frear, C. (2013) Review of emerging nutrient recovery technologies, EPA Region 10 AFO/CAFO Workshop, Portland OR, December 3, 2013
- Frear, C. (2013) Review of emerging nutrient recovery technologies, USDA NRCS/EPA Region 10 Nutrient Recovery Conference, Portland OR, November 19, 2013
- Frear, C. (2013) Review of emerging nutrient recovery technologies, EPA Region 10 Nutrient Recovery Conference, Seattle WA, July 30, 2013

Industry audiences—agricultural, including future industry, educational

Similarly, the team shared their results through presentations at industry-organized events and conferences specifically targeting cooperation between scientists and industry professionals:

- Frear, C., Ma, J., Zhao, Q. (2014) Emerging nutrient recovery technologies on large animal farms, presentation to the Sustainable Dairy Workshop, Twin Falls, ID, September 16-17, 2014.
- Zhao, Q., Kennedy, N., Chen, S., Frear, C. (2013) Commercialization of anaerobic digestion, ammonia, phosphorus and hydrogen sulfide scrubbing system, Washington Clean Technology Alliance Ag Tech Conference, Seattle WA, July 31, 2013.
- Kruger, C.E. (2015) Outputs of Organics Recycling as Inputs for Resilient Communities. Delivered at the BioCycle West Coast Conference, April 13-16, 2015 in Portland, Oregon.
- Kruger, C.E. (2014) Waste to Fuels Technology Research Update. Washington Organics Recycling Council's Annual Conference. November 18-19, 2014. Blaine, WA.
- Kruger, C.E. (2013) Saving the Planet with Soil Amendments? Northwest Biosolids Management Association. September 10, 2013. Chelan, WA.

- Kennedy, N. and Frear, C. (2013) Next generation food scraps/green waste organics recycle, Biocycle National Conference (2013), San Diego, CA, April 8-11, 2013.
- Kruger, C.E., and Yorgey, G.G. (2014). Are cows really worse for the climate than cars? WSU Vet Med Seminar.
- Frear, C.S., Kruger, C.E., Collins, H.P., Garcia-Perez, M., Stockle, C.O., Shumway, C.R., Astill, G., Ewing, T.W., Kennedy, N.P., Khalil, T., and Yorgey, G.G. (2013). Anaerobic digestion systems: Integrating emerging technologies to improve environmental and social impact. BioEarth Annual Meeting, Pullman, WA.

1.1.3 Technical support

Dr. Frear supplied considerable technical support to industry, government, non-governmental organizations (NGO), producers and third-party project developers. These included:

- Core panelist for the Environmental Protection Agency's (EPA) Nutrient Technology Challenge. Dr. Frear is part of a team of experts providing guidance to the EPA as they develop a challenge program looking to catalyze development of manure nutrient recovery technologies (anticipated launch in late 2015). The expert team's efforts are focused on detailing the scope, goals, rules, evaluation and awards.
- Technical review and awards panelist for the California Department of Food and Agriculture (CDFA) anaerobic digestion digester and research development program request for proposals.
- Participant in multiple meetings with the California NGO Sustainable Conservation on coordinating policy, research and extension activities related to organic management at the urban/agricultural interface, including AD, compost, vermicompost, nutrient recovery, and other technologies.
- Technical expert for project and policy development related to compost, AD, bioplastics, and compressed natural gas (CNG). Consulting entities included EPA, EPA Regions 9 and 10, US Department of Agriculture Natural Resource Conservation Service (USDA NRCS), USDA Rural Development, US Department of Energy (DOE), Dairy Management Incorporated, Walmart, Vermont Bio-methane Project Team, and various third party developers.
- Regular teleconference attendee to working groups from Washington State, EPA National Office, EPA Agstar, and American Biogas Council.
- Technical contributor to the USDA/EPA/DOE's Biogas Opportunities Roadmap (August 2014), for development of national programs and policies for enhanced adoption of AD systems in the US.
- Technical expert and academic reviewer for multiple federal grant programs (USDA REAP, USDA SBIR, NSF, DOE), peer-reviewed scientific journals and industry projects.

Dr. Frear and his team also conducted two important and contracted literature reviews related to AD systems and biorefining:

- Ma, J., Frear, C. (2015). Dairy manure management and anaerobic digestion: review of gaseous emissions, Report to SRA and EPA, March 11, 2015.
- Ma, J., Kennedy, N., Yorgey, G., Frear, C. (2013). Review of emerging nutrient recovery technologies for farm-based anaerobic digesters and other renewable energy systems, Report to the Innovation Center for US Dairy, November 6, 2013. Available at http://csanr.wsu.edu/wp-content/uploads/2014/07/ICUSD-Emerging-NR-Technology-Report-Final.121113B.pdf.

1.1.4 Training of future professionals

This biennium saw the successful training of four young professionals who transitioned to the academic and industry world, focused on resource management, sustainability and the biorefinery concept. Additional students are progressing in their academic studies.

- Nick Kennedy, M.Sc., WSU Associate in Research,
- Shannon Mitchell, Ph.D., postdoctoral researcher, and now future Assistant Professor at the University of South Alabama,
- Raul Pelaez-Samaniego, Ph.D., postdoctoral researcher, and now future Assistant Professor at the University of Cuenco, Ecuador,
- Jingwei Ma, Ph.D., postdoctoral researcher and now future Assistant Professor at Hunan University, China.

In addition, Dr. Frear coordinated with Bellingham Technical College to disseminate the already developed joint AD Technician curriculum to Quasar, supplier of farm-based and municipal digester systems. Quasar will use the curriculum to train their staff as well as regional municipal AD Technicians.

1.1.5 Extension products

With support from Appendix A, along with complementary support from the Washington Department of Ecology Waste to Fuels Technology Partnership, USDA National Institute of Food and Agriculture (award #2012-6800219814), and others, the extension team completed work on several durable products in the 2013-2015 biennium.

1.1.5.1 Formal extension publications

The extension team spent a considerable amount of time during this biennium working on a number of linked fact sheets covering biorefinery topics. These fact sheets were possible given additional leveraged funding from United States Department of Agriculture National Institute of Food and Agriculture (USDA NIFA) funding through a companion project to develop an "AD Systems Manual." These factsheets have been formally peer reviewed by subject matter experts through the WSU Extension Publications system:

- Yorgey, G.G., C.S. Frear, C.E. Kruger, and T.J. Zimmerman. (2014). **The rationale for recovery of phosphorus and nitrogen from dairy manure.** Washington State University Extension Fact Sheet FS136E. Washington State University, Pullman, WA.
- Galinato, S., Kruger, C.E., and Frear, C.S. (2015). **Anaerobic Digester Project and System Modifications**. WSU Extension Manual. EM090E.
- Mitchell, S.M., Kennedy, N., Ma, J., Yorgey, G.G., Kruger, C.E., Ullman, J.L., and Frear, C.S. (in press). **Anaerobic digestion effluents and processes: the basics**. WSU Extension Fact Sheet FS171E.
- Kennedy, N., G. Yorgey, C. Frear, D. Evans, J. Jensen, and C. Kruger. (in press). **Biogas upgrading on dairy digesters**. Washington State University Extension Publication, Pullman, WA.
- Kennedy, N.P., Yorgey, G.G., Frear, C.S., and Kruger, C.E. (in press). **On-farm co-digestion of dairy manure with high-energy organics**. WSU Extension Manual. Pullman, WA: Washington State University.

- Kennedy, N.P., Yorgey, G.G., Frear, C.S., and Kruger, C.E. (in press). **Project considerations for on-farm co-digestion of dairy manure**. WSU Extension Manual. Pullman, WA: WSU Extension.
- Galinato, S., Kruger, C.E., and Frear, C.S. (in review). **Economic feasibility of post-digester nutrient recovery using struvite crystallization and the WSU AIRTRAP system.** WSU Extension Fact Sheet.

1.1.5.2 Other durable extension products

In addition to formal Extension Publications, the team produced a number of articles and non-reviewed extension materials, including:

- A video, "**Anaerobic Digestion: Beyond Waste Management**," released in June 2013, in conjunction with the Anaerobic Digestion Systems Field Day.
- Several webpages with connections to a database of relevant publications on the WSU CSANR's website: **Anaerobic Digestion**, **Biochar**, **Biofuels**, **Energy**, **Farm Energy**, **Waste Management**, and **Compost** webpages.
- A **University Partnership Research Project** web profile page, developed in coordination with EPA Agstar (http://www.epa.gov/agstar/projects/profiles/WSU_AgSTAR_Site_Profile_508_030514.pdf).
- A one-day symposium on AD Systems and AD biorefinery modeling (Frear, C., and Kruger, C. (2014) **Modeling anaerobic digestion systems symposium**, Washington State University sponsored symposium as part of US Dairy Innovation Center Sustainability National Meeting, Seattle WA, November 20, 2014).
- Blog posts on the WSU CSANR's "Perspectives on Sustainability" Blog:
    - Kruger, C. 2015. **Does an anaerobic digester cost too much?** March 9, 2015. Available at http://csanr.wsu.edu/does-ad-cost-too-much/
    - Kennedy, N. 2014. **Dairy waste bio-refineries: An innovative way to further reduce greenhouse gases on dairies in Washington State**. September 3, 2014. Available at http://csanr.wsu.edu/dairy-waste-biorefineries/
    - Frear, C. 2014. **The reactive nitrogen "wicked problem" – critical nutrient, disastrous pollutant.** August 4, 2014. Available at http://csanr.wsu.edu/the-reactive-nitrogen-wicked-problem/
    - Yorgey, G.G. 2014. **Closing the nutrient loop**. July 2, 2014. Available at http://csanr.wsu.edu/closing-the-nutrient-loop/.
    - Kruger, C. 2014. **When engineering a green solution has gone too far.** May 12, 2014. Available at http://csanr.wsu.edu/too-green/
    - Frear, C. 2014. **The 'rest' of the food system.** January 22, 2014. Available at http://csanr.wsu.edu/the-rest-of-the-food-system/
- Kennedy, N., C. Frear, M. Garcia-Perez, C. Kruger, and S. Chen. 2013. **Dairy waste bio-refinery (a two page concept illustration and summary).** Available at http://csanr.wsu.edu/wp-content/uploads/2013/11/Dairy-Biorefinery-Concept-Handout-FINAL.pdf
- Kennedy, N. 2013. **Economics of Dairy Digesters in Washington State.** BioCycle 54(11), 36. Available at http://www.biocycle.net/2013/11/18/economics-of-dairy-digesters-in-washington-state/

- Proceedings published in association with the Waste to Worth Conference. Proceedings and, in the near future, presentation materials and recordings, are available at http://www.extension.org/pages/72719/agenda-for-waste-to-worth-2015 - .VVLfIflVikq:
    - University and anaerobic digestion industry partnerships: Lab testing
    - The dairy manure bio-refinery
    - Renewable natural gas: Biogas cleaning and upgrading 101
    - Renewable natural gas: Economics
    - Antibiotic degradation during anaerobic digestion and effects of antibiotics on biogas
    - Co-digestion: A primer on substrates and project considerations
    - Digested solids: forms, markets, and trends
    - Panel discussion: Expanding markets for manure treatment technologies
    - A primer on available and emerging N, P and salt recovery: Performance and cost
    - Anaerobic digestion projects: Environmental credits 101
    - Farm-based anaerobic digestion: Wastewater and nutrient considerations
    - Poultry digestion: Emerging farm-based opportunity
- A one-page summary of the organic waste biorefinery concept, and an accompanying graphic, available at http://csanr.wsu.edu/wp-content/uploads/2013/11/Biorefinery-Concept-Handout-FINAL.pdf.

1.2 Impacts of outreach and extension activities

Through these four core outreach activities—conference presentations, technical support, training of future professionals, and development of formal and other extension publications—the extension team shared the results described in other chapters of this report, as well as the results of related research on biorefinery technologies. The team estimates that close to 12,000 scientists, producers, industry specialists, regulators, policy-makers, and other interested parties across the country were reached, including:

- The 280 participants at the Waste to Worth conference, where the extension team gave 13 different presentations. An additional 80 participants attended a farm tour that was co-led by Dr. Frear. The associated farm tour video has already accumulated 43 views, even though it has not yet been released, and the conference and tours were summarized in local news articles.
- An estimated average of 20 professionals at each of the other 23 national and regional conference presentations.
- The dozens of scientists, students and colleagues that interacted and collaborated with the four professionals during their training at WSU, a number that will grow significantly as these professionals take on new positions in academia and industry.
- The curriculum disseminated through Quasar has the potential to reach dozens if not hundreds of current and future AD technicians, including those in Quasar's employment working at their AD facilities, as well as the regional municipal AD technicians they train.
- The WSU extension publications, articles, blog posts, and resources on WSU's webpages have been viewed over 13,000 times cumulatively. This includes the two formal

extension publications, which have had a cumulative 1,759 hits, and 604 downloads/views.

These statistics are considered conservative, as they do not include views or downloads of the additional research products posted on EPA's, eXtension's, or Washington State Department of Agriculture's (WSDA) webpages, nor do they include the numbers of stakeholders and professionals involved in the working groups that Dr. Frear has advised throughout this biennium.

Through these outreach activities, the team has increased the awareness of the potential and opportunities surrounding biorefinery technologies, and has shared tools, resources and successful experiences that can help diverse groups further develop and implement these technologies in their line of work. Such awareness and resources are critical to the advancement and adoption of technologies and processes in Washington State that create energy from livestock manure and other organic residues.

2. Nutrient Recovery Technologies for Dairy Application and Characterization of the Performance of Engineered Biochars as Soil Amendments

Waled Suliman, James B. Harsh, Nehal I. Abu-Lail, Ann-Marie Fortuna, Ian Dallmeyer, Hamid Iqbal, Matt Smith, Manuel Garcia-Pérez, and Markus Flury

2.1 Background

Washington State University (WSU), WSDA and Washington State continue to be interested in the development of technologies to remove nutrients—nitrogen and phosphorous—from manures, and to reduce leaching of nutrients from soils to groundwater tables. The 1.5 million tons of manure currently generated in the state of Washington contain more than 19,000 tons of phosphorus (P) and more than 75,000 tons of nitrogen (N). These nutrients tend to accumulate in lagoons prior to application of lagoon water to agricultural lands. Direct application of these waters to adjacent fields can result in rates of more than 600 kg N $ha^{-1}yr^{-1}$ and 160 kg P $ha^{-1}yr^{-1}$, much more than typically required. This over-application results in significant leaching of both nitrogen and phosphorus into the groundwater and runoff into rivers, streams, and other water bodies. The accumulation of nutrients in these systems can lead to eutrophication, posing a serious risk to the environment in the Pacific Northwest.

Biochar is a carbon-rich, porous material prepared via thermochemical decomposition of organic materials in an oxygen-limited environment (Ronsse et al., 2013; Crombie et al., 2013). Biochar is receiving growing attention as a soil amendment due to its potential to enhance soil fertility, soil moisture, and sequester carbon (Song and Guo, 2012) . The use of biochar as a soil amendment dates back to the Amazonian Dark Earths (known as Terra Preta) in the Amazon Basin, where charred organic materials appear to have been added purposefully to the soil to enhance its fertility. Some of these anthropogenically modified soils date back 7,000 years, and have long-lasting fertility resulting from biochar's presence and stability (Maia et al., 2011; Lehman and Joseph, 2009).

The addition of biochars enriched with N and P is an attractive agricultural management strategy to enhance soil fertility. The use of biochar in compost and in the recovery of N and P from anaerobic digestion (AD) processes can mitigate environmental issues such as greenhouse gas (GHG) emissions and nutrient and pathogen leaching in soils—a serious and persistent problem in agriculture. Washington State University's (WSU) biochar program is advancing the design and use of biochars to adsorb and retain nutrients both at the source—nutrient retention from AD effluents—and in the soils—through compost and biochar amendment. This research shows promise for addressing environmental concerns and creating a valuable market for engineered biochars, as well as for improving the hydrological and microbial transport properties of marginal soils. Producing engineered biochars that can improve the viability of amended soils offers a path to increasing productivity in regions of the state dominated by marginal soils, such

as the low-grade, sandy Quincy series soils found in Adams, Benton, Douglas, Franklin, Klickitat, Walla Walla, and Yakima counties (Hipple, 2012).

This project aims to engineer and evaluate biochars for use as soil amendments to reduce nutrient leaching and the transport of *Escherichia coli*.

2.1.1 The promise of biochar as a soil amendment

Biochars are significantly more stable than the fast and slow-cycling fractions of soil organic matter. The effects of biochar additions to soil can therefore have significant long-term benefits on soil fertility and carbon (C) sequestration (Lehmann et al., 2006; Lehmann, 2007). In addition to potential direct carbon sequestration, laboratory studies have shown that emissions of carbon dioxide (CO_2) and nitrous oxide (N_2O) were reduced in biochar-amended soils (Spokas et al., 2012).

Soil amendments using biochar, when properly managed, are a sustainable means of improving soil fertility in a way that is stable over the course of decades to centuries (Lehmann et al., 2003; Novak et al., 2009). This is especially true for sandy soils where low water holding capacity and significant leaching of soil nutrients are major hurdles to their sustainability (Uzoma et al., 2011). Recent research has shown that biochars have positive effects on a variety of soil properties essential for plant growth, such as soil pH (Novak et al., 2009; Sika, 2012; Basso et al., 2013), cation exchange capacity (CEC) (Lehmann and Joseph, 2009; Uzoma et al., 2011; Basso et al., 2013), soil water holding capacity (Uzoma et al., 2011; Basso et al., 2013), soil bulk density (Basso et al., 2013), and exchangeable basic cations (Sika, 2012).

While biochar has significant potential as a soil amendment, studies with freshly produced biochars have not been able to reproduce the effectiveness of the centuries-old Terra Preta soils in the Amazon Basin (Granatstein et al., 2009). A likely cause of this difference in biochar behavior is the low level of surface oxidation of the fresh biochar, when compared to the much higher oxidation levels achieved by the Terra Preta biochars, which have aged in an oxidizing soil environment for centuries (Solomon et al., 2007). Oxidation processes are known to significantly increase acidic surface oxygen complexes—hydroxyl, carbonyl and carboxyl groups (Chiang et al., 2002; Valdes et al., 2002; Park and Jin, 2005)—and the development of these acid groups is essential for improving the biochar's cation exchange and nutrient retention capacities. This project therefore aims to design and produce biochar with greater amounts of surface oxygenated complexes.

Biochar's ability to adsorb phosphate, on the other hand, appears to be related to the mineral fraction of the biochar (Agyei et al., 2000; Agyei et al., 2002; Namasivayam and Sangeetha, 2004; Oguz, 2005; Lu et al., 2009; Xue et al., 2009). Results from Yao et al. (2011) demonstrate that surface mineral complexes associated with magnesium were responsible for phosphate adsorption on biochar developed from anaerobically digested sugar beet tailings. This project therefore also aims to design biochar that can achieve such phosphorous adsorption.

2.1.2 The performance of biochar as a soil amendment

While greater scientific attention has resulted in an increasing number of biochar publications, the literature pertaining to the effects of biochar amendments on the properties of sandy soil

remain limited. A key aspect requiring further study is the effect of biochars on the hydro-physical properties of amended soils. As the hydro-physical properties of sandy soils are important limiting factors for agricultural productivity, further study is necessary to determine appropriate biochar properties and necessary applications rates that would make engineered biochar an effective amendment for sandy soils. This project aims to determine the effect of biochar on the hydro-physical properties of Quincy sandy soils, following the hypothesis that biochar additions to these soils will increase the water retention capacity and improve the physical properties of sandy soils.

Biochar is also attracting attention as a promising option to mitigate climate change through increased soil carbon storage and decreased CO_2 emissions from agricultural soils. Laboratory studies have shown that emissions of CO_2 were reduced in biochar-amended soils (Spokas and Reicosky, 2009). Further research is needed in order to verify these results and to determine how the surface chemistry of different biochars affects the emission of these gases. This study aims to evaluate the effect of biochar production conditions and application rate on CO_2 emissions from Quincy sandy soils under lab-controlled conditions.

Biochar and co-composted biochar may be useful amendments to reduce leaching of nutrients and contaminants from the compost itself. Biochar can potentially prevent the leaching of pollutants that may already be part of the compost, can reduce the leaching of nitrate from soil (Knowles et al., 2011; Clough et al., 2013), and can reduce pore water concentrations of metals (Brennan et al., 2014; Meng et al., 2014). However, it is not known whether biochar or co-composted biochar mixed with compost would improve the soil's retention capabilities for nutrients. The aim of this study was therefore to test whether adding a commercially available biochar to mature compost could reduce the leaching of nutrients from the compost. The results of this study have already been published (Iqbal et al., 2015; see Authors' note on page 14).

Finally, the transport of pathogenic bacteria through soils is also of concern in soil health, and particularly in the use of manure-based products as soil amendments for food crop production. Bacterial transport is a complex process that is impacted by many factors, such as the charge of the soil media. Biochars can also have a role in microbe retention into soil particles (Wang et al., 2011). The abiotic conditions that regulate pathogen transport through soils are dependent on both the specific pathogen and the soil conditions (Abit et al., 2012). The effect of biochar characteristics on the transport of microorganisms has been very poorly studied. This project aims to address this gap in knowledge by evaluating *E. coli* movement in biochar-amended sandy soils.

To achieve the biochar engineering, nutrient retention, and microorganism transport aims identified above, this project targeted five specific objectives:

1. Develop methods to produce engineered biochars with enhanced capacity to remove N and P, and that are compatible with the AD nutrient recovery system developed at WSU.
2. Characterize the physical and chemical properties of these biochars that are relevant to nutrient retention and microorganism transport.
3. Study the effect of engineered biochar on the physicochemical and hydrological properties of amended sandy soils.
4. Understand the influence of biochar characteristics on CO_2 emissions from a sandy soil.

5. Evaluate biochar's ability to reduce N, P, and *E. coli* leaching and movement in biochar-amended sandy soils.

As the results of all five objectives inform the integration of nutrient recovery technologies with the anaerobic digestion nutrient recovery system developed at WSU, this report presents the results of these five objectives first, and concludes with the integration recommendations.

2.2 Methods

2.2.1 Methods to produce engineered biochars with enhanced capacity to remove nitrogen and phosphorous

Based on small-scale studies conducted last biennium, a batch method was developed to treat large quantities of AD dairy fiber. Approximately 10 kg of untreated and calcium-modified biochars were produced from AD fiber—obtained from Andgar and the DeRuyter dairy farm—using a continuous auger pyrolysis reactor. 70 kg of the digested fiber were mixed and ground using hammer mills, and were then passed through a 1/8" screen. 30 kg of the digested fiber was pyrolyzed at 500°C under a nitrogen (N_2) flow of 8–12 standard liter per minute (SLPM). A continuous biochar removal system was used, which allowed the biochar to cool rapidly. In total 9.6 kg of biochar were produced.

To test the effects of calcium precipitates on the biochar's ability to adsorb nutrients, 35 kg of digested fiber was mixed with 120L of 0.5M calcium nitrate ($Ca(NO_3)_2$) solution, and agitated for five minutes using a 700 rpm grout mixer. After stabilization, the fiber was pressed through cheesecloth and washed with deionized water. The pressed fiber was dried at 105°C for two days and stored prior to pyrolysis. The final calcium-treated fiber was pyrolyzed following the same method utilized for the untreated fiber. Biochar yields showed no appreciable variation from the untreated samples: in total, 9.5 kg of biochar was produced.

From preliminary tests at the bench scale, recovery of ammonium from the digester effluent is significantly compromised by competitive adsorption from an assortment of cations within the wastewater. Due to this complication, recovery of phosphate was the primary focus for this scaled-up project. Here batch adsorption from AD fiber was tested. 70 kg of AD dairy and food co-digestion liquids were obtained from the DeRuyter dairy farm. This effluent was transported in sealed, five-gallon containers and allowed to settle for three weeks after arrival at the laboratory. These liquids were then mixed in a ratio of 11 kg of liquid to 1.5 kg of biochar, in six batches. The liquid effluent was sampled from three containers on days 2, 4, 6, 8, 11 and 15. After 15 days of contact between the biochar and the liquid, the biochars were filtered through a 300 mesh stainless steel screen, pressed and dried for three days at 105°C.

The effluent samples collected on days 2, 4, 6, 8, 11 and 15 were centrifuged and separated, to quantify the biochar's ability to remove phosphorous from the liquid. 300 mg of effluent were then digested using 3 mL of concentrated HNO_3 and 2 mL of 30% H_2O_2. The digested samples were diluted to 100 mL and analyzed by inductively coupled plasma mass spectrometry (ICP-MS).

2.2.2 Physical and chemical properties of biochar that are relevant to nutrient retention and microorganism transport

In order to tailor the engineering of biochar to specific applications, improved understanding of the effects of temperature and composition of the biochar is required. To fill this gap in understanding, biochars were produced following a thermo-series—pyrolysis temperatures from 300 to 700°C under constant nitrogen flow—using several different feedstock. Bulk characteristics of the resultant biochars were determined by elemental and proximate analyses, as well as by adsorption isotherms and microscopy. Changes in the finer chemical structures were followed by nuclear magnetic resonance and FT-Raman spectroscopy.

A spoon pyrolysis reactor available at WSU was used to generate all biochars used in this study. All biochars were produced from feedstocks that varied in their initial composition (Table 2.1): Douglas fir wood (DFW) and bark (DFB), hybrid poplar wood (HPW), spent brewers grain (SBG), and anaerobic digested fiber (ADF).

Table 2.1: Proximal analysis of starting feedstock

Sample	Extractive (wt. %)	Cellulose (wt. %)	Hemi-cellulose (wt. %)	Lignin (wt. %)	Insoluble Ash (wt. %)
DFW	9.6	41.1	16.2	28.5	0.0
HPW	10.9	40.7	15.4	32.9	0.0
DFB	24.2	24.6	10.8	32.9	0.1
SBG	38.4	19.0	18.5	26.5	0.7
ADF	18.2	23.9	14.4	36.0	0.7

The effect of post-pyrolysis oxidation on the yield and physical and chemical properties of various biochars—produced with different pyrolysis temperatures—was also studied. Changes in composition were examined by CHN-elemental analysis, proximate analysis, pH and electro conductivity (EC) in solution, cation exchange capacity (CEC), Brunauer Emmett Teller (BET) surface area, scanning electron microscopy (SEM) analysis, Boehm titration, and FT-Raman analysis.

2.2.3 Effect of engineered biochar on the physicochemical and hydrological properties of amended sandy oils

Six different biochars were produced at two pyrolysis temperatures—350°C and 600°C—from hybrid poplar wood (HP), pine wood (PW), and pine bark (PB). Samples of each of these six biochars were also treated with post-pyrolysis oxidation. The 12 different biochar samples (2 pyrolysis temperatures x 3 feedstock x 2 levels of post-pyrolysis treatment) were then mixed with Quincy sandy soil samples at an application rate of 2% by weight. In a Quincy sandy soil control and in all biochar-amended sandy soil microcosms, water content at field capacity (FC), available water holding capacity (AWC), permanent wilting point (PWP), water content at saturation point ($\Theta_{sat.}$), and water potential of biochar-soil mixtures were measured, as well as selected physical and chemical properties such as bulk density, porosity, EC and pH.

The key hydro-physical parameters listed above were obtained from soil water retention curves, which map the effect of water content on a soil's—or amended soil's—water potential. Curves were fitted to measured soil volumetric water contents using the Van Genuchten model (van Genuchten, 1980) through the SWRC-Fit version 1.3 software (Seki, 2007). The following parameters were obtained from these curves:

- the volumetric water content at field capacity (Θ_{FC}), defined as the volume of water held at a water potential (Ψ) between -10 to -30 Kpa.
- the permanent wilting point (Θ_{PWP}), defined as the moisture content in soils at which plants begin to wilt and cannot recover in a saturated atmosphere without increasing moisture in the soil, quantified as a water potential of -1.5 MPa, and
- the available water holding capacity (Θ_{AWC}), which represents the quantity of water that can be held and would be available to the plant, calculated as the difference between Θ_{FC} and Θ_{PWP}.

The osmotic potential is customarily ignored in soil-related studies, due to the lack of semipermeable membranes in soil-water systems such as those of interest in this project. However, it has been calculated here as a function of the EC values of biochars, to estimate the potential effect of biochar additions on this parameter.

The Quincy sandy soil's particle size followed an approximately Gaussian distribution, centered near 0.2 mm and with particles generally constricted to the 0.03 to 0.7 mm range (Figure 2.1). Both biochars had somewhat larger particles, with mean particle sizes near 0.3-0.4 mm. These samples also showed a strong asymmetrical distribution towards lower particle sizes, with distributions occurring over a range of 0.01 to 2 mm for both biochars (Figure 2.1).

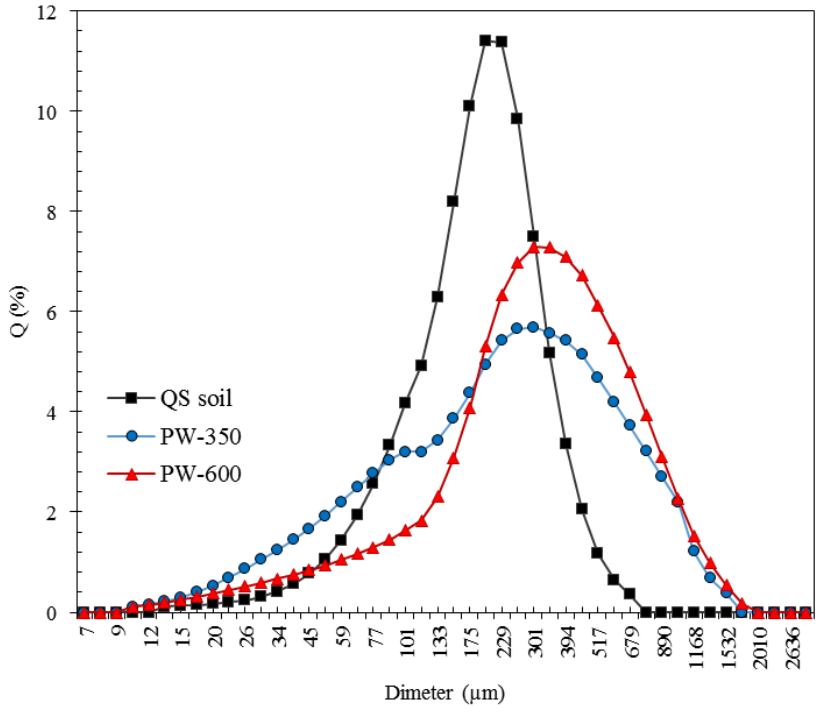

Figure 2.1: Particle size distribution of Quincy sandy soil and biochar from Pine Wood produced at 350 and 600°C.

2.2.4 Influence of biochar characteristics on carbon dioxide emissions from a sandy soil

Samples of Quincy sandy soil mixed with two different types of biochar (LB: low temperature biochar, produced at 350°C; and HB: high temperature biochar, produced at 600°C) at three different application rates (10%, 15%, and 20% by weight) were prepared. These samples—including a sample of Quincy sandy soil without biochar as a control—were incubated for 14 days, and the total amount of carbon (C) released as CO_2 was measured. The observed CO_2 production rates were subtracted from the CO_2 production of the biochar itself (without soil, data not shown), which occurs during the incubation period and is due to abiotic oxidation (Spokas and Reicosky, 2009; Zimmerman et al., 2011; Thomazini et al., 2015).

2.2.5 Biochar's ability to reduce nutrient leaching in amended sandy soils

> ***Authors' note:*** This study's results have been published in *Science of the Total Environment*:
>
> Iqbal, H., Garcia-Perez, M., Flury, M. 2015. Effect of biochar on leaching of organic carbon, nitrogen, and phosphorous from compost in bioretention systems. Science of the Total Environment 521-522: 37-45.
>
> Portions of this section—and of the associated *Results and discussion* section—were taken directly, with modest modifications, from this publication.

Column leaching experiments were carried out on eight different media: four pure media—100% compost, 100% biochar, 100% co-composted biochar, and 100% sand—and four media mixes—75% compost and 25% biochar, 75% compost and 25% co-composted biochar, fully mixed compost (30%) and sand (70%), and layered compost (30%) and sand (70%).

PVC columns were packed with each of the media or mixes being evaluated, and then irrigated with a flow rate of 77 mm hr^{-1} for 36 hours, representing a six-month, 24-hour storm in the Puget Sound area (Ecology, 2012). The leachate from each column was sampled at three-hour intervals, and analyzed for pH, electrical conductivity, dissolved organic carbon, N and P. Full details on the methodology are described in the peer-reviewed publication of this study (Iqbal et al., 2015).

2.2.6 Biochar's ability to reduce *Escherichia coli* movement in amended sandy soils

Biochars (PW-350, PW-600, PB-350, and PB-600) were sub-sampled and oxidized in air at 250°C for 30 minutes. One randomly selected biochar (PW-600) was mixed with sandy soil at different ratios to study the effect of application rate on *Escherichia coli* transport. All biochar samples were then mixed with soil at a 20% weight ratio. A biochar concentration of 20% was chosen to allow for the bacterial cells to meet significant numbers of biochar particles, especially at low bacterial concentration, as used here, and also to limit any analytical difficulties that arise from working with low concentrations.

Pathogenic and non-pathogenic *E. coli* strains (H7 and K12 respectively) were grown for 12 hours at 37°C. The cells were isolated at the late exponential phase of their growth. The culture was centrifuged at 5100 RPM for 10 minutes, and washed to re-suspend the cells in deionized water to an absorbance of 0.05 units at 600 nm. Bacterial cells were then pumped through the packed biochar-amended soil column at a speed of 1.16 m day^{-1}, and the absorbance measurements of the solutions leaving the columns were taken at 600 nm every 16 seconds through the use of a fraction collector (Figure 2.2). The adsorption kinetics of bacteria in composite soil were measured by comparing the concentration of bacteria leaving the soil matrix at a given flow rate to the known influx of bacteria.

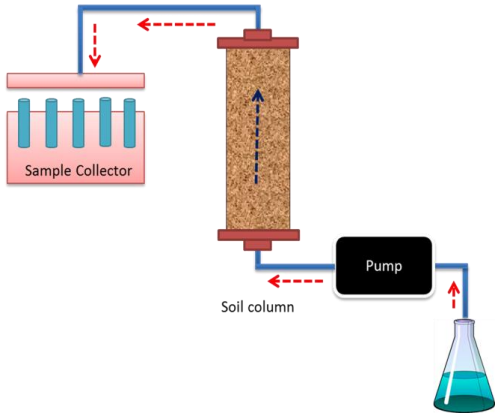

Figure 2.2: Soil column used for pathogen transport in biochar-amended soils.

2.3 Results and discussion

2.3.1 Production of engineered biochars with enhanced capacity to remove nitrogen and phosphorous

Based on poor performance during initial batch trials, the non-calcium treated biochar was eliminated from further tests. All the results presented here were obtained using calcium-treated biochar.

A total of 10.1 kg of enriched biochar was obtained after drying, an amount 12% greater than the 9 kg of biochar originally mixed with the liquid effluent (1.5 kg biochar x 6 batches). This increase in weight indicated there was significant retention of material from the solution.

The analysis of the P concentration in the effluent as a function of contact time with the biochar showed a sharp drop in phosphate in the first two days, followed by a slow release through day 8, when the P concentration reached a plateau at approximately 50% of the original concentration (Figure 2.3). These results suggest that the engineered biochar has a noticeable capacity for adsorbing P from the liquid effluent from AD.

The adsorption of P is dependent on many factors, including pH and competitive ions. The initial strong adsorption, followed by subsequent release of P suggests variation in the solubility of phosphate changes over the course of the trial, which could be due to changes occurring over the

course of the trial in either pH or the concentration of competitive anions such as sulfate. The batch adsorption was also noted to have a strong positive effect on odor control, suggesting additional applications for the biochar in addressing this issue, subject to further confirmatory studies.

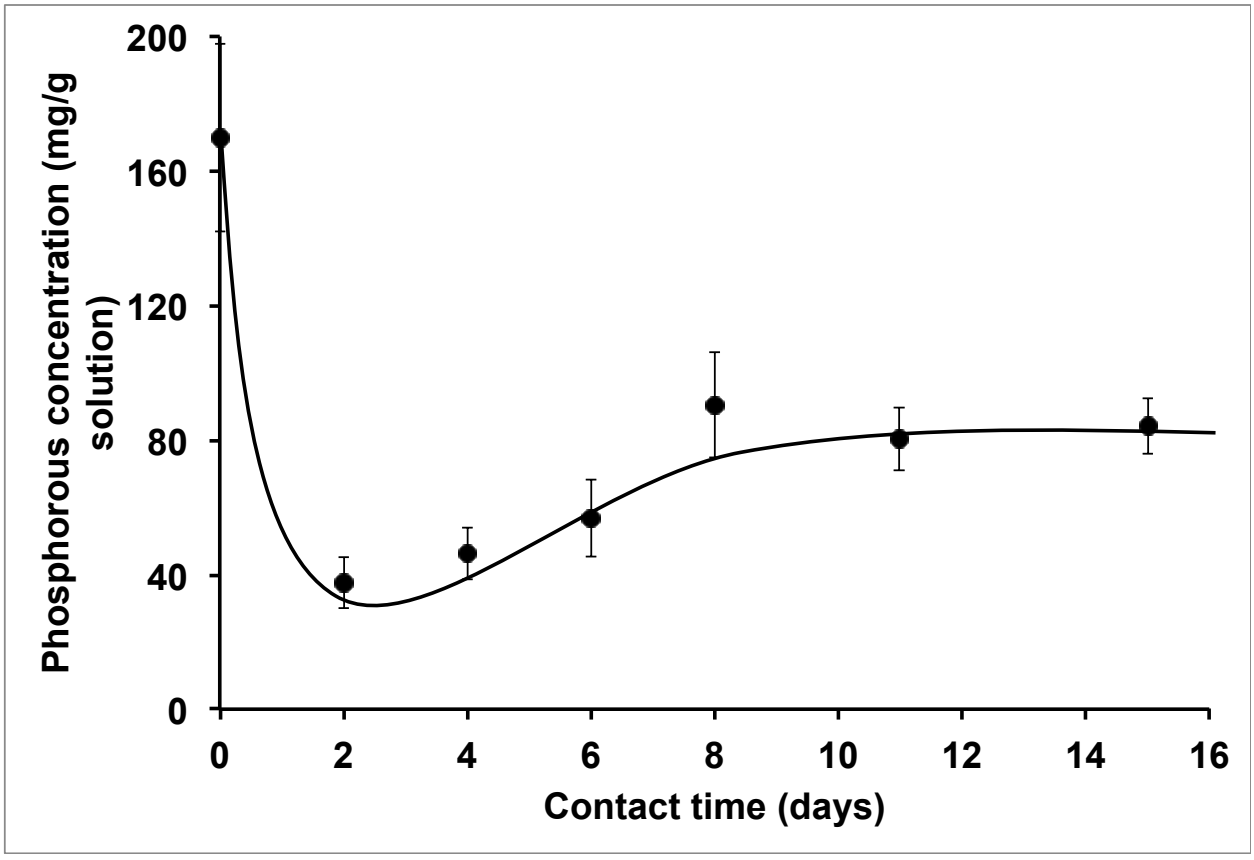

Figure 2.3: Phosphorous remaining in solution in the AD effluent, as contact time with calcium-treated biochar increased.

2.3.2 Physical and chemical properties of biochar that are relevant to nutrient retention and microorganism transport

Biochar yields decreased asymptotically with temperature for all feedstock species studied, with the highest yields being obtained from materials with high ash and lignin fractions (

Figure 2.4A, Table 2.1). As temperature increased, the fixed carbon content of the biochar also increased for each feedstock species (

Figure 2.4B). In contrast to yield however, a high ash fraction, specifically high alkali content, resulted in strong reductions in fixed carbon at 850°C. This effect is likely due to the catalytic effect of alkali metals during gasification reactions, as noted in the literature (Quyn et al., 2003; Yip et al., 2010). Both feedstock and pyrolysis temperature strongly affected the element composition of the resultant biochars. Despite initially consistent elemental (C, H, O) compositions, treatment at torrification temperatures resulted in strong variations in the oxygen content of the resultant biochars. Treatment at higher temperatures resulted in increasing elemental consistency between all materials studied (

Figure 2.4C).

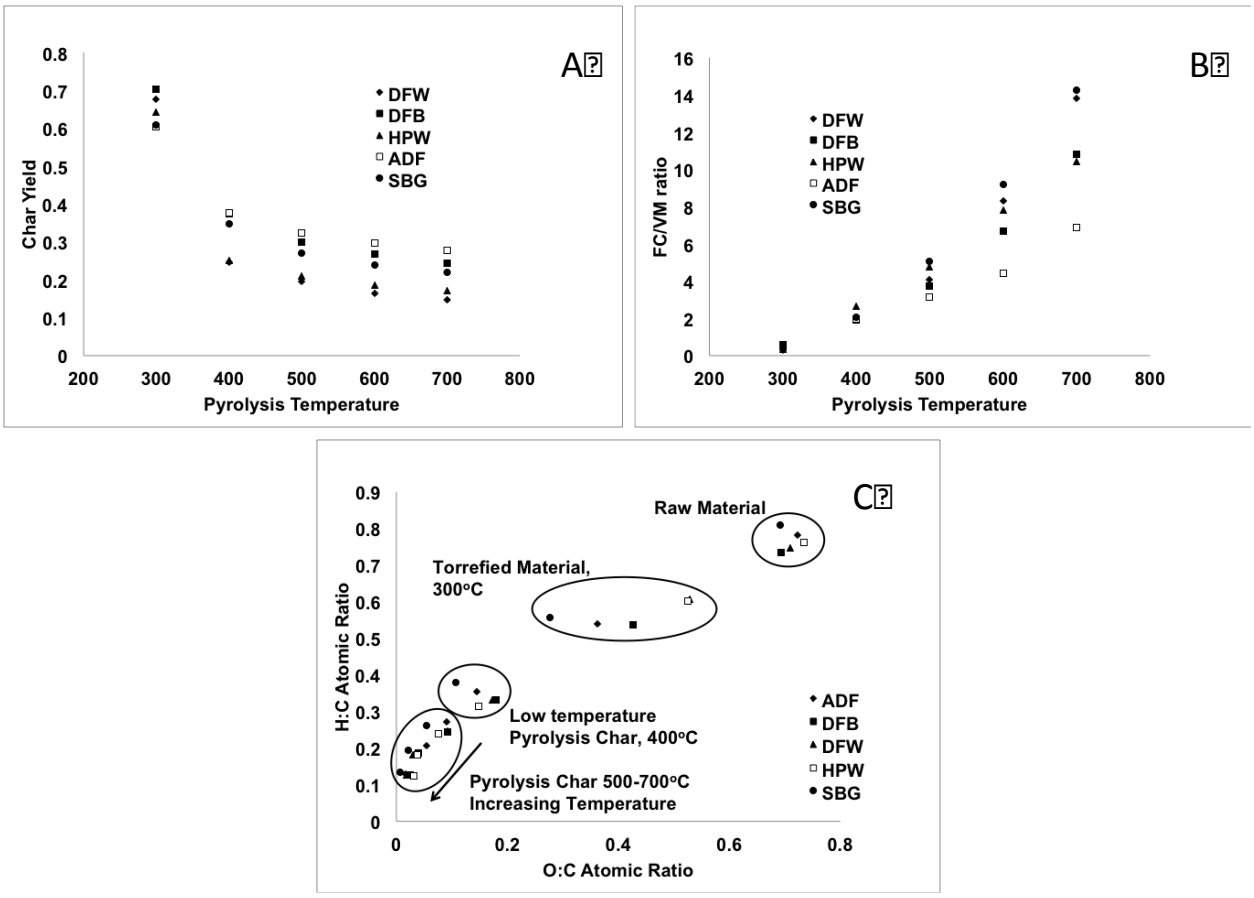

Figure 2.4: Effect of temperature on the bulk chemical properites of biochar: (A) biochar yield: the weight of biochar obtained, relative to the initial weight of oven-dry feedstock; (B) fixed carbon (FC)—solid carbon fraction stable under an inert atmosphere at 850°C—to volatile matter (VM)—fraction volatilized at temperatures between 105 and 850°C—ratio; and (C) H:C to O:C ratio, representing the elemental composition of the biochar.

Pyrolysis temperature has also been found to strongly affect the surface properties of biochar. While higher pyrolysis temperatures led to a rapid increase in the available surface area (Figure 2.5A), the surface chemistry needed for adsorption of ions was stripped (Figure 2.5B). The effect of temperature on the surface functional groups also impacted the charges of the biochar's surface (

Figure 2.5C). The z-potential is a property that has been correlated with the biochar–microbial interactions. The higher the pyrolysis temperature, the less negative the surface charge of the biochar was. Consequently, biochar produced at those higher temperatures should have a higher attraction for negatively charged compounds and microorganisms. These results clearly showed that it is a challenge to produce a biochar with both high surface area and high CEC—a property associated to the oxygenated functional groups on the surface.

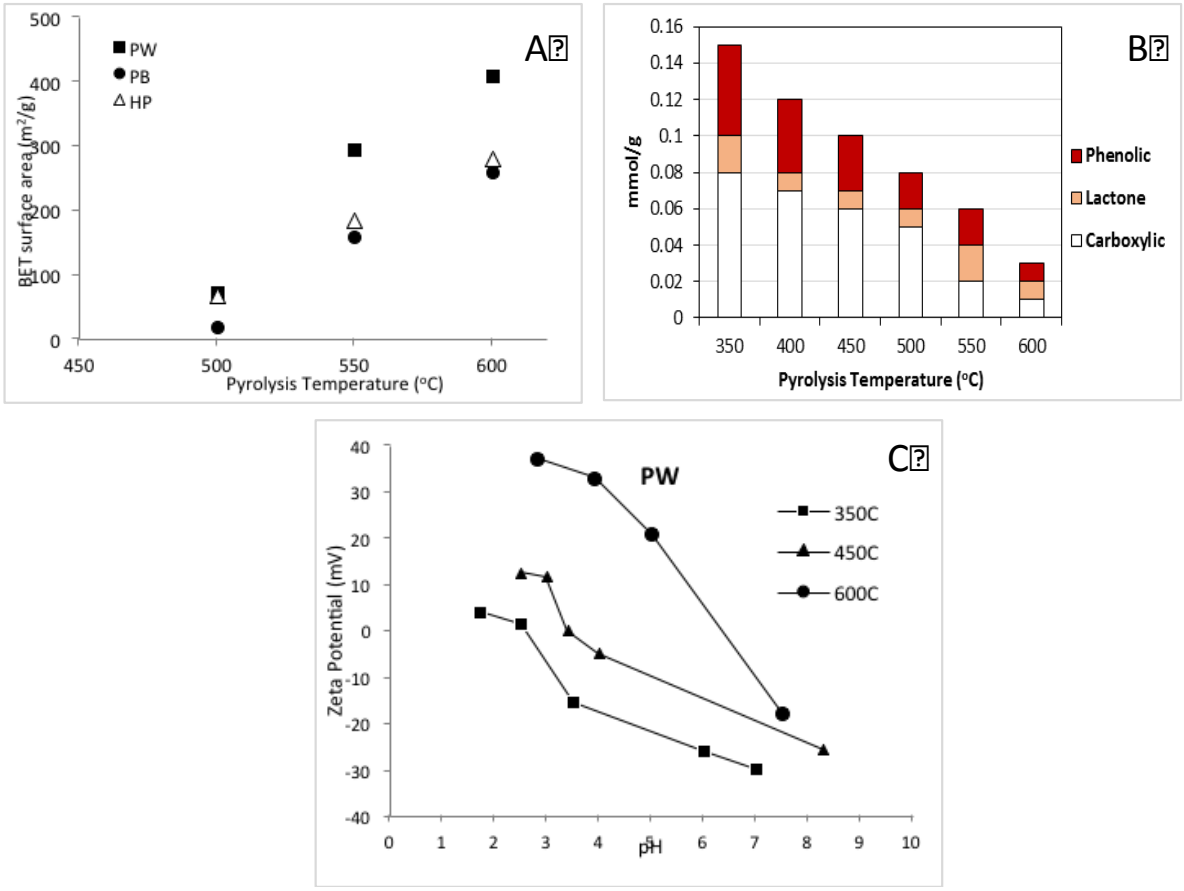

Figure 2.5: Effect of pyrolysis temperature on various surface properties of biochar: (A) surface area; (B) surface functional groups needed for adsorption of ions; and (C) Z-potential.

The Raman spectra of the thermoseries of biochars showed a narrowing of the G-peak as temperatures increased from 400 to 600°C (Figure 2.6). This narrowing is indicative of increasing order in the system. The loss of intensity near 1520 cm^{-1} is linked to reduction of ether groups as temperature increases. The dramatic reduction in intensity observed near 1450 cm^{-1} suggests that non-hexagonal defects—such as pentane-based ring systems—decreased with increasing temperature. The moderate increase in intensity in the region near 1450 cm^{-1} observed in biochar produced at 700°C suggests that point vacancies within largely hexagonal structures have developed. The observed increase in intensity and the downshift of the D-peak with increasing temperature is indicative of increased aromatic ring formation and increased cluster size. That the D-peak for biochars produced at 500 and 600°C was largely overlapping suggests that the primary difference between those two samples was a mild to moderate decrease in ether type groups within clusters.

The elemental and proximate analyses of the oxidized and unoxidized biochars suggest that the carbonaceous materials produced at low pyrolysis temperatures were more susceptible to low temperature, air oxidation post-pyrolysis than those obtained at high pyrolysis temperatures.

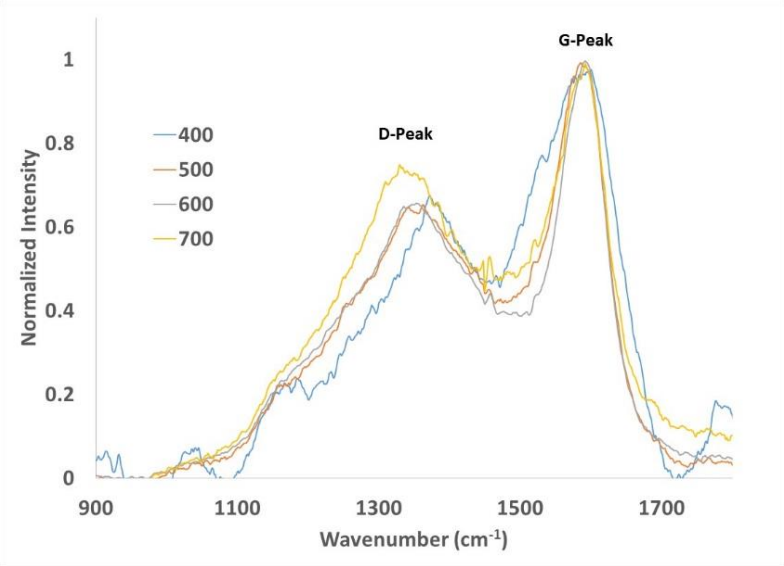

Figure 2.6: FT-Raman analysis of the effect of pyrolysis temperature on biochar from Douglas Fir Wood.

In summary, the results of this project showed that ash content, pH, apparent surface area, fixed carbon, and total carbon were positively correlated with pyrolysis temperature. Conversely, recovery yield, total N content, volatile matter (VM), and CEC showed negative correlations. The ratios of O:C and H:C, and total acidic functional groups tended to decrease with the pyrolysis temperature, and were directly related to the content of VM. While increasing the pyrolysis temperature did reduce biochar yields and did increase fixed carbon ratios, these results were strongly dependent on the initial feedstock. Spectroscopic results indicated that the reduced VM content observed in these analyses was likely a result of increased aromatic condensation and the reduction of non-hexagonal rings. Raman studies showed a marked increase in possible defects after treatment at 700°C. These defects may have played a role in the observed increase in microporous surface area and pore volume, and may also have provided additional reactive edge sites for chemical modifications.

2.3.3 Effect of engineered biochar on the physicochemical and hydrological properties of amended sandy oils

The application of biochar reduced the EC and bulk density of the sandy soil (Table 2.2), whereas an increase in pH was observed, particularly in the HP-350, HP-600 and PB-600-amended soil samples, which could be linked to the biochar's ash content. The decrease in bulk density is due to the low density of biochar, typically well below 1 g cm^{-3}. The observed increase in pH was likely an effect of both the mineral content of the biochar (alkali and alkaline oxides, and carbonates), as well as an effect of the slightly basic nature of the pi-pi systems present in aromatic carbons. The reduction of the EC suggests there were reduced free ion counts in the solution, indicating adsorption of said ions by the biochar. The lowest EC values were recorded for low-temperature biochars, which were previously shown to have the largest native CEC. As the EC is related to the free ion concentration in solution, the most probable

explanation for this effect is the destruction of exchange sites at higher pyrolysis temperatures. In all cases, however, the EC was reduced with biochar amendment.

Table 2.2: Effect of biochar application to sandy soil on the soil's physicochemical properties.

Sample ID	Bulk density ($g\ cm^{-3}$)	Organic Matter (%)	pH (1:5)	EC ($dS\ m^{-1}$)
Control	1.49	0.76	7.5	0.08
HP-350 soil	1.28	2.24	8.4	0.03
HP-600 soil	1.27	2.21	9	0.06
PW-350 soil	1.27	2.29	8	0.01
PW-600 soil	1.26	2.13	8	0.02
PB-350 soil	1.28	2.21	8.1	0.02
PB-600 soil	1.29	2.1	8.7	0.06

The soil water retention curves showed that the application of biochar affected the physicochemical and hydrological properties of interest (Figure 2.7). Biochar amendments significantly impacted soil water content at field capacity (Θ_{FC}). The Θ_{FC} of the sandy soil was increased by roughly 40 to 80% after amendment with biochar, with air-oxidized biochars having the larger effect (Table 2.3). The largest increase in Θ_{FC} was noted for HP350-amended samples, which retained 30.22% moisture at field capacity. Amended samples were also found to have increased water content at the permanent wilting point (Θ_{PWP}) relative to the control soil (Table 2.3). Water content at permanent wilting point presented weak dependencies on the biochar feedstock source as well as on pyrolysis temperature. The observed increases in Θ_{PWP} were small in comparison to the increases in water available at field capacity. Because of this, the majority of the total water potentially stored in the soil was available for plant growth, while in the case of soil without biochar additions, much of the water was easily lost by gravity.

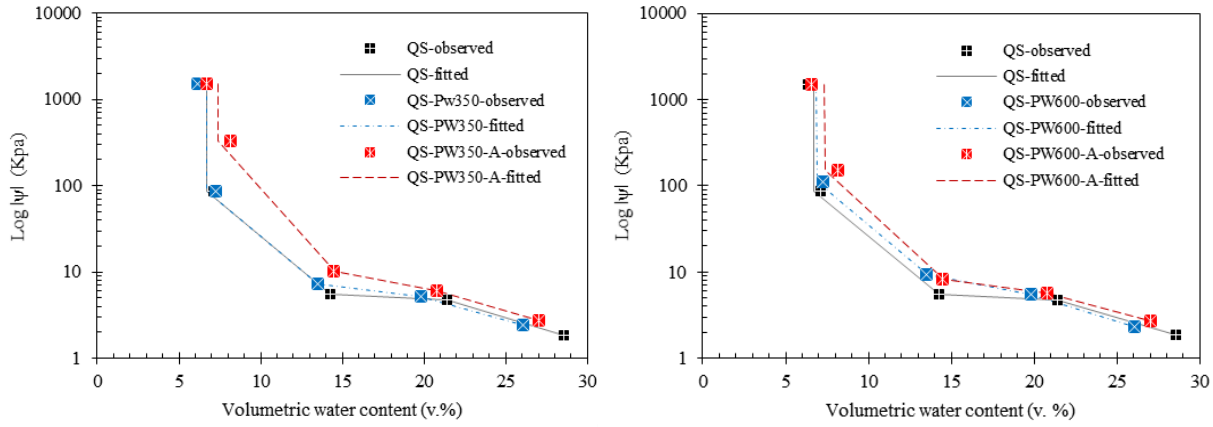

Figure 2.7: Predicted soil water retention curves (lines) and measured soil volumetric water contents (symbols) at different matric potentials. The soil water retention curve was fitted using the Van Genuchten model (van Genuchten, 1980) through the SWRC-Fit version 1.3 software (Seki, 2007).

In all cases, the application of either oxidized or unoxidized biochar was found to reduce the osmotic potential in the soil (Table 2.3). The effects of air oxidation were complex, but tended to increase the osmotic potential for lower temperature biochars, and reduce the osmotic potential for higher temperature biochars. This would suggest that destruction of the carbon matrix during pyrolysis results in the release of free ions to the solution from low temperature biochars, while acid groups are likely formed with minimal surface destruction on the high temperature biochars.

Table 2.3: Water-holding characteristics of biochar-amended soils.

Property	QS	QS-PW350		QS-PW600		QS-PB350		QS-PB600		QS-HP350		QS-HP600	
		UO	AO	UO	AO	UO	AO	UO	AO	UO	AO	UO	AO
θ_{FC} (%)	16.9	26.6	27.1	25.7	27.5	23.7	25.9	25.4	27.2	28.7	30.2	25.5	25.9
θ_{PWP} (%)	5.3	6.2	6.7	6.6	6.6	6.4	6.6	6.4	5.9	6.1	6.3	6.8	6.5
θ_{AWC} (%)	11.6	20.4	20.4	19.2	20.9	17.3	19.3	19.0	21.3	22.6	23.9	18.7	19.3
θosm. (-KPa)	2.9	0.4	0.7	0.7	1.4	0.7	1.8	2.2	1.4	1.1	0.4	2.2	0.7

Abbreviations: QS: Quincy sandy soil (control); UO=unoxidized biochar; AO=oxidized biochar; Θ_{FC} = water content at field capacity; Θ_{PWP}= water content at Permanent Wilting Point (−1.5 MPa); Θ_{AWC} = available water holding capacity; Θ_{osm}=Osmotic water content.

The addition of biochar was generally found to be beneficial to the hydro-physical properties of sandy soil, an effect that was linked to the pyrolysis temperature and biomass feedstock. However, additional research is needed to determine how crop yields might respond to the observed improvement in soil quality indicators when grown on amended Quincy sandy soils.

2.3.4 Influence of biochar characteristics on carbon dioxide emissions from a sandy soil

Biochars produced from pine wood at 350°C (LB) and 600°C (HB) significantly reduced CO_2 emissions compared to the control. Unexpectedly, biochar produced at low temperature led to reductions in CO_2 emissions as the application rate increased from 10% to 20% by weight (Figure 2.8). This reduction was likely due to the associated increase in abundance of functional groups on the surface of the LB biochars. High-temperature biochar showed the opposite trend: application rates of 20% showed higher CO_2 emissions compared to soils amended at 10 and 15% biochar (Figure 2.8). This increase could be linked to abiotic CO_2 production from chemisorptions of oxygen to the biochar's surface, a similar process to what happened in the case of the biochar control incubation. This trend has also been documented by Thomazini et al. (2015). In general, the CO_2 released from biochar-amended Quincy sandy soil was always less than that of the soil alone, regardless of the biochar production conditions and the application rate (Figure 2.8). This conclusion provides preliminary evidence that net carbon sequestration occurs after biochar application to sandy soils, an observation that supports the findings of Zimmerman et al. (2011).

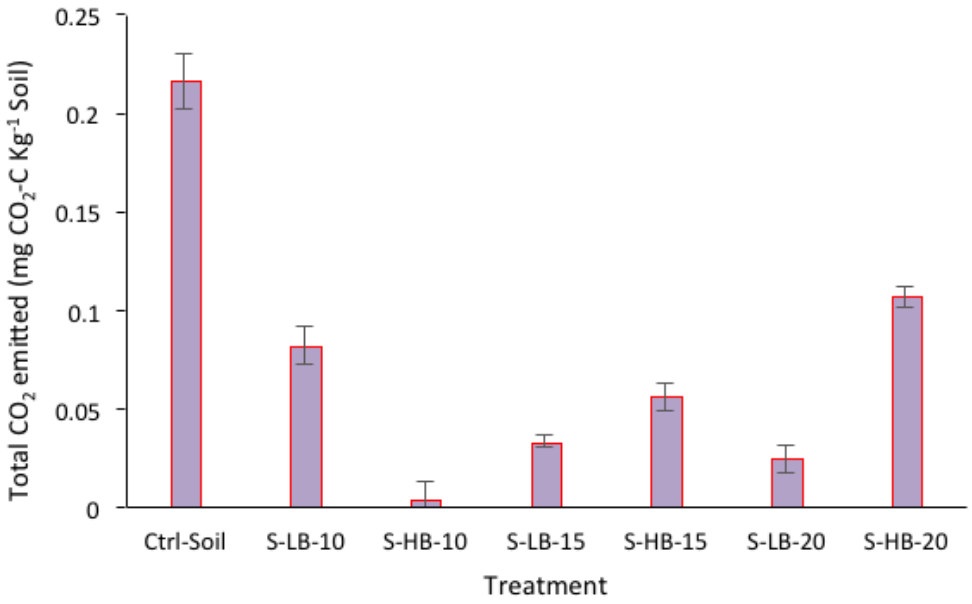

Figure 2.8: The total CO_2 emitted from soil and biochar treatment after 14 days of incubation.

2.3.5 Biochar's ability to reduce nutrient leaching in amended sandy soils

Analysis of the chemical and physical properties of the pure media showed that compost contained the highest amounts of nutrients, and that the co-composted biochar adsorbed N and other nutrients, as has been observed by others (Prost et al., 2013). The biochar—both alone and co-composted—had by far the highest surface area. These and other, more detailed results are presented in the peer-reviewed publication of this study (Iqbal et al., 2015; see Authors' note on page 14).

The leachate from the compost had the most N, though the co-composted biochar had adsorbed some N during composting, leading to some leaching (Figure 2.9). Adding biochar and sand to compost reduced—but did not eliminate—the leaching of total N and nitrate/nitrite (Figure 2.9(b)). The mixing of biochars with compost did not decrease the P leaching, most of which leached as ortho-phosphorous (Figure 2.9(c) and (d)).

As the compost was the major source of nutrients, the amount of each nutrient in the leachate was dependent on the total amount of compost in the column. The concentration of nutrients in the leachate was therefore normalized by the mass of compost used in each treatment. In comparison to pure compost, the biochar amendments did not reduce total N and nitrate/nitrite leaching (Figure 2.10(a)). However, the soil amendments were able to significantly reduce both total N and nitrate/nitrite leaching. The amounts of total N leached from the compost and compost–biochar treatments—most of which was nitrate/nitrite—were 7 to 8% compared to 4 to 5% for the compost–sand mixes.

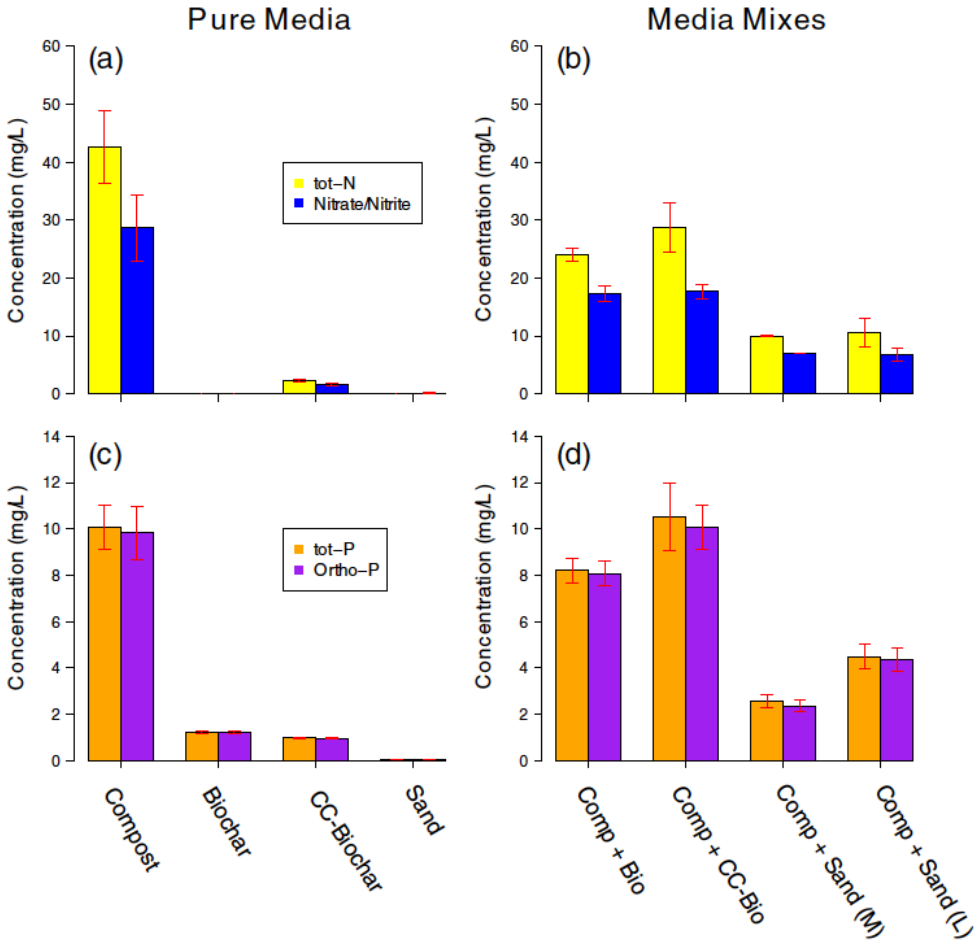

Figure 2.9: Nitrogen (top panels) and phosphorous (bottom panels) leached from pure media (left panels) and media mixes (right panels). Data represent averages of three replicates from composite samples, and error bars are ± one standard deviation (extracted from Figure 5 in Iqbal et al., 2015).

There was no significant difference in the leaching of P from compost–biochar and compost–sand (layered) compared with the pure compost (Figure 2.10b). However, in the compost–co-composted-biochar mix, more P was leached from there than from the compost–sand (mixed). In soils, P leaching is generally slowed down by the presence of Al and Fe oxides (Sposito, 2008). Iron concentrations in the sand (2.2 g kg^{-1}) were almost seven times higher than in the biochar (0.3 g kg^{-1}); therefore, the sand had a higher capacity for suppressing P leaching. Biochar itself leached a substantial fraction of its initial P, though that initial amount was an order of magnitude smaller than that of the P in the compost, and so biochar leaching was deemed negligible.

In summary, adding biochar to mature compost did not affect the leaching of nitrate/nitrite nor ortho-phosphorus under unsaturated flow conditions. Co-composting the biochar did not make a significant difference in terms of its effect on leachates, and co-composting did not appear to have any advantage when incorporating biochar into bioretention systems. While not effective in preventing leaching of nitrate/nitrite and ortho-phosphorus, biochar applied to bioretention

systems may help retain metal contaminants. Many metals, however, will readily form soluble complexes with dissolved organic carbon. The presence of excess dissolved organic carbon from when compost is applied to the bioretention systems (results not shown) may circumvent the sorption capacity of biochars for metals.

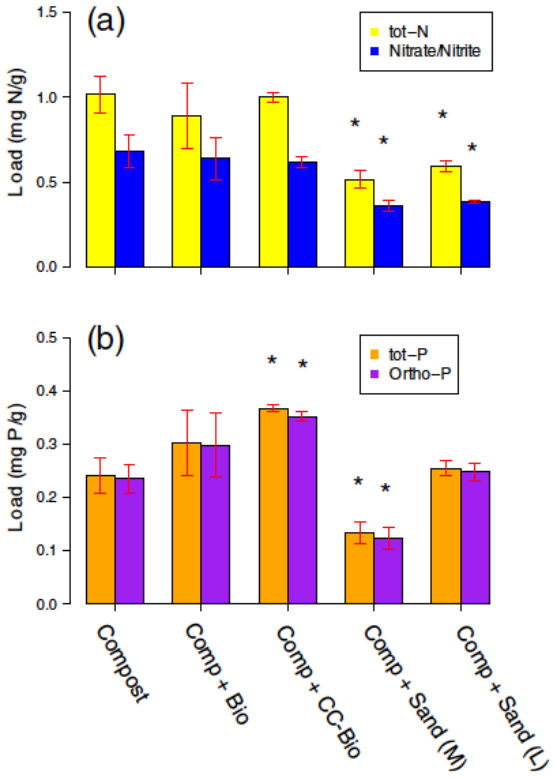

Figure 2.10: Nitrogen and phosphorous loads in the leachate, normalized by the mass of compost used in each treatment. Data represent averages of three replicates from composite samples, and error bars are ± one standard deviation. Asterisks indicate significant differences (p=0.05) compared to pure compost (extracted from Figure 6 in Iqbal et al., 2015).

2.3.6 Biochar's ability to reduce *Escherichia coli* movement in amended sandy soils

Each bacterial strain— O157:H7 and K12—exhibited different behavior in response to biochar additions (Figure 2.11). Transport of the pathogenic strain (O157:H7) through heavily amended soils was severely inhibited (Figure 2.11A). In contrast, the non-pathogenic strain (K12) showed only minimal variations in transport patterns between the control and amended soils (Figure 2.11B). The transport of both *E. coli* O157:H7 and K12 was reduced with biochar additions as low as 1% ($p < 0.05$). As with the control sample, both strains showed similar transport behavior when biochar was added at 1% and 5% concentration levels (Figure 2.11). As amendment rates increased from 5 to 20%, differences in transport between O157:H7 and K12 became more pronounced. While the pathogenic strain exhibited significant decreases in the normalized effluent concentrations $[(C/C_o)_{max}]$, dropping from 0.87 to 0.64 to 0.21 as amendment rates increased from 5 to 10% to 20%, no significant changes were observed in the transport of K12.

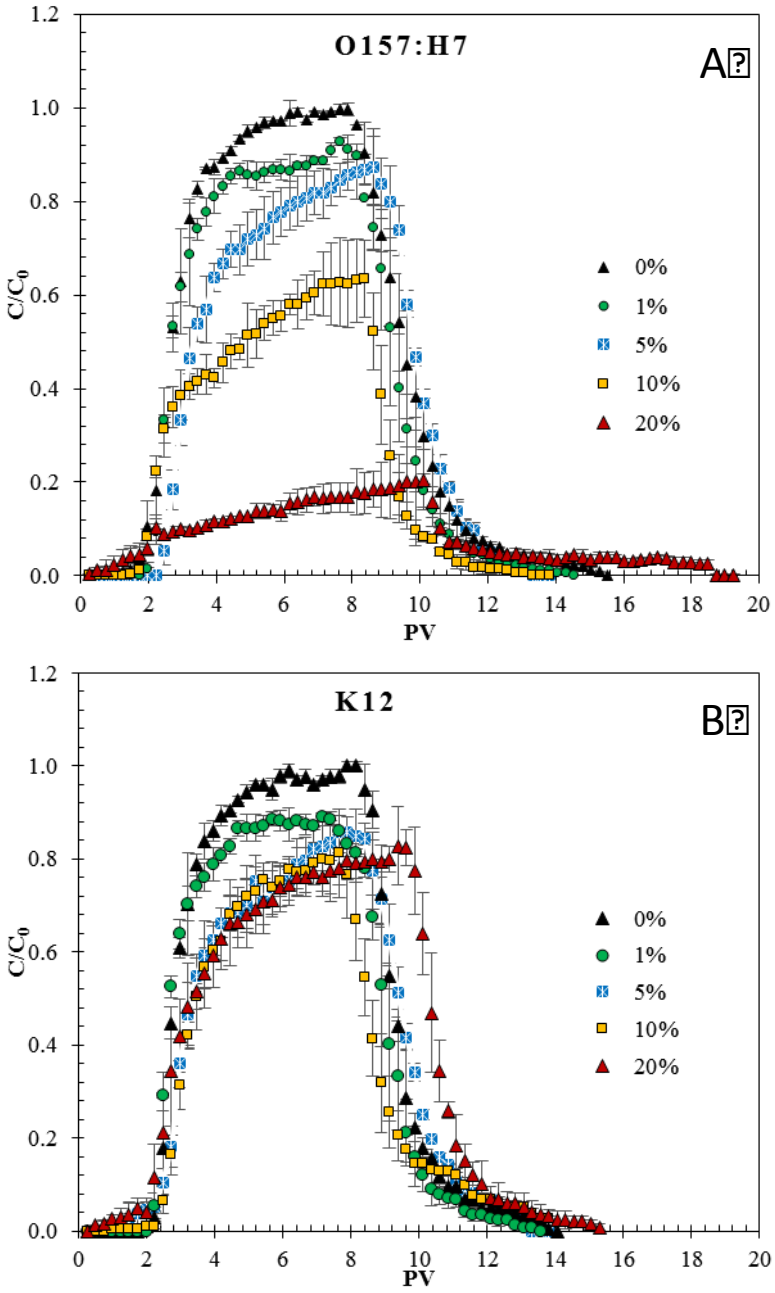

Figure 2.11: Breakthrough curves for *E. coli* (A) O157:H7, and (B) K12 for the column study evaluating the effects of application rates of PW600 biochar on bacterial transport. Error bars indicate variation between triplicate experiments.

Post-pyrolysis oxidation of the biochar had only a relatively minor influence on the transport of non-pathogenic *E. coli* (K12), with nearly the same recoveries from effluent from beds amended with both oxidized and unoxidized biochars (Figure 2.12). In contrast, oxidation was found to promote the transport of pathogenic *E. coli* (O157:H7) relative to the unoxidized biochar-amended soil, though transport was still less than in the non-amended control (Figure 2.12). This

indicates that oxidation of biochar created unfavorable attachment conditions for *E. coli* (O157:H7) during transport events. Results generally indicate that transport of *E. coli* in high temperature biochar-amended soil is governed by surface negative charge density and oxygen content, which both increased meaningfully with oxidation.

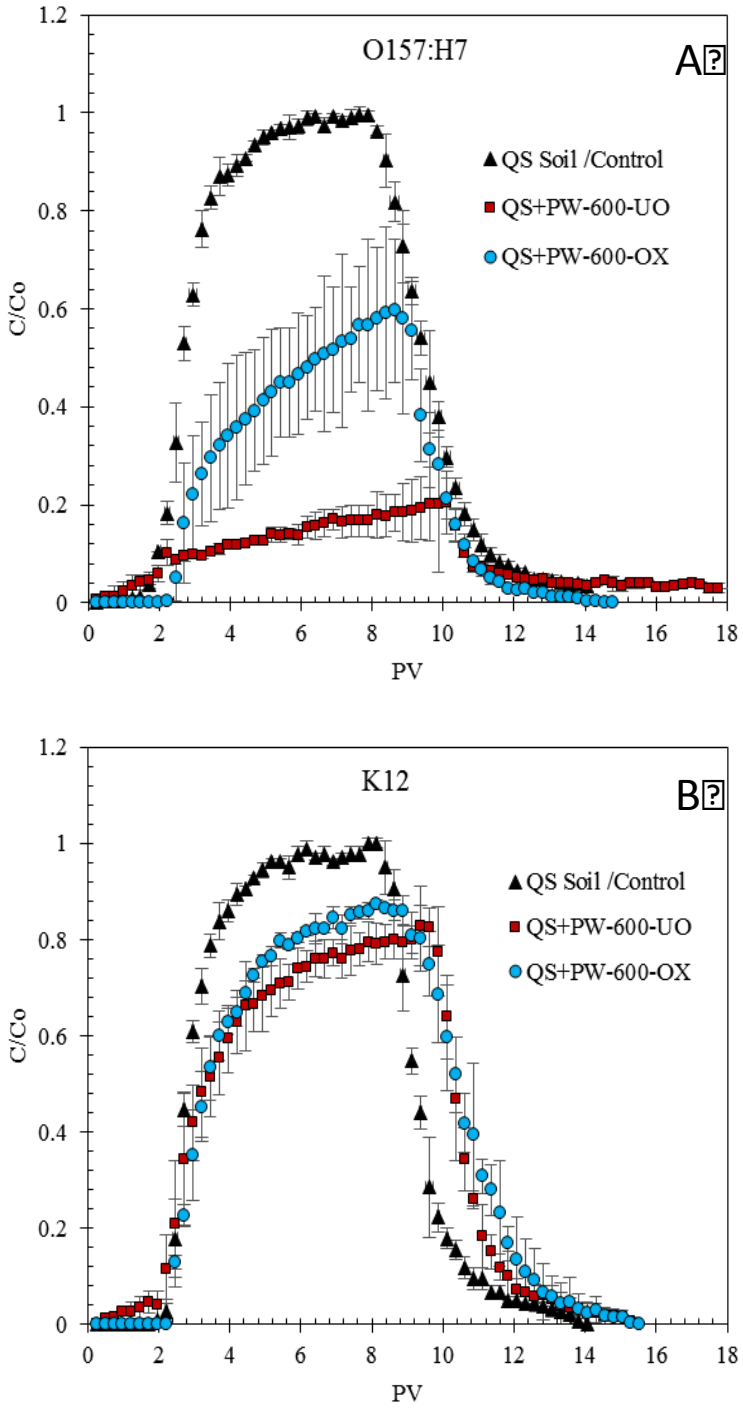

Figure 2.12: Breakthrough curves of *E. coli* (A) O157:H7, and (B) K12 for experiments in columns packed with oxidized and unoxidized PW600 biochars. Error bars indicate variation between triplicate experiments.

The transport capacities of *E. coli* K12 and O157:H7 were both reduced significantly in soils amended with non-oxidized biochar (Figure 2.12). However, the addition of oxidized biochar enhanced the transport of bacteria, indicating that air oxidation changes the surface properties of biochar and limits the efficiency of biochar in reducing *E. coli* transport. Regardless of oxidation status, high-temperature pine wood biochar (600°C) was the most effective biochar amendment in limiting the transport of bacteria through soil columns during this study. This is likely due to the high surface area and low negative surface charges comparable to biochar produced at 350°C. Moreover, *E. coli* O157:H7 was more sensitive to biochar addition than *E. coli* K12, likely due to differences in cell properties.

2.4 Proposed scheme for the integration of anaerobic digestion, nutrient recovery and biochar production

The results of this project, in combination with results obtained during the 2011–13 biennium (Frear et al., 2013) form the basis for a proposed new scheme to integrate pyrolysis and biochar production with anaerobic digestion (Figure 2.13). This scheme incorporates mineral deposition on the fiber surface during ammonia stripping, which reduces the overall complexity of integration while still allowing for the production of biochar with a high affinity towards phosphates.

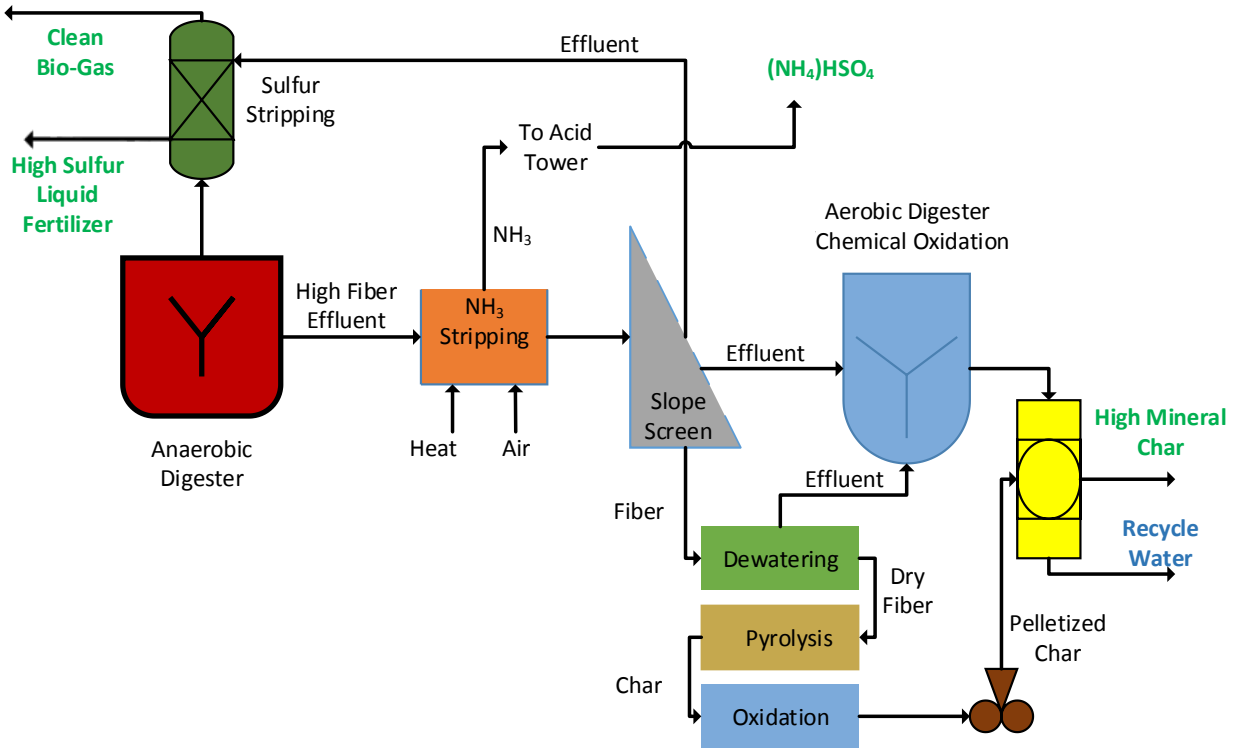

Figure 2.13: Proposed scheme for the integration of anaerobic digestion with nutrient recovery and biochar production.

2.4.1 Key considerations

Ammonia stripping of high fiber effluent: Previous studies have indicated that alkaline oxide/hydroxide precipitation on dairy fiber at elevated pH is a highly effective method to produce biochars with elevated phosphate adsorption capacity. The high mineral content of effluent water can provide an excellent source of alkalines. Previous results also indicated that the pH of the effluent during ammonia stripping reaches values as high as 9.7. Based on these parameters, it appears that performing ammonia stripping prior to fiber removal will allow the incorporation of alkaline precipitates on the fiber surface. Pyrolysis of this fiber will result in the stabilization of the mineral complexes, avoiding excessive solvation when the biochar comes in contact with liquid solutions.

Oxidation of the biochar: Previous studies have confirmed that oxidation by air at 250°C or by ozone rapidly increases the concentration of carboxylic groups at the surface of the biochar. These groups have been found to be responsible for elevated cation exchange capacity in near neutral solutions. Oxidation is an essential step for the production of biochars intended to control heavy metal cations in solution, though the interference from more prevalent ions such as sodium and calcium must be considered.

Aerobic digestion and chemical oxidation: Attempts to directly filter effluent water have indicated that the high carbon content and fine particles of the effluent rapidly saturate and plug biochar-based filters. Oxidation of these residual carbon species increases filter life and assists in the degradation and removal of potentially hazardous organics.

Use of a biochar–sand bed: Biochar-based filters tend to get compacted in filter set up, due to their high friability and water-holding capacity. This reduces their hydraulic conductivity and results in significant pressure losses. Briquetting or pelletization will help minimize this effect, however inclusion of sand is strongly recommended to minimize the effects of compaction and channeling within the filter.

2.5 Conclusions

The results from this project emphasize the importance of production conditions and secondary treatments on the efficacy of biochar for specific tasks. Both pyrolysis temperature and initial feedstock play a critical role in the surface area and chemical properties of the biochar, as well as the recalcitrance of the final material. Production temperature has also been found to moderately affect hydrological properties when used as a soil amendment, as well as the CO_2 released from soil after treatment. High temperature biochars resulted in slightly higher available water capacity, and a lower amendment rate to minimize CO_2 losses from soil. Untreated biochars were not found to significantly alter leaching of N or P from a mixed compost–biochar column. However, batch adsorption studies using biochar containing a calcium precipitate on the surface showed significant reductions in phosphate concentrations in AD effluent. Secondary oxidation has been found to strongly affect the transport of microbial species through a biochar–soil column. Oxidation increased the transport of a pathogenic strand of E. coli (O157:H7) due to reduced interaction of this gram negative strain with the negatively charged surface of the

biochar. This study highlights the requirements for specific material applications and associated design parameters for successful adoption of biochar-based materials.

2.6 References

Abit, S.M., Bolster, C.H., Cai, P., Walker, S.L. 2012. Influence of feedstock and pyrolysis temperature of biochar amendments on transport of *Escherichia coli* in saturated and unsaturated soil. Environmental Science and Technology 46(15), 8097-8105.

Agyei, N., Strydom, C., Potgieter, J. 2000. An investigation of phosphate ion adsorption from aqueous solution by fly ash and slag. Cement and Concrete Research 30(5), 823-826.

Agyei, N.M., Strydom, C., Potgieter, J. 2002. The removal of phosphate ions from aqueous solution by fly ash, slag, ordinary Portland cement and related blends. Cement and Concrete Research 32(12), 1889-1897.

Basso, A.S., Miguez, F.E., Laird, D.A., Horton, R., Westgate, M. 2013. Assessing potential of biochar for increasing water-holding capacity of sandy soils. GCB Bioenergy 5(2), 132-143.

Brennan, A., Jimnez, E.M., Puschenreiter,M., Alburquerque, J.A., Switzer, C. 2014. Effects of biochar amendment on root traits and contaminant availability of maize plants in a copper and arsenic impacted soil. Plant Soil 379, 351–360.

Chiang, H.-L., Huang, C.P., Chiang, P.C. 2002. The surface characteristics of activated carbon as affected by ozone and alkaline treatment. Chemosphere 47(3), 257-265.

Clough, T.J., Condron, L.M., Kammann, C., Müller, C. 2013. A review of biochar and soil nitrogen dynamics. Agronomy 3, 275–293.

Crombie K., Mašek O., Sohi S.P., Brownsort P., Cross A. 2013. The effect of pyrolysis conditions on biochar stability as determined by three methods. GCB Bioenergy 5, 122–31. doi:10.1111/gcbb.12030.

Ecology, 2012. Stormwater Management Manual for WesternWashington. Washington State Department of Ecology, Publication Number 12-10-030. Olympia, WA.

Frear, C., Kennedy, N., Zhao, Q., Liu, J., Zhao, B., Ma, J., Yu, L., Bule, M., Chen, S., Gao, A., Garcia-Perez, M., Smith M., Suliman, W., Pang, C., Kantor, S., Yorgey, G., Kruger, C. 2013. Anaerobic digestion-related research and development summary for WSU ARC/WSDA Appendix A Funds, 2011-2013. Washington State Department of Agriculture, Olympia, WA.

Granatstein, D., Kruger, C., Collins, H., Garcia-Perez, M., Yoder, J. 2009. Use of biochar from the pyrolysis of waste organic material as a soil amendment. Final Project Report, Vol. 09-07-062, Center for Sustaining Agriculture and Natural Resources, Washington State University. Wenatchee, pp. 168.

Hipple, K.W. 2012. Washington Soil Atlas. National Resource Conservation Service, U.S. Department of Agriculture. 121 pp. Available at http://www.nrcs.usda.gov/Internet/FSE_DOCUMENTS/nrcs144p2_034094.pdf.

Iqbal, H., Garcia-Perez, M., Flury, M. 2015. Effect of biochar on leaching of organic carbon, nitrogen, and phosphorus from compost in bioretention systems. Science of the Total Environment 521-522, 37-45.

Knowles, O.A., Robinson, B.H., Contangelo, A., Clucas, L. 2011. Biochar for themitigation of nitrate leaching from soil amended with biosolids. Science of the Total Environment 409, 3206–3210.

Lehmann, J. 2007. Bio-energy in the black. Frontiers in Ecology and the Environment 5(7), 381-387.

Lehmann, J., Gaunt, J., Rondon, M. 2006. Bio-char sequestration in terrestrial ecosystems–a review. Mitigation and Adaptation Strategies for Global Change 11(2), 395-419.

Lehmann, J., Joseph, S. 2009. Biochar for environmental management: An introduction, in: Lehmann, J., Joseph, S. (Eds.), Biochar for Environmental Management: Science and Technology. Earthscan, Washington DC, pp. 1-9.

Lehmann, J., Pereira da Silva, J., Jr., Steiner, C., Nehls, T., Zech, W., Glaser, B. 2003. Nutrient availability and leaching in an archaeological Anthrosol and a Ferralsol of the Central Amazon basin: fertilizer, manure and charcoal amendments. Plant and Soil 249(2), 343-357.

Lu, S., Bai, S., Zhu, L., Shan, H. 2009. Removal mechanism of phosphate from aqueous solution by fly ash. Journal of Hazardous Materials 161(1), 95-101.

Maia, C., Beata, M., Etelvino N. 2011. Advances in Biochar Research in Brazil.

Meng, J., Feng, X., Dai, Z., Liu, X., Wu, J., Xu, J. 2014. Adsorption characteristics of Cu(II) from aqueous solution onto biochar derived from swine manure. Environmental Science and Pollution Research 21, 7035–7046.

Namasivayam, C., Sangeetha, D. 2004. Equilibrium and kinetic studies of adsorption of phosphate onto ZnCl2 activated coir pith carbon. Journal of Colloid and Interface Science 280(2), 359-365.

Novak, J.M., Busscher, W.J., Laird, D.L., Ahmedna, M., Watts, D.W., Niandou, M.A.S. 2009. Impact of biochar amendment on fertility of a southeastern Coastal Plain soil. Soil Science 174(2), 105-112.

Oguz, E. 2005. Sorption of phosphate from solid/liquid interface by fly ash. Colloids and Surfaces A: Physicochemical and Engineering Aspects 262(1), 113-117.

Park, S.-J., Jin, S.-Y. 2005. Effect of ozone treatment on ammonia removal of activated carbons. Journal of Colloid and Interface Science 286(1), 417-419.

Prost, K., Borchard, N., Siemens, J., Kautz, T., Sequaris, J.-M., Möller, A., Amelung,W. 2013. Biochar affected by compostingwith farmyardmanure. Journal of Environmental Quality 42, 164–172.

Quyn, D.M., Wu, H., Hayashi, J.-i., Li, C.-Z. 2003. Volatilisation and catalytic effects of alkali and alkaline earth metallic species during the pyrolysis and gasification of Victorian brown coal. Part IV. Catalytic effects of NaCl and ion-exchangeable Na in coal on char reactivity. Fuel 82(5), 587-593.

Ronsse F., van Hecke S., Dickinson D., Prins W. 2013. Production and characterization of slow pyrolysis biochar: influence of feedstock type and pyrolysis conditions. GCB Bioenergy 5, 104–15. doi:10.1111/gcbb.12018.

Seki, K. 2007. SWRC fit - a nonlinear fitting program with a water retention curve for soils having unimodal and bimodal pore structure. Hydrology and Earth Systems Science Discussions 4(1), 407-437.

Sika, M.P. 2012. Effect of biochar on chemistry, nutrient uptake and fertilizer mobility in sandy soil. Stellenbosch: Stellenbosch University.

Solomon, D., Lehmann, J., Thies, J., Schäfer, T., Liang, B., Kinyangi, J., Neves, E., Petersen, J., Luizão, F., Skjemstad, J. 2007. Molecular signature and sources of biochemical recalcitrance of organic C in Amazonian Dark Earths. Geochimica et Cosmochimica Acta 71(9), 2285-2298.

Song W., Guo M. 2012. Quality variations of poultry litter biochar generated at different pyrolysis temperatures. Journal of Analytical and Applied Pyrolysis 94, 138–45. doi:10.1016/j.jaap.2011.11.018.

Spokas, K., Reicosky, D. 2009. Impacts of sixteen different biochars on soil greenhouse gas production. Annals of Environmental Science 3, 179-193.

Spokas, K.A., Cantrell, K.B., Novak, J.M., Archer, D.W., Ippolito, J.A., Collins, H.P., Boateng, A.A., Lima, I.M., Lamb, M.C., McAloon, A.J., Lentz, R.D., Nichols, K.A. 2012. Biochar: A aynthesis of its agronomic impact beyond carbon sequestration. Journal of Environmental Quality 41(4), 973-989.

Sposito, G. 2008. The Chemistry of Soils. 2nd Ed. Oxford University Press, New York, NY.

Thomazini, A., Spokas, K., Hall, K., Ippolito, J., Lentz, R., Novak, J. 2015. GHG impacts of biochar: Predictability for the same biochar. Agriculture, Ecosystems and Environment 207, 183-191.

Uzoma, K., Inoue, M., Andry, H., Zahoor, A., Nishihara, E. 2011. Influence of biochar application on sandy soil hydraulic properties and nutrient retention. Journal of Food, Agriculture and Environment 9(3&4), 1137-1143.

Valdes, H., Sanchez-Polo, M., Rivera-Utrilla, J., Zaror, C.A. 2002. Effect of ozone treatment on surface properties of activated carbon. Langmuir 18(6), 2111-2116.

van Genuchten, M.T. 1980. A closed-form equation for predicting the hydraulic conductivity of unsaturated soils. Soil Science Society of America Journal 44(5), 892-898.
Wang, L., Xu, S., Li, J. 2011. Effects of phosphate on the transport of *Escherichia coli* O157:H7 in saturated quartz sand. Environmental Science and Technology 45(22), 9566-9573.
Xue, Y., Hou, H., Zhu, S. 2009. Characteristics and mechanisms of phosphate adsorption onto basic oxygen furnace slag. Journal of Hazardous Materials 162(2), 973-980.
Yao, Y., Gao, B., Inyang, M., Zimmerman, A.R., Cao, X., Pullammanappallil, P., Yang, L. 2011. Removal of phosphate from aqueous solution by biochar derived from anaerobically digested sugar beet tailings. Journal of Hazardous Materials 190, 501-507.
Yip, K., Tian, F., Hayashi, J.-i., Wu, H. 2010. Effect of alkali and alkaline earth metallic species on biochar reactivity and syngas compositions during steam gasification. Energy and Fuels 24(1), 173-181.
Zimmerman, A.R., Gao, B., Ahn, M.-Y. 2011. Positive and negative carbon mineralization priming effects among a variety of biochar-amended soils. Soil Biology and Biochemistry 43(6), 1169-1179.

3. Gypsum as a Replacement for Sulfuric Acid in Bio-Ammonium Sulfate Production in Dairies

Quanbao Zhao and Craig Frear

3.1 Background

Production of ammonium sulfate from gypsum and gypsum-like materials is a known and well-studied process. However, its application within a biological ammonia stripping system to produce ammonium sulfate is problematic. A scientific and engineering study is needed to adapt known aspects of the reaction to this particular situation, and to specify the appropriate system parameters. The development of a viable gypsum replacement to the present use of concentrated sulfuric acid has the potential for great savings, particularly in regard to operating cost and environmental sustainability, as well as the potential for organic certification. Chou et al. (1995, 2005) tested ammonium sulfate production with the gypsum produced from a flue gas desulfurization (FGD) process. Ammonium sulfate could be produced with up to 99% purity using available ammonium carbonate and FGD. However, this or any other system must be adapted to the specific challenges of the situation here, including low solubility of gypsum, the presence of ammonium and carbon dioxide components as separate gases (as opposed to being already produced as ammonium carbonate), low NH_3 concentration in the ammonia stripping gas stream, and the corresponding separation of the products.

The aim of this proof-of-concept project was to explore mechanisms to overcome the specific challenges to the production of ammonium sulfate using gypsum. Researchers at Washington State University (WSU) collaborated with colleagues at Illinois State University (ISU) carrying out similar experiments. Given the interest in scaling such ammonium sulfate production up to a commercial scale, an additional collaboration with an industry partner, DVO Incorporated, allowed testing of experimental approaches at a larger scale.

3.2 Methods

3.2.1 Experimental scale

Ammonia gas was obtained by pumping air (800-1,000 mL min^{-1}) through 10% ammonium hydroxide solution, producing an ammonia gas stream with a concentration of approximately 8,000 ppm (Figure 3.1). A multi-channel peristaltic pump was used for stripping the ammonia, as well as for adding air to the gas stream to dilute the ammonia concentration. The carbon dioxide (CO_2) gas was released from a CO_2 gas cylinder, and the flow rate (0-400 mL min^{-1}) was controlled by a flow meter (Figure 3.1). Diluting air (800-1,000 mL min^{-1}) was pumped into a vessel of water to gain moisture, to avoid taking moisture out of the gypsum solutions. The resulting gas stream produced within the mixing chamber flowed through two reactors—R1 and then R2—that contained 150 mL of saturated gypsum solution each. The gas stream then flowed

through to reactor R3, which consisted of 150 mL of 10% sulfuric acid solution to trap the remaining ammonia gas (Figure 3.1). The total gas flow rate was 1.0 L min^{-1}, and the CO_2 flow rate was originally held constant at 0.10 L min^{-1}. Twenty percent more gypsum was added than the theoretical requirement for 40% ammonium sulfate production. The experiment was conducted at room temperature: 20°C.

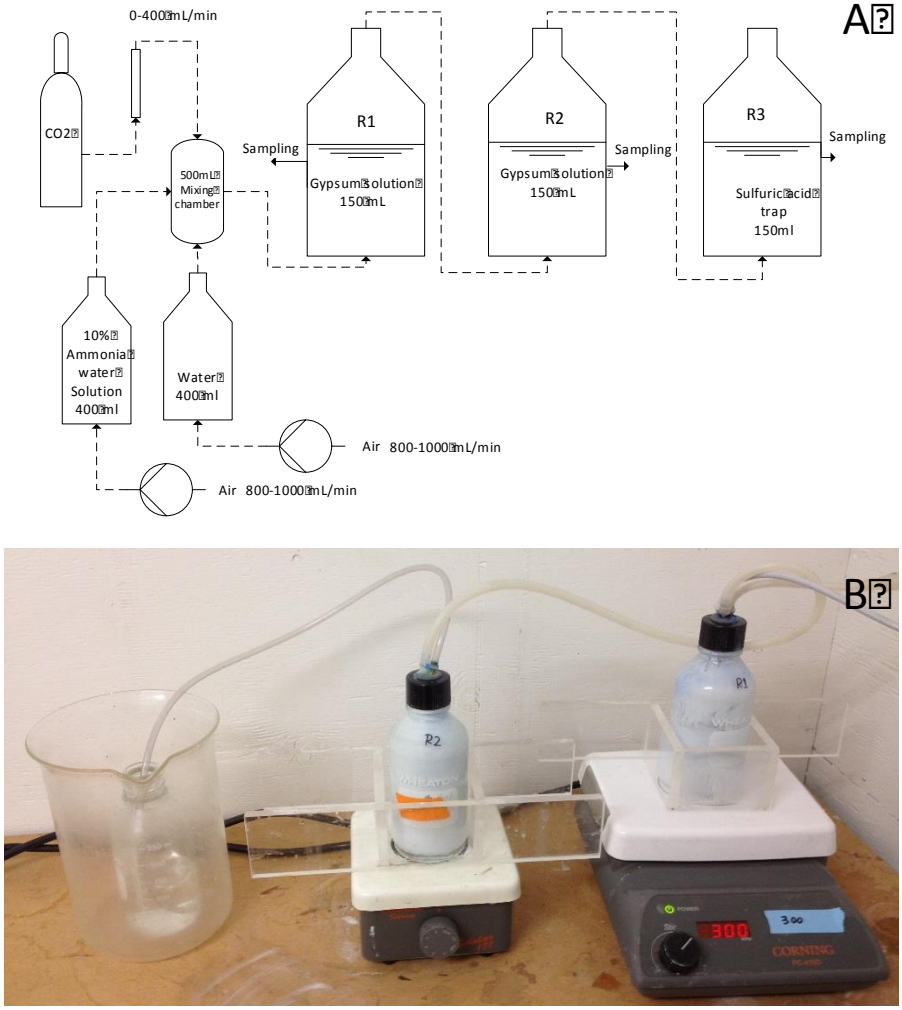

Figure 3.1: Experimental setup: (A) flow chart; (B) the reactors: R1, R2, and R3.

3.2.2 Industry scale-up

After consultation with WSU and ISU, industry partner DVO Incorporated (Chilton WI) completed scale-up tests, attempting to determine whether production of saturated levels of ammonium sulfate solution could in fact be achieved using typical ammonia stripping concentration of gases and stoichiometric levels of gypsum. The experiment was conducted at a scale of 25 L (Figure 3.2).

Figure 3.2: Scale-up apparatus.

3.3 Results and discussion

3.3.1 Experimental scale

During the experiment the total ammonia-N concentration (TAN) increased slowly to 5.6% by mass after 24 hours of reaction in R1 (Figure 3.3A). In R2 the TAN level was only 0.7% after 24 hours reaction. R1 captured the majority of the ammonia, with only a small portion of ammonia passing through R1. The majority of what passed through was later captured by R2, leaving no unreacted ammonia within the R3 acid trap. The pH increased in both reactors during the

reaction, as excess ammonia in the reactor increased (Figure 3.3B). The pH increased from 7.32 to 9.0 for R1, and to 8.2 for R2 after 24 hours reaction. The pH in R3 did not change much (Figure 3.3B).

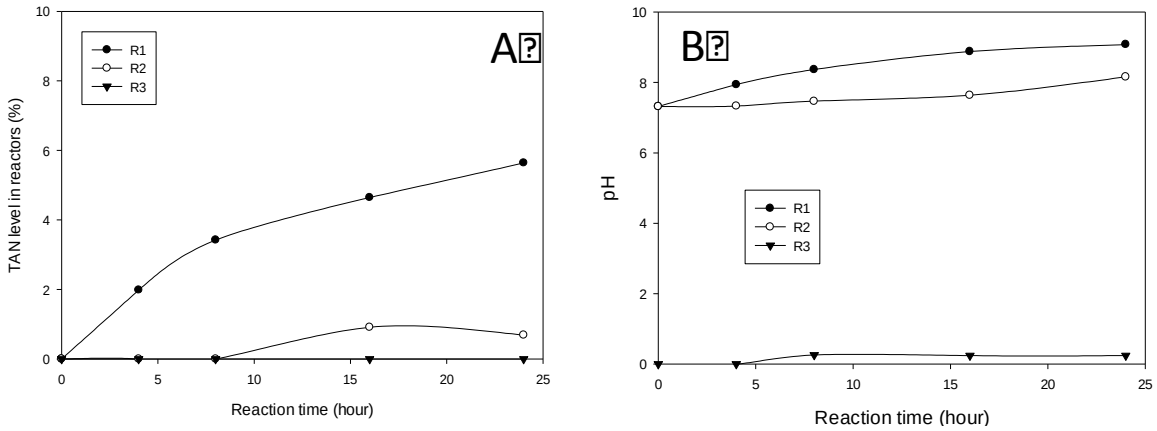

Figure 3.3: TAN (A) and pH (B) in the reactors with premixed ammonia gas and CO_2.

During the experiment it was noted that both the mixing chamber and the mixed gas inlet tubing to R1 contained solid ammonium bicarbonate, which eventually constrained the gas flow (Figure 3.4). To solve these problems of clogging and ammonia loss due to the formation of ammonium bicarbonate, the pre-mixing chamber was removed. After removing the pre-mixing chamber and directly injecting ammonia gas and CO_2 gas into R1, the production rate of ammonium sulfate increased. The TAN concentration reached the highest level of 9.5% after 12 hours reaction (Figure 3.5A). This level of TAN is higher than that of saturated ammonium sulfate (approximately 8%), which suggests that other forms of ammonium salt were produced, likely ammonium bicarbonate. After 12 hours reaction, solid ammonium bicarbonate was formed in the pipeline between R1 and R2, which supports the hypothesis that ammonium bicarbonate was formed in R1. A portion of the ammonia was not captured by R1, but was later captured by R2. Little ammonia was released from R2 until the TAN concentration in R2 was over 5%. As before, the pH increased in both reactors during the reaction (Figure 3.5B). The pH increased from 7.32 to 8.6 for R1, and to 8.0 for R2 after 24 hours reaction. The pH increase in R3 was very small, as little ammonia went in to R3 until the end of the reaction (Figure 3.5B).

Colleagues at ISU completed similar experimental trials. Full details of their results will be submitted soon to a peer-reviewed journal for publication. However, highlights of their results are:

- Saturated solutions of ammonium sulfate (approximately 40% ammonium sulfate) could be produced from gypsum reactions using ammonia and CO_2 concentrations similar to commercial-scale production of these gases.
- The rate of production could be enhanced if the concentration of ammonia was held constant to that produced at commercial-scale ammonia stripping facilities (approximately 1%) while CO_2 concentrations were allowed to increase considerably. Twelve percent appears to be the point at which performance started to level off somewhat. Higher concentrations of CO_2 are presumably feasible through the use of

engine exhaust or gas stripping streams, although additional testing is required to validate these assumptions.

- Ammonia concentrations above what would be expected from a saturated ammonium sulfate solution were also consistently seen, but further analysis did not confirm the existence of ammonium carbonate. This analysis instead appeared to show the presence of dissolved ammonium.

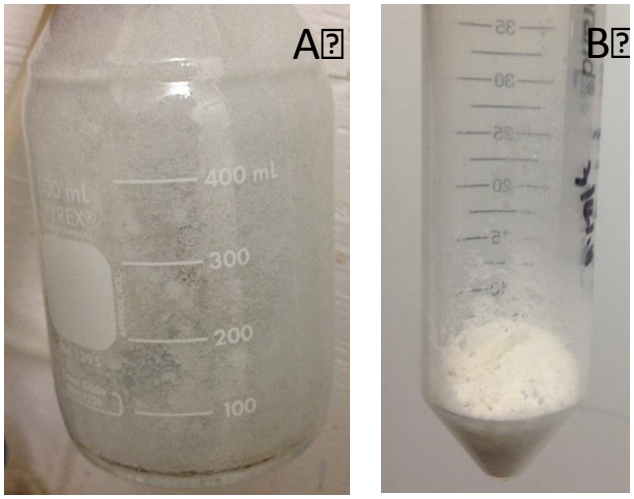

Figure 3.4: Ammonium bicarbonate production (A) inside the mixing chamber; (B) collected from the tubing.

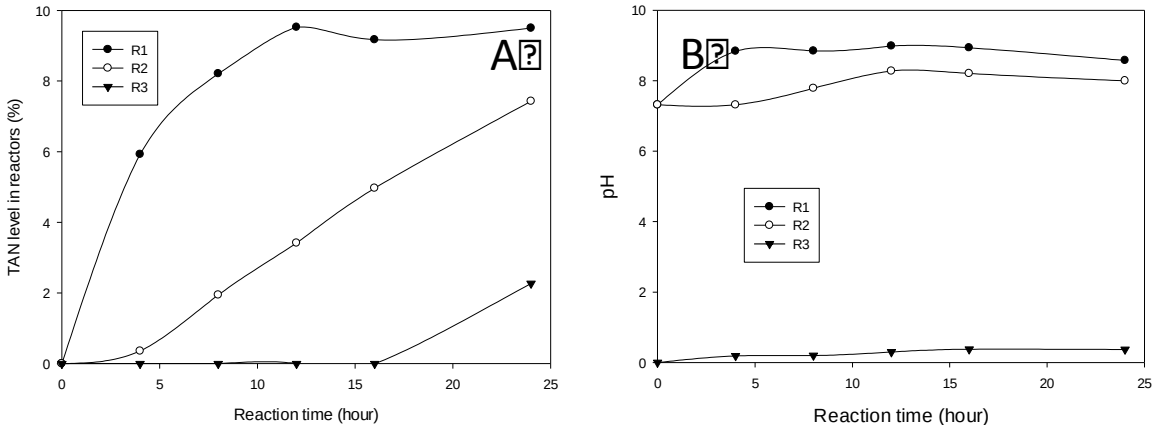

Figure 3.5: TAN (A) and pH (B) in the reactors without premixing of ammonia and CO_2.

3.3.2 Industry scale-up

The results of the scaled-up experiment were similar to the laboratory studies described above, confirming the potential for achieving ammonium sulfate saturation, and highlighting the need for higher concentrations of CO_2. A procedure for settling and subsequent washing allowed for

an effective separation of the ammonium sulfate solution produced from the additional insoluble calcium carbonate solids.

3.4 Conclusions

Several conclusions can be drawn from this set of experiments.

- Reacting gypsum slurry with ammonia and CO_2 gases can achieve desired levels of saturated ammonium sulfate. However, the concentration of both gases in these initial trials was higher than is presently being produced within farm-scale ammonia stripping systems. *Further study is therefore required to evaluate the system and its ability to produce saturated levels of ammonium sulfate at or near existing commercial concentrations of the gases.*
- The results from ISU and additional experimentation with zero inputs of CO_2 (results not shown) suggest that a preferred process is one that utilizes higher concentrations of CO_2. This gas is essential in helping increase gypsum solubility by liberating calcium ions from gypsum. *Further experimentation is needed to validate the optimal CO_2 concentration required. Levels of CO_2 above those produced by the ammonia stripping system could be supplied by engine exhaust.*
- While concerns arose about ammonium bicarbonate production within this experiment, which was conducted at 20°C, the ammonia stripping process can also produce ammonia and CO_2 at temperatures as high as 50°C. At this temperature, the ammonium bicarbonate will disassociate, reducing concerns about clogging. *On the other hand, data from this set of experiments showed that an intriguing alternative production system could be the production of ammonium bicarbonate, rather than using gypsum to directly produce ammonium sulfate. The ammonium bicarbonate could later be used in multiple ways, including to produce ammonium sulfate, aqua, or for direct use as fertilizer.*

Although the reaction with gypsum has been shown to be viable, industry partners are concerned with the high capital and operating costs the process would incur, as well as with the lengthy reaction time when compared to the use of sulfuric acid. Commercialization is therefore on hold pending an economic analysis, and comparison with other means of producing ammonium sulfate for organic certification, such as using organic acids.

3.5 References

Chou, M.I.M., Bruinius, J.A., Li, Y.C. 1995. Manufacture of ammonium sulfate fertilizer from FGD-gypsum. Preprints of Papers, American Chemical Society, Division of Fuel Chemistry 40 (CONF-950801).

Chou, M.I.M., Bruinius, J.A., Benig, V., Chou, S.F.J., Carty, R.H. 2005. Producing ammonium sulfate from flue gas desulfurization by-products. Energy Sources 27(11), 1061-1071.

4. Expansion and Scale-Up of Hydrogen Sulfide Scrubbing Using Bubble Column and High pH Ammonia-Removed Effluent

Nick Kennedy, Quanbao Zhao, and Craig Frear

4.1 Background

Biogas derived from the anaerobic digestion (AD) of dairy manure consists of methane (CH_4; 55–65%), as well as contaminants such as carbon dioxide (CO_2; 30–45%) and low concentrations of hydrogen sulfide (H_2S; 300–4,500 ppm) (Liebrand and Ling, 2009). Without pretreatment, these contaminants limit the use of the resultant biogas to feed combined heat and power (CHP) systems on-site. Multiple economic assessments have suggested that a higher value use of this biogas is possible by either removing these contaminants and thereby meeting natural gas regulations, or by purifying and compressing the biogas for use as a vehicle fuel (Coppedge et al., 2012). Numerous upgrading techniques were developed to simultaneously remove CO_2 and H_2S from biogas, including physical and physico-chemical absorption in organic and inorganic solvents (Ryckebosch et al., 2011) and pressure swing adsorption (PSA) (Ryckebosch et al., 2011).

Unfortunately, the costs associated with the chemical absorbents and the uptake of CO_2 (due to its higher concentration in the biogas) increase the overall cost of biogas upgrading. The multiple units of operations needed for the upgrading of biogas are often too expensive for them to be adopted on a small- to large-scale farm. Therefore, reductions in the construction, operation or maintenance costs of this process could provide dairy digester operators with a more feasible way to upgrade biogas to higher value products (Regenis, 2014, personal communication).

In previous Appendix A-funded research (2011–13), proof-of-concept work was completed that evaluated the use of ammonia-stripped, high pH effluent as media for selectively scrubbing H_2S from raw biogas (Kennedy et al., 2013, 2015). That study showed that 95% of H_2S could be scrubbed from biogas using only high pH ammonia-stripped effluent operated within a simple, process-controlled bubble column. While the concept has important and vital implications to AD, the costs of operating engine and generator sets and of producing renewable natural gas fuel remain obstacles to its adoption. A couple of important science and engineering studies are needed so as to both scale-up the selective H_2S scrubbing process and expand the simple H_2S scrubbing concept to sequential scrubbing of CO_2 as well. These two studies were investigated from 2013 to 2014, and are the focus of this chapter.

4.2 Methods

4.2.1 Scale-up scrubbing system

Washington State University (WSU) scientists and project engineers from the patent licensee (DVO, Incorporated, Chilton WI) designed and constructed a two-tower bubble column for commercial-scale testing (Figure 4.1). The design built upon previous work completed by Kennedy et al. (2015), where manipulating bubbles and reactor height were shown to selectively favor the absorption of H_2S over CO_2 in a bubble column reactor. Testing was completed at a 2,200-cow dairy near Chilton, WI outfitted with an anaerobic digester and an ammonia stripping system.

Figure 4.1: Two-stage H_2S scrubbing system designed and constructed by DVO, Inc.

4.2.1.1 Design concept

In this two-stage system, high pH effluent (around pH 9.3) discharged from the dairy's ammonia stripping system was sent at 35–45 gallons per minute (top green pipe, Figure 4.1) to Tank 1 (T1) and Tank 2 (T2) at a 50:50 ratio. The pressure of T1 and T2 was 1.2–1.5 PSI and 0.5 PSI, respectively. Approximately 1,240 gallons of effluent (around 48 cm above installed diffusers) was continually contained within T1. The two tanks were connected to each other via a U-shaped green pipe at the bottom of the reactors (Figure 4.1) to allow effluent from T1 to pump to T2, creating a continually flowing system from digester to T1 to T2. 3,000 gallons (around 101 cm above installed diffusers) was continually contained within T2. Raw biogas (above 2,000 ppm) was fed at approximately 250 cubic feet per minute to T1 (not shown in picture) utilizing a

Rotron blower. Large bubble diffusers (120 Flex Cap) were utilized in both T1 and T2 to distribute biogas as bubbles through the high pH effluent. After the raw biogas was sent to T1, partially cleaned biogas was sent through T2 to achieve higher purification. Due to the physico-chemical reaction between both H_2S and CO_2 and the high pH effluent, a reduced pH effluent resulted in T2. To compensate for this, a portion of the effluent going to T2 was sent back to the ammonia stripping system to increase the pH of the effluent. This recharged effluent was returned to T2 to provide a better purification media for biogas coming off of T1. The portion of spent effluent from T2 was sent to a lagoon for storage, and ultimately used for land application. Hydrogen sulfide, CH_4, CO_2, and pH were monitored prior to entering T1, from T1 to T2, and after leaving T2.

4.2.2 Expansion to sequential scrubbing of carbon dioxide

Based on the results of the commercial-scale testing of H_2S and CO_2 removal from raw biogas, scientists at WSU and project engineers at DVO, Inc. decided to evaluate the possibility of expanding the two-staged system to a three-staged or more system to increase the removal efficiency of CO_2. If complete removal of H_2S and CO_2 can be achieved, the cleaned biogas could be compressed and utilized as a transportation fuel.

A three-stage process that utilizes two regeneration steps (aeration) and three absorption steps (bubble columns with biogas passing through effluent) was designed (Figure 4.2). This concept is slightly different from pressure swing absorption (PSA) in that the commercial process does have a regeneration step—some spent effluent is sent back to the nutrient recovery system where it is mixed and re-aerated—but the three-stage process described here would include dedicated aeration units in series with absorption units.

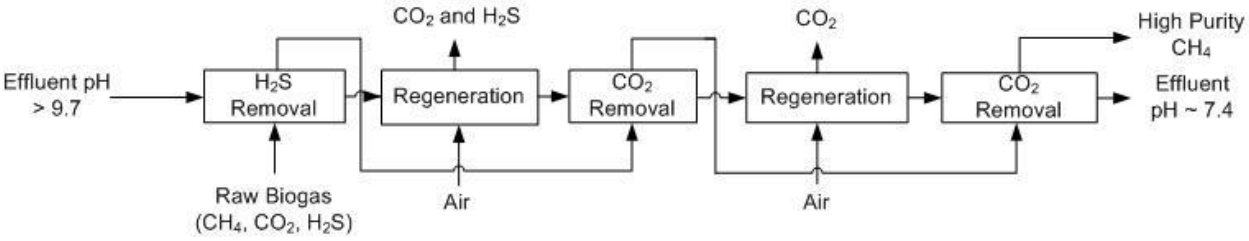

Figure 4.2: Schematic of the stepwise removal of both H_2S and CO_2 from biogas.

Hydrogen sulfide (and some CO_2) is expected to be completely removed within the primary absorption unit (labeled as H_2S removal), since it has a lower initial concentration in the biogas than CO_2, and thus is easier to completely remove. The subsequent step is a regeneration step to raise the pH back to above 9 by eliminating both H_2S and CO_2 from the effluent. This step is achieved by re-aerating the effluent. After the pH has reached around 9, the effluent is sent into another reactor where CO_2 can be removed from the biogas that has already been purified of H_2S. This process can be repeated as many times as needed to completely remove CO_2 from the biogas, resulting in a product with high purity of CH_4, which can be used in a variety of ways including electricity, pipeline-quality gas, or as a vehicle fuel. Lab-scale testing was conducted at WSU to determine whether or not the pH of the effluent could be continually raised to levels high enough to continue the absorption process downstream.

4.2.2.1 Lab-scale testing

A bubble column reactor was constructed for lab-scale testing (Figure 4.3). A lab-scale ammonia stripping process (4 in Figure 4.3) allows for the effluent coming off the digester to be used as an absorbent of H_2S and CO_2 from biogas. The bubble column was constructed out of acrylic plastic with a diameter of 0.072 m. Biogas containing concentrations of CH_4, CO_2, and H_2S typical in biogas produced at agriculture digesters (66%, 34%, and 0.08%, respectively) was obtained from Ideal Specialty Gas and Analytical Services (Houston TX) and stored in a gas cylinder for use during experiments (5 in Figure 4.3). The pretreated and now alkaline effluent was sent to the top of the bubble column reactor to a height of 1.25 L by a peristaltic pump (Cole Parmer, Vernon Hills, IL). Once the effluent was completely pumped into the bubble column, the inlet was shut off to ensure no biogas or liquid would escape during the experiment. The biogas flowed into the reactor at the bottom of the bubble column through an air-stone and was controlled by a rotameter (Cole-Parmer, IL) (2 in Figure 4.3). The air-stone had a pore diameter of 140 μm. The air-stone dimensions were 3.8 x 3.8 cm and it was constructed out of glass-bonded silica (Aquatic Ecosystems, Apopka, Florida). The bubble column was operated in batch mode with respect to the liquid and continuously with respect to the gas phase. A separate tank of air was included and connected to the same tube as the biogas tank (Figure 4.3). This air tank was used to regenerate the effluent once the effluent had become completely saturated in H_2S and CO_2. A three-way valve was incorporated to be able to shut off the biogas from entering the bubble column and allow air to enter, and *vice versa*.

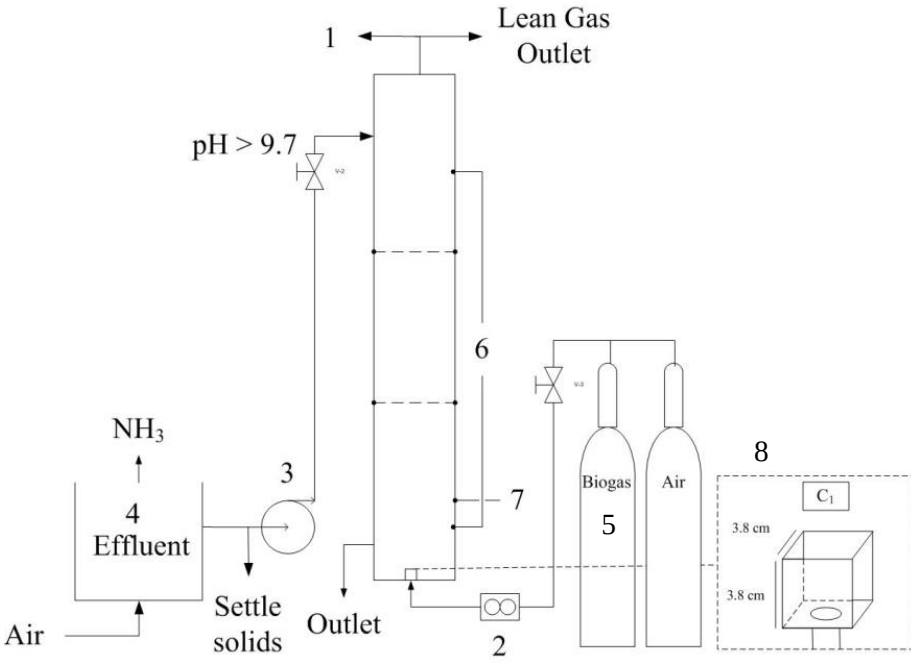

Figure 4.3: Schematic of the lab-scale bubble column reactor used for the purification of the biogas and the regeneration of the effluent.

The gas coming out of the reactor during the regeneration process was tested periodically with a gas chromatographer (Shimadzu Corp., Japan, Model GC-2014) equipped with a flame ionization detector and length of 30 m × id 0.25 mm × film thickness 0.25 μm capillary column

(HP-INNOWax, Agilent Technologies, Palo Alto, CA), to determine how much CH_4, CO_2 and H_2S is eliminated from the effluent once it became saturated during the biogas purification step. Liquid samples were taken periodically to test the total inorganic carbon in the effluent (results not shown).

4.2.2.2 Experiment #1 – Regeneration of the effluent

An initial experiment was performed to confirm that it was possible to regenerate the effluent by re-aerating it after the initial purification step. This test was performed at 16°C because it has been shown that H_2S selectivity is enhanced at a lower temperature (Wallin and Olausson, 1993). In both this and the coupled purification and regeneration steps experiment (described below) the bubble column was operated at ambient pressure.

4.2.2.3 Experiment #2 – Coupled purification and regeneration steps

After the concept of regenerating the effluent was evaluated, the researchers wanted to test if coupled steps of purification, regeneration, purification, regeneration, and purification were possible. A higher temperature (35°C) was used during the regeneration step to see if this step could be shortened. One idea was to use a heat exchanger before the initial purification process to lower the temperature of the effluent coming off the ammonia stripping process (more selectivity for H_2S removal), and then use another heat exchanger to heat up the effluent coming out of the purification process (faster regeneration). The operating conditions for this experiment were the following:

- biogas flow rate: 0.5 L min^{-1},
- airflow rate: 2.5 L min^{-1},
- effluent volume: 1.25 L.

Included in this test was the ammonia stripping process of fresh AD effluent, post-fiber separation.

4.3 Results and discussion

4.3.1 Scale-up scrubbing system

4.3.1.1 Hydrogen sulfide removal

Biogas coming off the digester (purple line in Figure 4.4) was at an H_2S concentration above 2,000 ppm, which is typical for dairy digesters. After reacting with the high pH effluent in T1, the concentration was drastically reduced (red line in Figure 4.4), achieving roughly 70% removal efficiency. Higher removal efficiency was achieved after this partially cleaned biogas was fed to T2. Biogas leaving the system from T2 achieved greater than 95% removal efficiency throughout the entire 7-hour trial (green line in Figure 4.4). Spikes in H_2S from the digester were seen throughout the experiment, bumping the initial H_2S entering T1 to as high as 3,000 ppm. However, due to the two-staged system, only minimal changes in the removal efficiency of the biogas coming off of T2 resulted, showcasing the resistant ability of this two-staged bubble column system. Spikes in H_2S are common due to the complexity of the AD process and due to changes in feedstock entering the anaerobic digester.

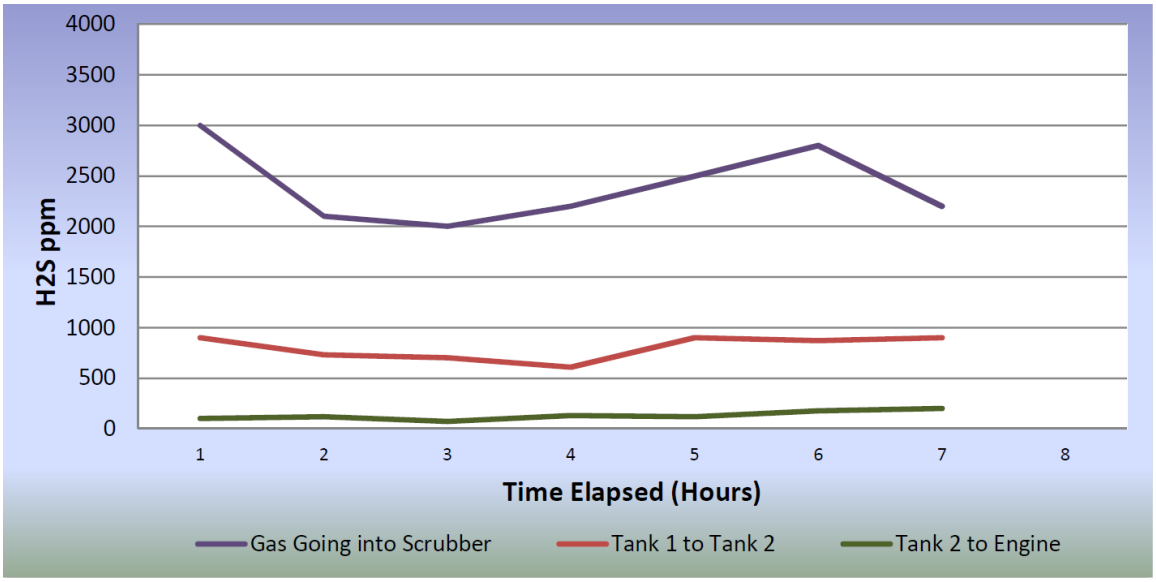

Figure 4.4: Hydrogen sulfide removal at different stages during the purification process (results from one of the tests performed by project engineers at DVO, Inc.).

The phenomena behind this absorption process are the physico-chemical reactions taking place between H_2S and the high pH effluent. Due to the effluent coming off the ammonia stripping system with a pH above 9, H_2S at the surface of the biogas bubbles instantaneously disassociated into HS^- and H^+ upon contact with the effluent, resulting in its removal from the gaseous stream. However, there is only so much absorption that can occur and at some point equilibrium was reached between the gas and the liquid, resulting in the inability of the effluent to absorb more H_2S. This is why this two-staged countercurrent system is unique. By splitting the effluent 50:50 from the nutrient recovery (NR) system to T1 and T2 and sending in recharged effluent from the NR system to T2, H_2S absorption was able to resume when the partially cleaned biogas was sent from T1 to T2, resulting in a higher removal efficiency (above 95%).

However, competition is taking place between H_2S and CO_2. Under these conditions, carbon dioxide will also move from gaseous form ($CO_{2aqeous}$) to its liquid forms ($CO_{2liquid}$, H_2CO_3, HCO_3^-, and CO_3^{2-}). All of these reactions produce a hydronium ion (H^+), adversely affecting the pH of the effluent. For H_2S to disassociate into the effluent, a high pH is crucial. This is where another unique component of this two-stage system came into play. Studies by Kennedy et al. (2015) showed that large bubbles and minimal height increased the removal efficiency of H_2S. These parameters decreased the absorption of CO_2, thus creating conditions to selectively remove H_2S over CO_2. Engineers at DVO Inc. utilized this same technique in the two-staged system by using diffusers to produce large bubbles and having T1 at a lower height than T2. In addition, pressurizing T1 should further promote selectivity, since Henry's law is a function of pressure and temperature. Any increase in pressure will enhance the movement of H_2S from gas to liquid if a flux promoting this movement exists. During contact in T1, H_2S was preferentially scrubbed, as demonstrated by the fact that the percent reduction in H_2S concentration from digester to T1 is much higher compared to the reduction from T1 to T2. However, due to the rather low ability to enhance selectivity in a bubble column when compared to other absorption apparatuses (e.g. packed-bed), complete removal of H_2S was not achieved in the first stage. The addition of another reactor (T2) with partially alkaline effluent was able to remove the rest of the

H_2S in the biogas coming out of T1, and achieve substantially higher removal efficiency compared to the majority of the absorption apparatuses on the market today.

4.3.1.2 Reduction in pH

In addition to monitoring the H_2S concentration at different stages of the purification unit, the pH was also monitored. Effluent coming from the ammonia stripping system had a pH around 9.3 before entering T1 (purple line in Figure 4.5). As effluent left T1, the effluent's pH dropped to around 8.3, with similar results seen as the effluent left T2 (red and green lines, respectively, in Figure 4.5). The pH leaving T2 was consistently below 8.5 throughout the entire experiment. The pH decreased in T1 and T2 due to the physico-chemical reactions taking place between H_2S and the effluent and CO_2 and the effluent, albeit CO_2 no doubt had a higher effect on pH due to its higher concentration in raw biogas (CO_2 was roughly 37%, compared to H_2S at 2,000 to 3,000 ppm). It is worth noting that the pH never dropped down to as low as the results of experiments by Kennedy et al. (2015). The ability for the effluent to remain slightly alkaline even after biogas passed through T2 leads to the speculation that effluent coming out of T2 could be utilized to further remove CO_2 contained within the purified biogas.

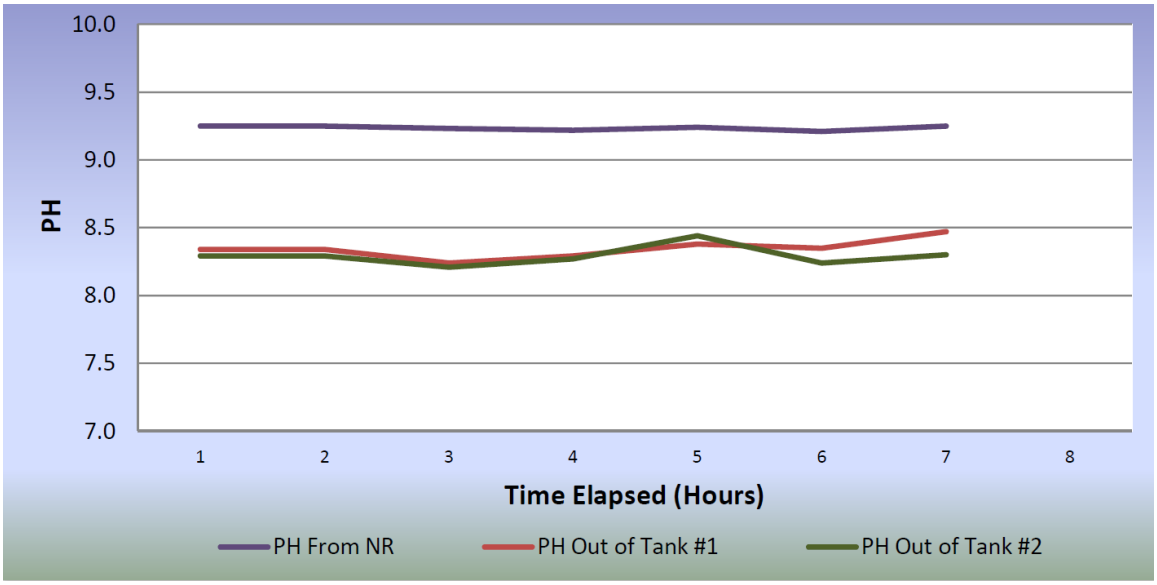

Figure 4.5: pH at different stages of the purification unit (DVO, Inc.).

4.3.1.3 Methane removal

The CH_4 concentration was also monitored throughout the purification process. Initially, the percentage of CH_4 coming off of the digester into T1 was rather low, at around 54%. The purification unit was able to boost this percentage significantly during the first hour of operation due to the removal of CO_2 and H_2S (Figure 4.6). The percentage of CH_4 coming out of T2 at the beginning of operation was boosted to around 61%, an increase of roughly 13% (Figure 4.6). Thereafter, levels tapered off and became relatively stable throughout the experiment, resulting in a boost of around 5%. Methane does react with alkaline absorbents but is quite resistant to absorption due to its Henry's constant, which is why chemical absorption is such a highly utilized biogas upgrading technique in the industry (e.g. water scrubbing). However, some CH_4 absorption will occur and must be weighed against the benefits of creating a biogas free of H_2S.

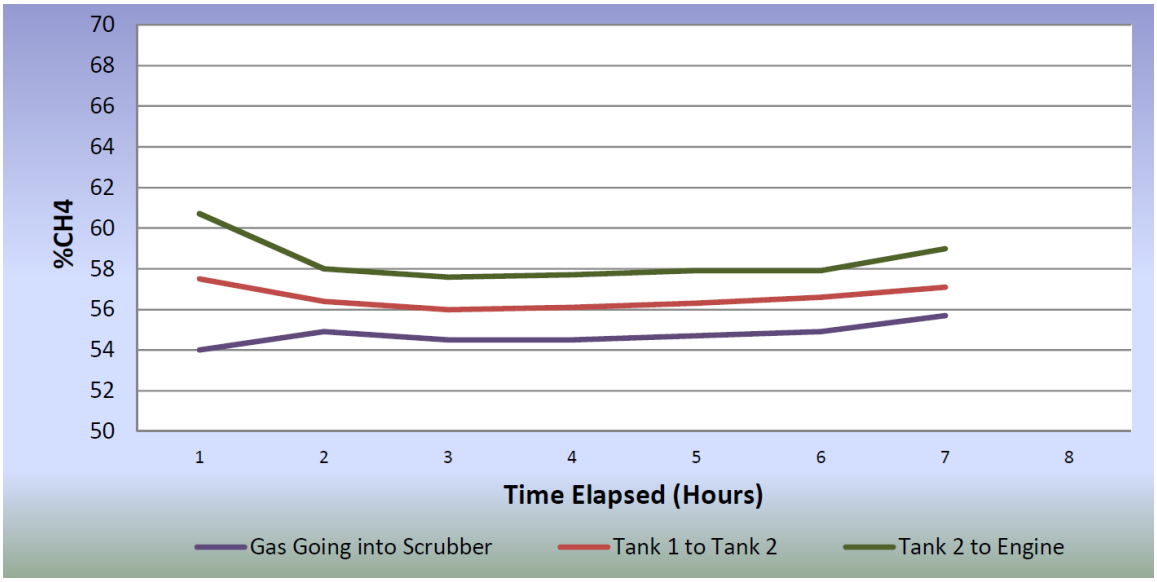

Figure 4.6: Percent change in CH_4 concentration at different stages of the purification unit (DVO, Inc.).

4.3.1.4 Carbon dioxide removal

The CO_2 concentration was monitored at various stages of the purification unit (Figure 4.7). As the biogas was fed into T1, a slight drop in CO_2 resulted due to the physico-chemical reaction taking place between CO_2 and the high pH effluent. At each stage in the purification unit, the CO_2 removal efficiency improved, with the highest removal efficiency seen after biogas was bubbled through T2 (around a 10% increase in CO2 removal) (Figure 4.7). As mentioned earlier,

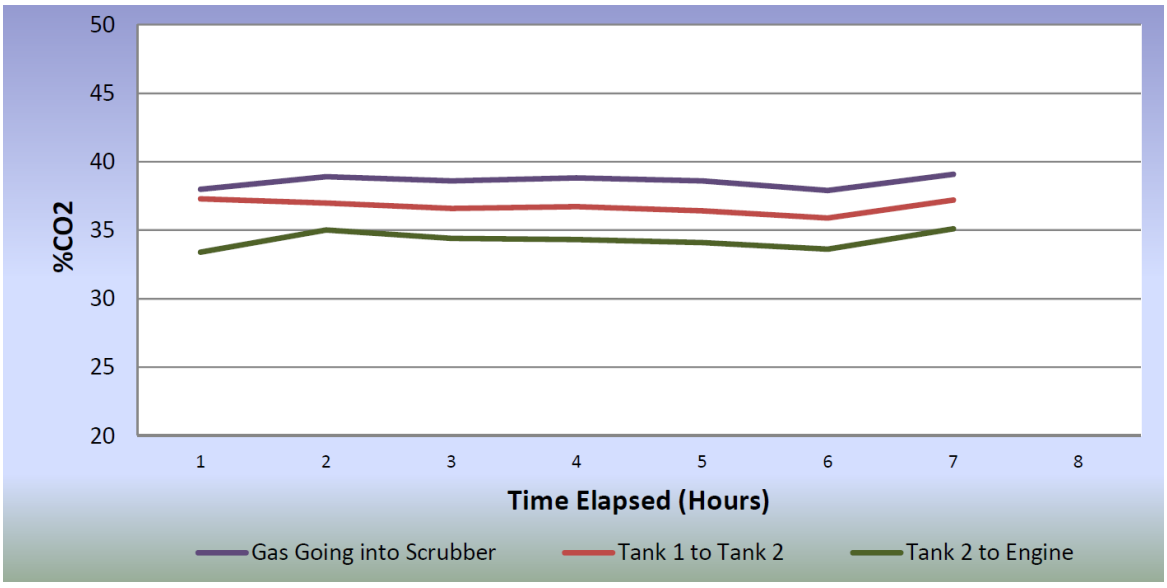

Figure 4.7: Percent change in CO_2 concentration at different stages of the purification unit (DVO, Inc.).

the effluent remained slightly alkaline after leaving T2. Therefore, additional bubble columns could be added to the back end of the main two-stage scrubber to further decrease the CO_2 content. This addition must be weighed, of course, against any added capital and energy costs. Though the multi-step design of the scrubber might seem overly complex—particularly if an added step is included at the end—it is not uncommon to have multiple steps in biogas purification units, as is exemplified in PSA.

4.3.2 Expansion to sequential scrubbing of carbon dioxide

4.3.2.1 Experiment #1 – Regeneration of the effluent

At the beginning of the biogas purification process, the pH increased from around 9.5 to 9.8 (Figure 4.8), as the pH probe needed to reach steady state. After a steady pH had been obtained, the biogas was injected into the bubble column through the air-stone. A fast drop of pH resulted from the absorption of H_2S and CO_2 in the purification step (Figure 4.8). This process took about 30 minutes to complete before a steady pH of around 7.4 was achieved (Figure 4.8).

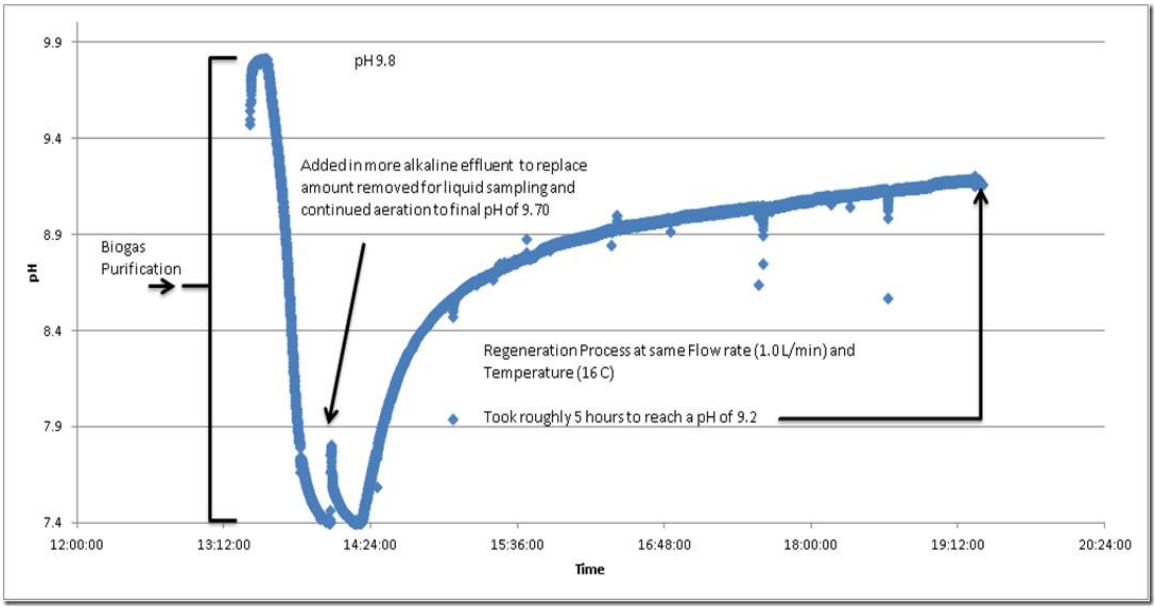

Figure 4.8: The effect the two-step biogas purification and regeneration process had on the effluent pH.

It is important to note that H_2S re-entered the gaseous phase once the pH dropped below 9, which led to the removal efficiency of H_2S suffering from the extended purification process. Liquid samples were taken to test the total inorganic carbon in the effluent (results not shown). Therefore, fresh pretreated effluent was added into the bubble column to reach the same liquid volume used, which is why there was a slight increase in pH after a pH of 7.4 was reached. Thereafter, biogas was injected into the effluent until the pH dropped back to 7.4. Once this pH was obtained, the biogas was shut off and the air tank was injected into the bubble column at 1.0 L min^{-1} through the air-stone to see if CO_2 and H_2S could be eliminated from the effluent, and if the pH of the effluent could be raised, for continued use as an absorbent of CO_2.

The pH began to increase after the air tank was injected into the bubble column, and after about 5 hours of aeration the pH was about 9.2 (Figure 4.8). This step took about 10 times longer than the purification process. It is worth noting that since the H_2S was completely removed from the biogas in the first step, and since CO_2 can be absorbed at a lower pH level, such a high pH did not need to be achieved in the regeneration step. Targeting a somewhat lower pH would have drastically reduced the regeneration time. The temperature of the effluent is an important factor due to Henry's constant being a function of temperature and pressure. If the temperature had been higher, the solubility of the gases would have decreased. This should benefit the removal of CO_2 and H_2S during the regeneration step.

The gas coming out of the reactor during the regeneration process was tested periodically with a gas chromatograph to see how much CH_4, CO_2 and H_2S was eliminated from the effluent during the regeneration step. Initially, a significant quantity of CO_2 (0.05% of the concentration in the biogas) was eliminated from the effluent, which began to decrease in concentration thereafter (Figure 4.9). Even though it decreased over time, CO_2 continued to be eliminated throughout the regeneration experiment (Figure 4.9). And since CO_2 is slightly acidic, any amount that was eliminated from the effluent affected the pH of the effluent throughout the five-hour experiment (Figure 4.8).

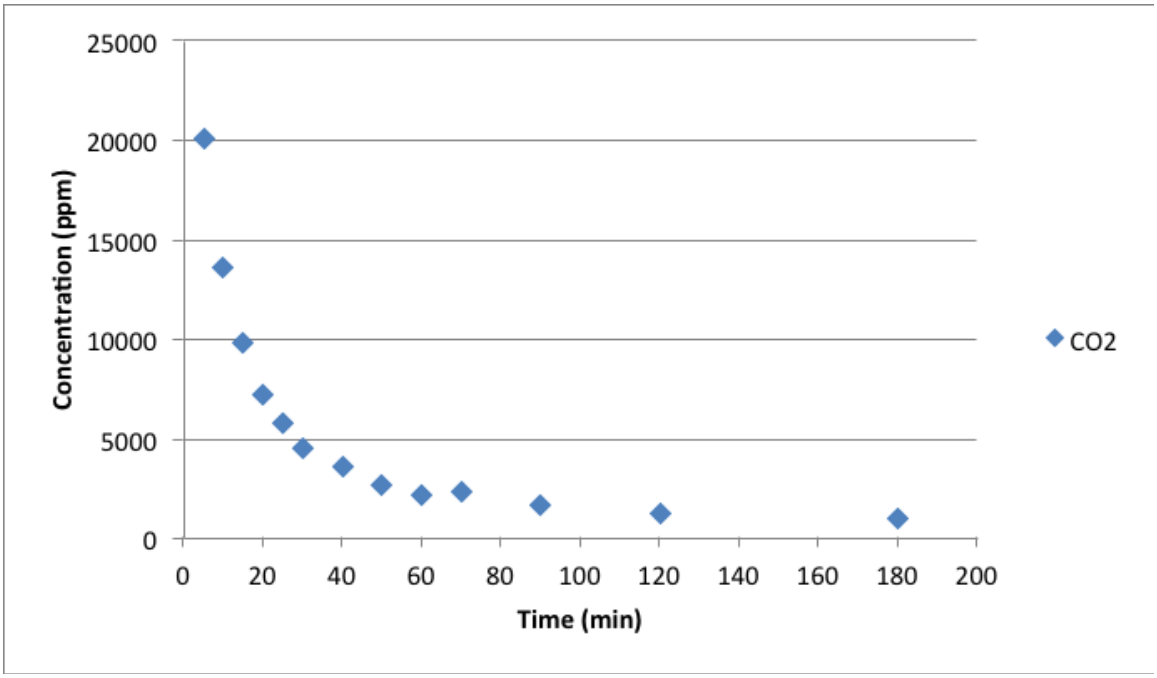

Figure 4.9: Concentration of CO_2 over time during the regeneration experiment.

A similar trend was found with the H_2S concentration profile (Figure 4.10). This trend, however, was not as consistent as the CO_2 trend (Figure 4.9), which could be due to a lack of precision on the gas chromatographer, or a variety of other reasons. Nonetheless, results show that, over time, H_2S was being eliminated as well (Figure 4.10), which effectively increased the pH of the

effluent. The highest concentration eliminated from the effluent was around 7 ppm (0.008% of the initial concentration in the biogas; Figure 4.10).

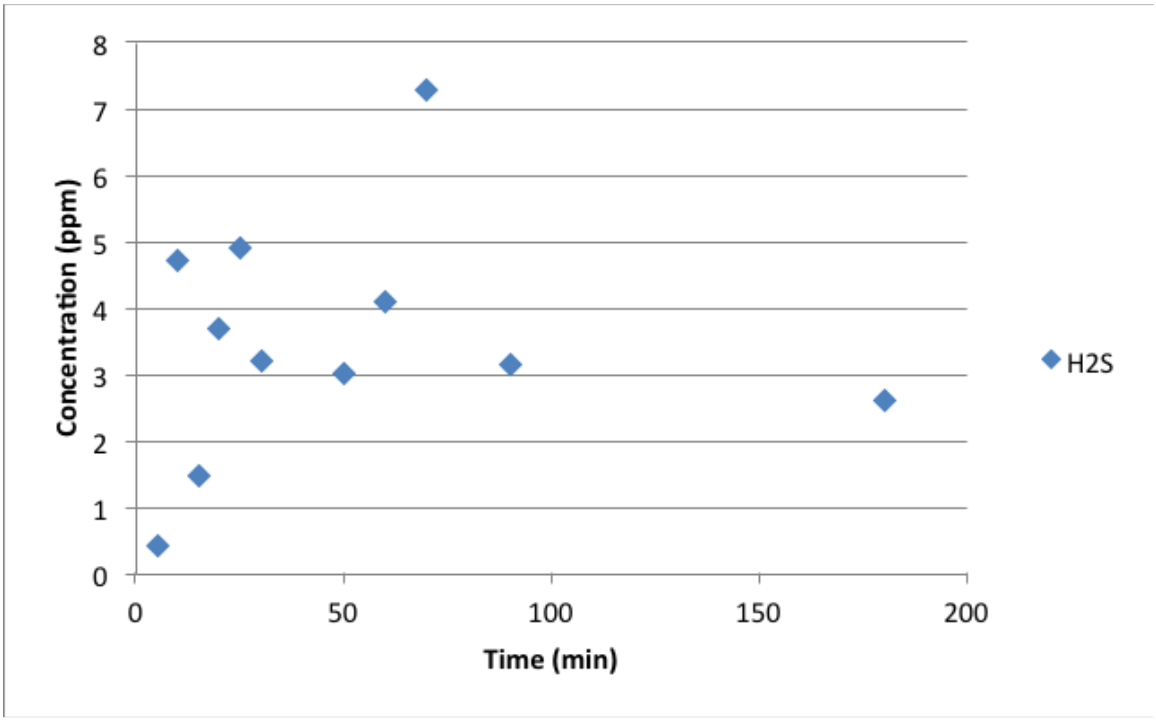

Figure 4.10: Concentration of H_2S over time during the regeneration experiment.

Methane is not as soluble as CO_2 and H_2S in liquid, and therefore should not absorb into the effluent. However, the researchers wanted to see how much CH_4 was eliminated during the regeneration process. The amount of CH_4 eliminated during the regeneration process was rather low: 0.008% after 1 minute, when compared with the initial concentration in the biogas, and after around 50 minutes it dropped to around 0 ppm (Figure 4.11). This CH_4 could be from the purification step (highly plausible) or could be supersaturated CH_4 from the AD process (not as plausible). Both could contribute, but if it were supersaturated CH_4 from the AD process it should have already been eliminated during the ammonia stripping process.

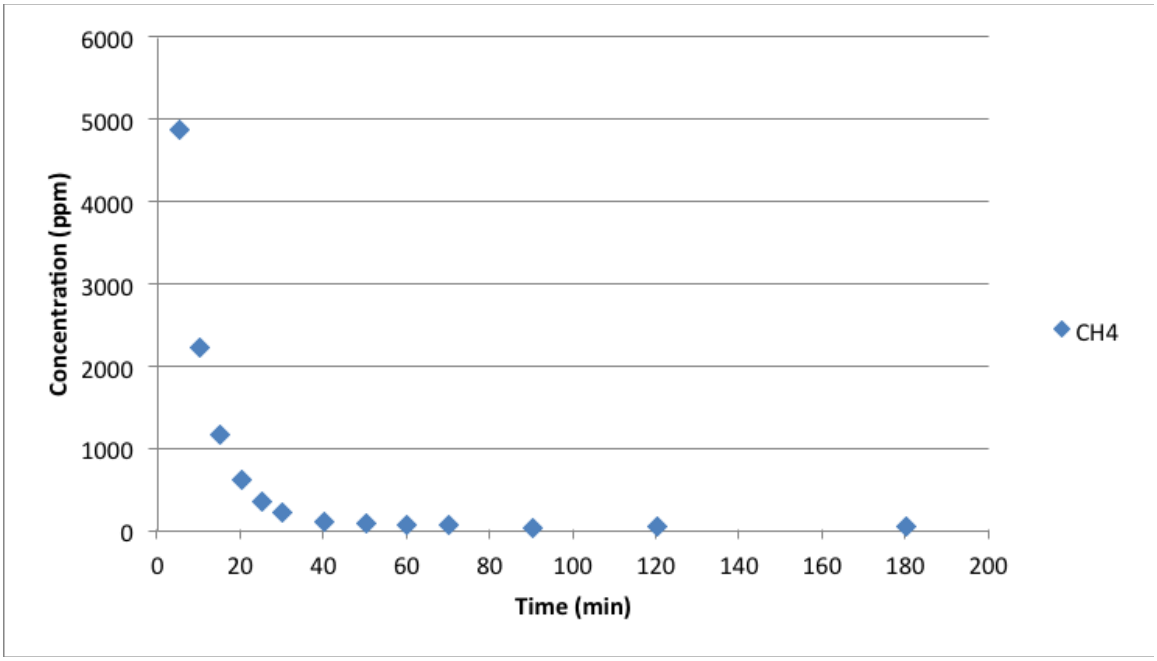

Figure 4.11: Concentration of CH_4 against time during regeneration experiment.

4.3.2.2 Experiment #2 – Coupled purification and regeneration steps

The ammonia stripping process took roughly 20 hours to reach a pH of around 9.2 (approximately 9.6 at adjusted lower temperature) (Figure 4.12). This was lower than the pH

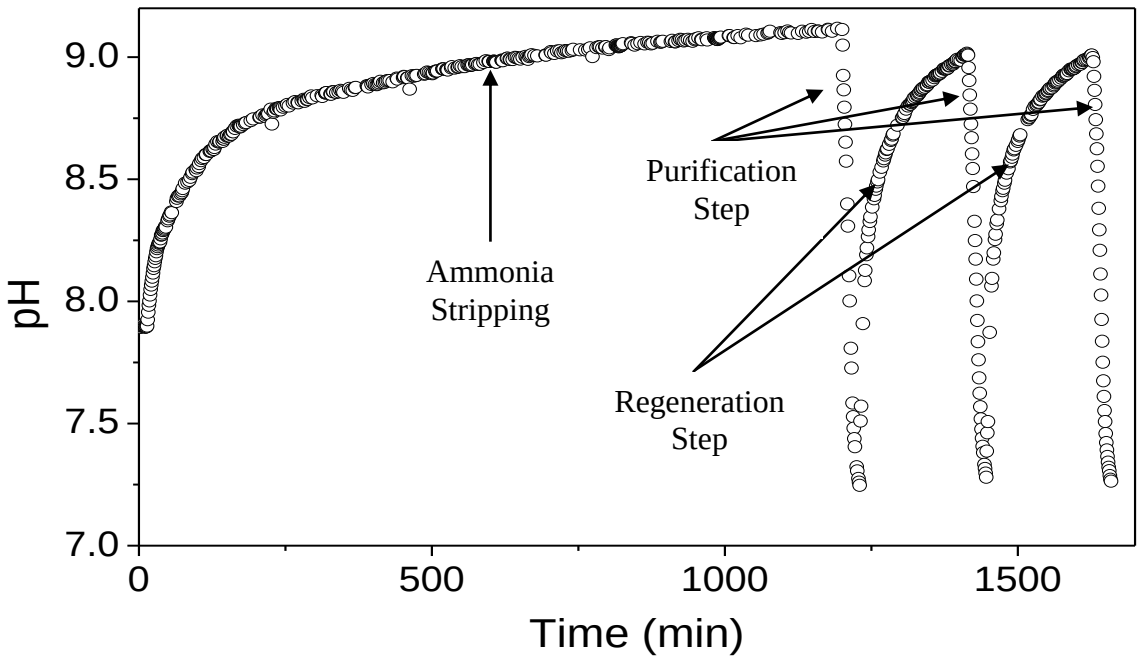

Figure 4.12: Fluctuation in pH with ammonia stripping and sequential regeneration and purification at 35°C.

achieved during experiment #1 due to the higher temperature of the effluent (35°C compared to l16°C). Thereafter, the air was shut off and the biogas was injected into the bubble column, which asted about 30 minutes before the pH leveled off at around 7.4 (Figure 4.12). After the pH stabilized, the biogas was shut off and the air was injected into the effluent, eliminating CO_2 and H_2S that was saturated in the effluent. This regeneration of the effluent raised the pH to around 9.0 and took around 3 hours to complete (Figure 4.12). This is much faster than the five hours it took in experiment #1, due to the higher temperature and higher flow rate used in this test. The biogas purification and regeneration process was performed again using the same effluent, and similar results were achieved. At the end of the coupled tests, a final purification step was performed to lower the pH of the effluent back to near neutrality, so as to mimic real-world application (i.e. stored in a lagoon and used as fertilizer).

Tail gas leaving the top of the system during the sequential regeneration and purification experiment was captured and evaluated to determine the extent to which the biogas could be purified of CO_2 using this methodology (Figure 4.13). Note that the three runs shown are not sequential: the biogas exiting run one was not sent through to run two and so on. Instead, original raw biogas—as defined by the gas cylinder used in the set-up—was used for each of the three runs.

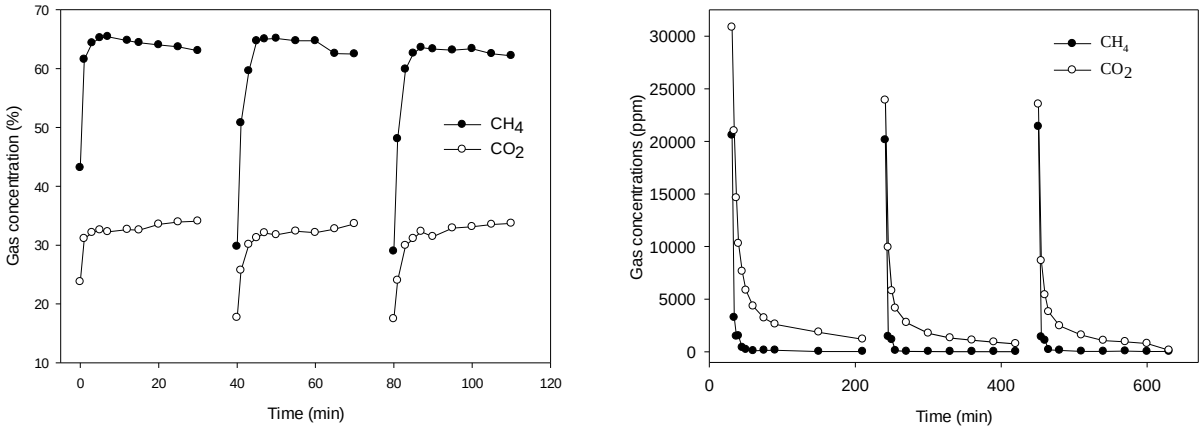

Figure 4.13: Component gas concentrations leaving the top of the apparatus after the gas purification processing (left panel), and after the effluent regeneration processing (right panel)—three separate runs.

There was no accumulation effect that continued to raise the CH_4 percentage and lower the CO_2 percentage (Figure 4.13). Future tests are needed to evaluate this, hopefully at larger scale, if the technology concept warrants it. Regardless, these results do show that by regenerating the AD effluent via three-hour, 35°C, air-stone aeration and achieving rises in pH, CO_2 (with some residual loss of CH_4) can be absorbed into solution and removed from the biogas.

Analysis of the area under the curves (Figure 4.13, left panel) using individual and average mass point analysis determines that, in *each individual step*, 10–25% of the CO_2 content can be removed from the raw biogas. This means that if a sequential approach could be completed, a series of four purification steps (with associated regeneration steps) could conceivably achieve

near 0% CO_2 content. The approximate amount of dissolved CH_4 lost during each individual purification process step was about 1%–2.5%. When expanded to four sequential operations, this could result in 4–10% loss of CH_4 to the solution and, ultimately, to the environment.

The gas component analysis of the regeneration step showed improved regeneration performance in the first of the three runs (Figure 4.13, right panel). This is due to the fact that prior to these three runs, a lengthy 24-hour ammonia stripping run was completed to remove ammonia, leaving a higher effluent pH for the succeeding first run. Subsequent runs (two and three) did not have this luxury. Regardless, the data show that the regeneration step resulted in immediate loss of some CH_4 and a considerable amount of CO_2 with continued release, albeit at lower values of CO_2 over the course of the three hours (Figure 4.13).

4.4 Conclusions

4.4.1 Bubble column scale-up for removal of hydrogen sulfide

Rapid movement from lab-scale to commercial-scale is rather rare in engineering. However, through a collaborative and interdisciplinary effort between scientists at WSU and project engineers at DVO, Inc., this purification concept was able to move from lab-scale to commercial-scale in under a year—an achievement in itself. Project engineers at DVO, Inc. were able to expand upon the lab-scale results obtained at WSU and push the envelope of this novel purification process by expanding the concept into a two-stage purification process. This innovative, two-stage bubble column reactor was able to utilize H_2S selectivity parameters discovered by scientists at WSU—column height and bubble size—and pressure to remove over 95% of the H_2S contained within the raw biogas that was produced at a 2,200-cow digester located in Chilton, WI. The absorption media used during experimentation was a high pH effluent produced as a byproduct from an ammonia stripping system, thus showcasing the integration of unit operations for more sustainable and economic use of byproducts. In addition to removing H_2S, some CO_2 was also removed, leading to a system that (a) strips and recovers ammonia gas from the manure, (b) scrubs the raw digester gas of nearly all H_2S, and (c) increases the methane concentration at the expense of some CO_2 removal.

The economic potential of the system is considerable. Manure laden with ammonia may well—under possible future regulation—warrant recovery and use. In addition, anaerobic digester economics are presently swinging the industry towards CNG business plans, which necessitate scrubbing of the biogas to high methane purity. Many of the existing commercial biogas scrubbing technologies are susceptible to H_2S corrosion, and therefore require separate H_2S scrubbing systems in addition to their CO_2 units. Use of such a simple H_2S scrubber in synergy with ammonia stripping could resolve these existing concerns, while also somewhat reducing the CO_2 mass in need of scrubbing. Commercial application is negatively impacted, however, by the need to link the technology with viable ammonia stripping units capable of supplying the required alkaline effluent. On-farm ammonia stripping systems are still uncertain in regard to their economic viability due to a combination of capital and operating costs and immature markets for the bio-derived ammonium fertilizers.

4.4.2 Sequential treatment for complete carbon dioxide removal

If complete CO_2 and H_2S removal can be achieved, this simple purification process can be used to upgrade biogas to CNG standards, a higher value use of biogas compared to electrical generation. This concept was tested and proved at the lab scale by performing a four-stage sequential purification and regeneration process. Nutrient recovery effluent was tested to see if a sequential biogas purification and regeneration process was feasible. Results showed that post-purification aeration could return effluent to alkaline conditions, thus allowing for continual biogas purification to remove CO_2 that could not be removed during the initial biogas purification step. Future tests at commercial scales are needed to determine the validity of this process. However, lab-scale experiments showed that a four-stage process should be able to completely remove H_2S and CO_2 from biogas.

The relative simplicity and low parasitic load of this system make it an ideal biogas purification process for digesters located on dairy operations where other purification processes—membrane separation, pressure swing adsorption, cryogenic separation—may be too expensive or labor intensive. However, the length of reaction, the reliance on suitable ammonia stripping effluent, and the relatively high potential for loss of methane are aspects that might negatively impact its commercialization.

4.5 References

Coppedge, B., Coppedge, G., Evans, D., Jensen, J., Kanoa, E., Scanlan, K., Scanlan, B., Weisberg, P., Frear, C. 2012. Renewable Natural Gas and Nutrient Recovery Feasibility For DeRuyter Dairy: An Anaerobic Digester Case Study For Alternative Offtake Markets and Remediation of Nutrient Loading Concerns Within The Region.

Kennedy, N., Zhao, Q., Jiang, A., Frear, C., Dvorak, S. 2013. Methods and apparatus for removal of H_2S and CO_2 from biogas. USPTO Application 20130309759. Publication date 11/21/13.

Kennedy, N., Zhao, Q., Ma, J., Chen, S., and Frear, C. 2015. The selective removal of H_2S over CO_2 from biogas in a bubble column using pretreated digester effluent. Separation and Purification Technology 144, 240-247.

Liebrand, C., Ling, K. 2009. Cooperative approaches for implementation of dairy manure digesters. USDA Rural Development. Washington, D.C., http://hdl.handle.net/10113/35107.

Ryckebosch, E., Drouillon, M., Vervaeren, H. 2011. Techniques for transformation of biogas to biomethane. Biomass and Bioenergy 35(5), 1633-1645.

Wallin, M.A.T.S., Olausson, S. 1993. Simultaneous absorption of H_2S and CO_2 into a solution of sodium carbonate. Chemical Engineering Communications 123(1), 43-59.

5. Improving Pretreatment Technologies of Manure Fiber and Crop Residues for Enhanced Methane Production

Ping Ai, Liang Yu, Dianlong Wang, and Shulin Chen

5.1 Background

Biogas is one of the most popular forms of renewable energy that can be produced from organic wastes. It is mainly produced from various agricultural residues such as wheat straw, corn stalks, and livestock manure (Li et al., 2015; Saady and Massé, 2015). To ensure the feedstock resources are adequate for biogas production, significant research has focused on enhancing the digestibility and improving the productivity of anaerobic digestion (AD) of lignocellulosic materials such as crop residues and manure fiber (Hendriks and Zeeman, 2009; Yue al., 2014).

Crop residue is one of the most abundant, low-cost, and renewable lignocellulosic materials in the world. It is made up of natural polymers that contain cellulose, hemicellulose and lignin (García et al., 2014). The use of crop residues as feedstock for an anaerobic digester could enhance the AD's profitability by producing more biogas (Li et al., 2015; Saady and Massé, 2015). Manure fiber is also a plentiful, and an important source of lignocellulose. The composition of manure fiber depends mainly on the animal feed. Several studies (Wen et al., 2004; Yue et al., 2010; Teater et al., 2011) have demonstrated the potential manure fiber has as a lignocellulose feedstock for the production of biofuels and value-added chemicals. The use of manure fiber for biogas production could also help avoid the environmental pollution caused by spills when manure is being stored, loaded, transported, or applied to the land.

The challenge for using crop residues or manure fiber in AD is the low digestibility of these materials. Many large-scale biogas plants that use lignocellulosic materials as feedstock have low efficiency and a long hydraulic retention time due to this difficulty in degradation. In particular, the crystalline structure of cellulose has been reported to limit the utilization of lignocellulose (Sun et al., 2007). Pretreatment of these materials is therefore needed to loosen the plant cell-wall structure and allow the enzymes or microbes to access and use the material during AD (Zhou et al., 2012; Martinez et al., 2005). Pretreatment is an important step in breaking down the chemical structure of the lignocellulose and enhancing the conversion efficiency of cellulose and hemicellulose to sugars. Furthermore, whether the pretreatments have different effects on different substrates is still uncertain.

Various pretreatment methods using ammonia, alkali, acid, and steam explosion have been studied (Bauer et al., 2014; Baboukani et al., 2012). Soaking in aqueous ammonia (SAA) has been shown to be an attractive pretreatment method, as it is effective in delignification as well as the swelling of biomass (Kim et al., 2008). Soaking aqueous ammonia at low temperature minimizes the interaction between the ammonia and the hemicellulose, which is retained within the solid structure. The retained xylan can then be hydrolyzed to fermentable pentose during the

AD, thus enhancing the conversion efficiency (Kim and Lee, 2007; Zuo et al., 2012). The delignification reaction that occurs in the alkaline hydrolysis results in an increase of the internal surface area, a decrease in the degree of polymerization, a decrease in crystallinity, the separation of structural linkages between lignin and carbohydrates, and the disruption of the lignin structure (Sun and Cheng, 2002).

Ozonation is traditionally used in advanced oxidation processes for wastewater, as well as for the reduction of sewage sludge (Cesaro and Belgiorno, 2013). Ozone pretreatment can be carried out at room temperature and pressure, and can be highly efficient at removing lignin. Recent research concluded that combining ozone and SAA treatments (ozone and soaking in aqueous ammonia, OSAA) offers a unique dual benefit, as it can produce hydrolysable biomass with a low lignin content through a low temperature and pressure process (Gao et al., 2012). The SAA treatment can only hydrolyze the lignin into the ammonia effluent, while OSAA can oxidize the lignin, producing small organic molecules in the hydrolysate (Li et al., 2010).

Past research on ozone and SAA pretreatment have not provided an explicit explanation for the synergistic effect of ozone and SAA on biogas production (Yu et al., 2014), nor has it explored these effects in different types of substrate such as crop residues and manure fiber. Therefore, there is still a need for studies to optimize the OSAA pretreatment parameters for anaerobic digestion with different types of lignocellulosic materials.

The objectives of this study were to (1) explore the mechanism by which the OSAA pretreatment of crop residue and manure fiber degrades the lignocellulosic materials, and (2) optimize the parameters of the OSAA pretreatment—including pretreatment time—for biomethane production.

5.2 Methods

5.2.1 Feedstock and inocula

The two feedstock studied were crop residues and manure fiber. Crop residues—or straw—were collected from fields in Pullman, WA. After collection, the straw was air dried, ground with a laboratory grinder and passed through a 2 mm aperture standard screen (Tyler Standard Screen Scale). The processed substrate was then sealed in plastic bags and stored at room temperature for further use. The total solid (TS) and volatile solid (VS) content of straw were 77.42% and 65.20%, respectively. It was composed of 37.46% cellulose, 31.70% hemicellulose, 2.96% lignin, and 3.93% ash. Manure fiber was obtained from a dairy farm in the same region. Inoculated sludge was taken from an anaerobic digester that had been operating for two years. The sludge had a concentration of 12.95 g L^{-1} TS (6.62g L^{-1} VS), and a pH of 7.8, and was used as inoculum for the anaerobic tests.

5.2.2 Pretreatment methods

Different groups of experiments were carried out, in which either the ozonolysis time was kept constant while the SAA time varied; or the SAA time was kept constant while the ozonolysis time varied (see details in section 5.2.5, below).

5.2.2.1 Ozone pretreatment procedure

The processed straw and dairy fiber samples (20 g) were adjusted for moisture (40%, w/w) and placed into an enclosed stainless steel reactor, with 1 cm bed height to ensure equal contact time between all particles with the ozone, and operated in a semi-continuous mode. The ozone, produced by an Ozone Generator manufactured by Pacific Ozone, CA, USA, was applied at a concentration of 35±5 mg L^{-1}, and at a flow rate of 10 g h^{-1}. The processed samples were then dried at 50°C and stored in a freezer for further analysis.

5.2.2.2 Soaking aqueous ammonia (SAA) pretreatment procedure

After the ozone pretreatment, the samples were pretreated by soaking in aqueous ammonia using 26-28% (w/w) ammonium hydroxide solution, with a solid-to-liquid ratio of 1:10, at 50°C for the time required according to the experimental design (see Experimental setup, below). After completion of the soaking, the AD fiber was separated from the liquid via vacuum filtration with a 0.1 mm mesh, and the filter cake was washed with 1 L distilled water to achieve a neutral pH. The processed samples were then dried again at 50°C.

5.2.3 Enzymatic hydrolysis tests

Samples containing 3 g of dry solid fiber pretreated with OSAA were mixed with 60 mL of an acetic acid-sodium acetate buffer (0.2 M, pH=4.8) in a 100 mL shake flask, achieving a dry matter concentration of 6.0%. 0.5 g mixed cellulases (β-glucanase ≥ 6×10^4 U, cellulose ≥ 600 U, and xylanase≥10×10^4 U from Imperial Jade Bio-Technology Co., Ltd) were added to each flask. During the enzymatic hydrolysis, the flasks were shaken at 150 rpm at 50°C for 60 hours. The amount of hydrolyzed sugars in aliquots extracted at 12, 24, 36, 48 and 60 hours was then determined using high performance liquid chromatography. All tests were conducted in duplicate. The mean value was then calculated.

5.2.4 Batch anaerobic fermentation tests

The batch anaerobic digestion was fulfilled using a 0.5 L reactor, with 15 g of dry processed materials used for each run. To avoid acidification, 1.5 g $NaHCO_3$ was added into the reactors. Deionized water was added to achieve a final total solids loading of 7%. All reactors were capped with rubber stoppers and put into a water bath at 37°C. Prior to the fermentation test, the reactors were flushed with nitrogen to remove oxygen from the headspace, to maintain an anaerobic environment. The biogas volume produced was determined by the drainage method, and the biogas was collected for the gas component analysis using a 1 mL plastic syringe. Biogas volume and composition were measured at 24-hour intervals. Liquid samples were taken at 3- to 4-day intervals, to measure volatile fatty acids and chemical oxygen demand. To minimize the effect of random errors, each run was duplicated and the average data are reported.

5.2.5 Experimental setup

The experimental activity was structured in two parts:

1) The first part was focused on the definition of the optimal pretreatment characteristics, based on how the sugar production and weight loss varied with treatment times. Only one feedstock was used in this first part: crop straw. The pretreatment conditions consisted of two groups: in the first group the ozone time was kept constant at 45 minutes, while the SAA time varied from 0 to 10 hours; in the second group the SAA time was kept constant

at 4 hours, while the ozone time varied from 0 to 75 minutes (Table 5.1). Straw samples used in each test had 10g TS.

Table 5.1: Soaking aqueous ammonia (SAA) and ozone time setup for pretreatment trials

Experimental batch No.	SAA experiments group						Ozone experiments group					
	1	2	3	4	5	6	7	8	9	10	11	12
SAA time (h)	0	2	4	6	8	10	4					
Ozone time (min)	45						0	15	30	45	60	75

2) The second part of the experimental activity dealt with the anaerobic digestion test, evaluating the effect of the different ozone and SAA pretreatments on biogas production. Processed crop straw and manure fiber were pretreated with different combinations of ozone and SAA time (Table 5.2), similar to what was described in the first part, above, and then used as substrates for anaerobic digestion. 30 g TS of raw material was used in the pretreatment procedure, and 15 g TS of the processed material was added to each anaerobic digestion.

Table 5.2: Pretreatment conditions for anaerobic digestion trials

Substrate	Pretreatment condition	SAA experiments group				Ozone experiments group			
		1	2	3	4	5	6	7	8
Crop straw	SAA time (h)	0	3	6	9	6			
	Ozone time (min)	90				0	45	90	135
Manure fiber	SAA time (h)	0	3	6	9	6			
	Ozone time (min)	90				0	45	90	135

5.2.6 Analytical methods

Total solids (TS), volatile solids (VS) and chemical oxygen demand were measured using standard methods (APHA, 1998). The samples were heated overnight at 105°C to determine TS, and ashed at 550°C to determine VS. The pH was measured using a pH meter (FE20 LAB). The composition of the fiber was measured using the Laboratory Analytical Procedure (LAP) developed by the National Renewable Energy Laboratory (NREL) (Sluiter et al., 2005).

Glucose and xylose in the hydrolysate were analyzed using an Agilent1220 chromatography system equipped with a 4.6×150 mm Zorbax carbohydrate analytical column (Agilent, Palo Alto, California, USA), and a refractive index detector. The mobile phase was 75% acetonitrile, with a flow rate of 0.8 mL min^{-1}. Samples were filtered through a 0.22 μm membrane before injection.

Total reducing sugar concentration was determined by the DNS reagent (3, 5-dinitrosalicil acid). 2 mL of the DNS solution were added into 1 mL of the sample and the mixture was kept at 100°C for 2 minutes. The solution was then analyzed by spectrophotometer (UV752, wavelength 540 nm) to determine the yield of reducing sugars; a glucose solution was used as the standard (Wood et al., 2012).

The volatile fatty acid concentrations in the effluent—including acetate, propionate, butyrate, i-butyrate, valerate, and caporate—were determined daily with a gas chromatograph (Shimadzu Corp., Japan, Model GC-2014) equipped with a flame ionization detector and a capillary column with length of 30 m × id 0.25 mm × film thickness 0.25 μm (HP-INNOWax, Agilent Technologies, Palo Alto, CA). The liquid samples were first centrifuged at 12,000 rpm for five minutes, then acidified with formic acid, filtered through a 0.22 μm membrane, and finally measured for free acids. The temperatures of the injector and detector were 250°C and 300°C, respectively. Initial oven temperature and time was 70°C for three minutes, followed by an increase of 15°C min^{-1} to a final temperature of 230°C for three minutes. Nitrogen was used as a carrier gas, with a flow rate of 0.93 mL min^{-1}.

Weight loss was used to quantify the dry mass reduction after pretreatment:

$$W=1- (M_1-M_2)/M_1*100 \quad (1)$$

Where W is weight loss (%), M_1 is dry mass before pretreatment (g), and M_2 is dry mass after pretreatment (g).

5.3 Results and discussion

5.3.1 Effect of different pretreatments on enzymatic hydrolysis

5.3.1.1 Fermentable sugars concentration in the enzymatic hydrolysate

A set of experimental runs using straw as the raw material were first performed to analyze the influence of SAA and ozone pretreatment time on hydrolysis efficiencies. The optimal reaction times were then selected for subsequent experiments.

The glucose, xylose, arabinose and reducing sugar concentrations varied with SAA pretreatment length—which ranged from 0 to 10 hours, while the ozone time remained constant at 45 minutes (Figure 5.1(a)-(d)) and, to a lesser degree, with ozone pretreatment length—which ranged from 0 to 75 minutes, while the SAA time remained constant at 4 hours (Figure 5.1(e)-(h)).

SAA time exerted a great impact on the release of mono-sugars and reducing sugars. The 45-minute ozone-only pretreatment (SAA time 0 hours) showed glucose concentrations that were obviously lower than those of samples that also had aqueous ammonia soaking (Figure 5.1(a)). Even when only soaked for two hours, the glucose concentration was 50% greater than without SAA pretreatment. Further increases in soaking time—from 4 to 10 h—led to notably smaller increases in glucose (Figure 5.1(a)). There was no explicit positive correlation between xylose concentration and ammonia soaking time (Figure 5.1(b)). The behavior of glucose and xylose indicated that the SAA had greater effect on the decrystallization of cellulose than on the solubilization of hemicellulose (Hendriks and Zeeman, 2009). The concentration of arabinose was below 1.30 g L^{-1} for all pretreatments (Figure 5.1(c)). The 2-h and 4-h SAA pretreatments resulted in 48.23 g L^{-1} and 54.89 g L^{-1} of reducing sugar in the hydrolysate, respectively, compared to the 30.15g L^{-1} achieved when SAA was not applied (SAA 0h) (Figure 5.1(d)), while additional minor increases seen under SAA pretreatments of 4 h and 8 h. All these results indicate that without an additional SAA pretreatment, the hydrolysis efficiency of the ozone pretreatment was inadequate.

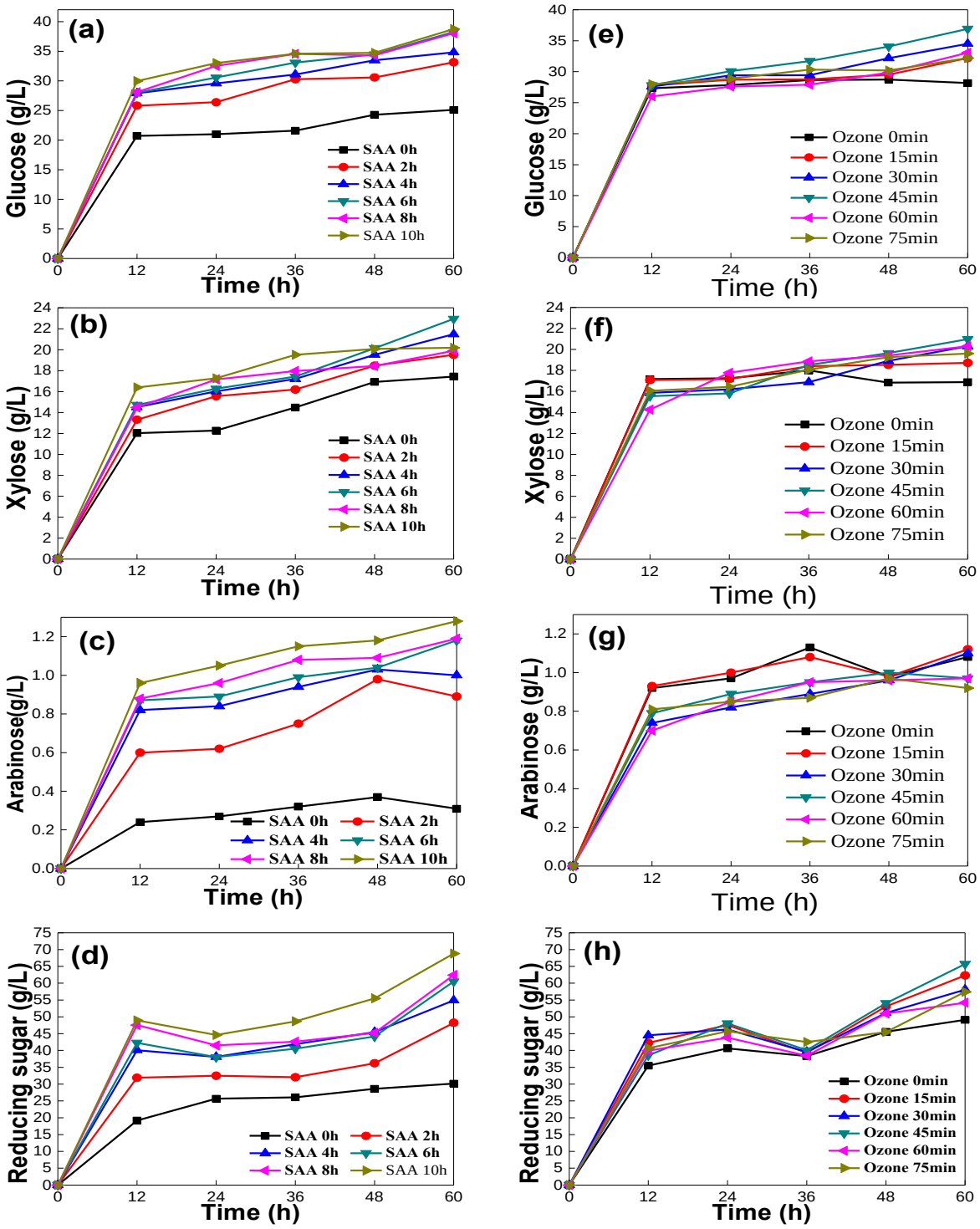

Figure 5.1: Changes in glucose, xylose, arabinose and reducing sugar in the enzymatic hydrolysis process, after different pretreatments: (a)-(d) results from the SAA experiments, with constant ozone time of 45 minutes; (e)-(f) results from ozone experiments with constant SAA time of 4 hours.

The release of glucose from ozone-pretreated straw was completely different from that of straw under the SAA pretreatment. The glucose levels varied with ozone pretreatment time, but not unidirectionally. The straw pretreated with ozone for 45 minutes presented the highest glucose levels, while those obtained in the 0-min and 75-min pretreatments were relatively lower, although the differences from 0 to 75 min were relatively small (Figure 5.1(e)). For xylose (Figure 5.1(f)), the variations in concentration did not present a unidirectional trend with increasing ozone time, and the final values were mostly very close to each other, except for the ozone 0-min pretreatment. Interestingly, the 0-min and 15-min ozone pretreated samples obtained the highest arabinose concentrations (Figure 5.1(g)). This result suggested that the ozone pretreatment might have caused the formation of an inhibitory compound (Travaini et al, 2013). The maximum reducing sugar concentration (65.71 g L^{-1}) after 60 hours of enzymatic hydrolysis was obtained in the sample pretreated with ozone for 45 minutes (Figure 5.1(h)). This maximum was 33.86% higher than the minimum concentration (49.09 g L^{-1}) obtained in the sample not pretreated with ozone (0 min). This 33.86% difference was considered too small when compared to the 2-fold greater variation observed in the results with different SAA pretreatment times. Therefore, in pursuit of an evident variation in sugar concentration between samples, an expanded ozone time range (0 min-135 min) was selected for subsequent trials.

5.3.1.2 Weight loss after different pretreatments

Weight losses as the time of the SAA pretreatment varied from 2 to 10 hours ranged from 26.40% to 40.27% (Figure 5.2(a)). The weight loss of the SAA 0-h pretreated sample is not shown because it did not undergo any ammonia aqueous pretreatment. Weight loss reached its highest level under the SAA 10-h pretreatment, which was consistent with the higher fermentable sugar concentrations achieved with the same pretreatment.

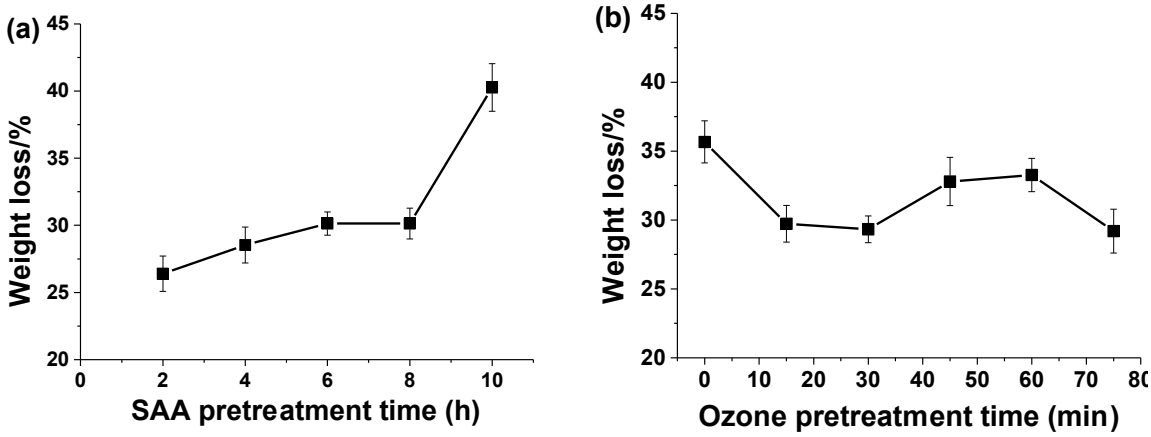

Figure 5.2: Weight loss after pretreatment with different methods: (a) varying SAA pretreatment times, and (b) varying ozone pretreatment times.

Unlike the increasing trend in weight loss as SAA time increased (Figure 5.2(a)), weight losses fluctuated with increasing ozone pretreatment times, and varied less overall (Figure 5.2(b)). The observed range of 29.20%-32.67% was close to that reported using a different pretreatment method (25%-50%, McIntosh, 2011). The small change in weight loss was consistent with the fermentable sugar results, which showed that extending the pretreatment time did not have much effect on sugar recovery. The weight loss for samples pretreated with ozone for 45 and 60

minutes was higher than for the 75-min ozone pretreatment, implying that extending the pretreatment time might not lead to improving the hydrolysis during the ozone pretreatment.

5.3.1.3 Lignocellulose content after enzymatic hydrolysis

A minor reduction of hemicellulose was observed in the ozone experiments, from 37.89% in the control to 31.94-32.99% in the ozone 15-75 min experiments (Figure 5.3). The minimum decrease in hemicellulose (down to 34.44% after pretreatment) occurred in the ozone 0 min test, which only pretreated the samples with SAA for 4 hours. This suggests that the ozone pretreatment was able to enhance hemicellulose reduction. Furthermore, the change in hemicellulose content exhibited an irregular relation with the length of the ozone pretreatment time, similar to the trend observed in fermentable sugar and weight loss, discussed above. These results are also consistent with an earlier report that found that increasing ozone time did not increase the pretreatment effect when exceeding an optimal time (Zhang et al., 2009).

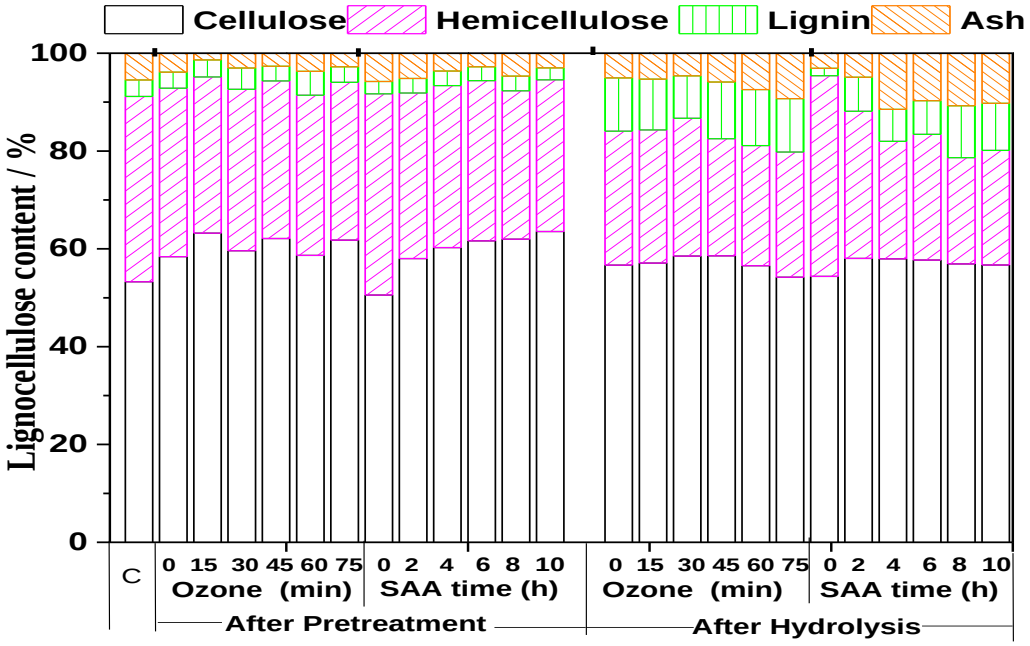

Figure 5.3: Lignocellulose content after pretreatment and after enzymatic hydrolysis. The lignocellulose content (%) is shown relative to the sum of cellulose, hemicellulose, lignin and ash.

We did not observe a significant shift in lignin content after pretreatment. The lignin content was 3.36% in the control and changed to 2.99%-4.89% in the ozone 0-75 min trials. Although ozone was expected to be effective in removing lignin, the remaining lignin content in the pretreated samples was similar to that of the raw materials, a result similar to that reported by García-Cubero et al. (2010). However, the lignin content rose considerably in all trials after enzymatic hydrolysis. The relative percentage of lignin increased to 8.67%-11.58%, although lignin was degraded in the hydrolysis process. This could be due to the hemicellulose content continuing to decrease to 23.95%-27.38%, a higher rate of degradation than lignin.

The relative percentage of cellulose increased to 58.39%-63.21% after OSAA pretreatments, then decreased to 54.18%-58.56% after the enzymatic hydrolysis process. The explanation for

these changes was that the cellulose degradation during hydrolysis was considerably higher than during the OSAA pretreatment. In the SAA experiments, a steady increase in cellulose content accompanied a decrease in hemicellulose content as the SAA time increased. The cellulose content was 53.28% in the raw material, and 58.01%, 60.27%, 61.64%, 61.96%, 63.54% in SAA 2-h, 4-h, 6-h, 8-h, and 10-h samples, respectively. The cellulose content was only 50.56% in the SAA 0-h pretreatment owing to the absence of the ammonia pretreatment. This increase in cellulose could be due to the fact that cellulose had a lower decomposition rate relative to hemicellulose during the OSAA pretreatment.

Although the ammonia pretreatment has been reported to have a minor effect on the solubilization of hemicellulose (Hendriks and Zeeman, 2009), the results obtained here suggest that the combination of SAA and ozone promoted the decomposition of hemicellulose. The lignocellulose content variation in SAA experiments was consistent with another existing report (Li et al., 2010). Even though the cellulose content increased with the SAA pretreatment time, there was an insignificant decrease in the cellulose remaining after enzymatic hydrolysis with SAA time (56.60%-58.05%). Meanwhile the hemicellulose content decreased greatly (21.72%-30.08%) during the hydrolysis process. In conclusion, SAA times between 2 and 10 hours did not significantly affect the lignocellulose content after hydrolysis as much as they did the content after pretreatment. However, the effect of SAA and ozone times on lignocellulose content may not be the same for anaerobic digestion with different feedstock. Crop straw and manure fiber should be tested further.

5.3.2 Biogas production with different pretreatment methods

Daily biogas yield and cumulative biogas production with different feedstock—straw and manure fiber—were compared under the same types of pretreatment conditions as described above. For each feedstock, two groups of experiments (SAA experiments and ozone experiments) were conducted to explore the effect of SAA and ozone times on anaerobic digestion (Table 5.2).

5.3.2.1 Biogas production from crop straw

The SAA experiments using crop straw as a substrate showed that, compared to the SAA 0-h pretreatment, other SAA runs—even soaking for just 2 hours—caused considerable improvements in the biogas daily yield and cumulative production (Figure 5.4(a)-(b)). The sample pretreated with ozone for only 90 minutes (SAA 0 h) obtained the lowest cumulative biogas production: 133.67 mL g^{-1} TS. Moreover, after subsequent pretreatments by SAA for 3, 6, and 9 h, the cumulative biogas production increased to 286.33, 324.33, and 365.67mL g^{-1} TS respectively, a 214.21%- 272.81% increase compared to the SAA 0-h pretreatment. This result implied that the OSAA pretreatment, which combines ozone and SAA pretreatments, significantly improved biogas yield.

In ozone experiments, the advantage of the OSAA pretreatment was verified once again. The cumulative biogas production was 219.00, 282.00, 298.10 and 306.33 mL g^{-1} TS for ozone times 0, 45, 90, and 135 minutes, respectively (Figure 5.4(c)-(d)). Compared to the ozone 0-h pretreatment (only pretreated by SAA for 6 h), other ozone runs increased biogas production by 28.77%, 36.07% and 39.88% (45, 90, and 135 minutes of ozone pretreatment, respectively). The increase in biogas production across ozone experiments was inferior to that across SAA experiments, suggesting that the SAA pretreatment performed a major function, while the ozone

pretreatment fulfilled a subordinate function, explaining the synergistic pretreatment effect of OSAA. It is worth noticing that there was no obvious increase of biogas production when the ozone pretreatment time varied from 45 to 135 minutes, although this time range was broader than in the earlier group of ozone experiments, confirming that it is not feasible to greatly enhance biogas yield by increasing ozone time alone within an OSAA process.

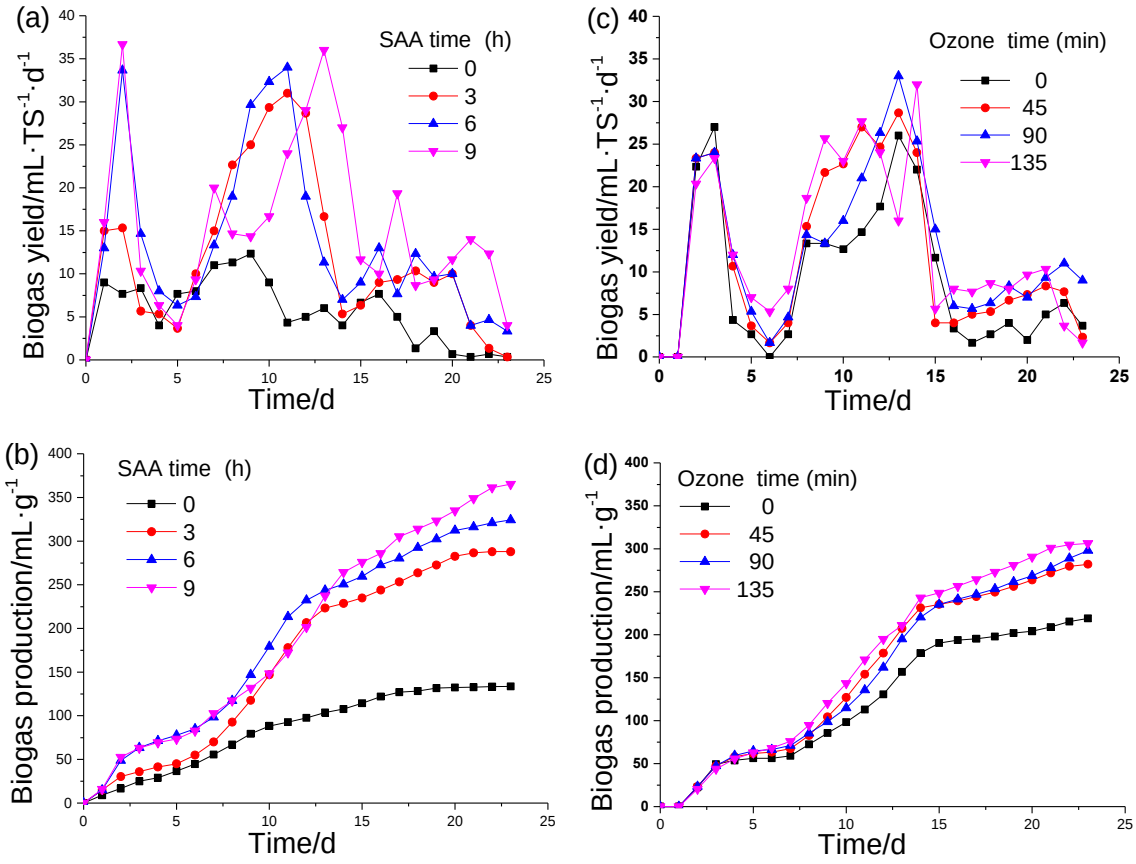

Figure 5.4: Daily biogas yield and cumulative biogas production of crop straw with different pretreatments: (a) Biogas yield with SAA time, (b) Cumulative biogas production with SAA time, (c) Biogas yield with ozone time, (d) Cumulative biogas production with ozone time. Note that (a)-(b) show results from the SAA experiments with constant ozone time of 90 minutes, and (c)-(d) show results from ozone experiments with constant SAA time of 6 hours.

5.3.2.2 Biogas production from manure fiber

It is well known that manure fiber has a lower biochemical methane potential than raw straw. In the SAA experiments with manure fiber as a substrate, the cumulative biogas production was 188.50, 200.10, 201.10 and 205.13 mL g^{-1} TS for SAA pretreatment times of 0, 3, 6, and 9 hours, respectively (Figure 5.5(a)-(b)). In ozone experiments, the cumulative biogas production was 97.10, 150.77, 195.20 and 197.7 mL g^{-1} TS in ozone time 0, 45, 90 and 135 minutes, respectively (Figure 5.5(c)-(d)). Besides the fact that biogas production from dairy manure was lower than the production from crop straw, the trends of biogas production with increased SAA or ozone pretreatment times were also quite different from the behavior of crop straw. The increase in biogas production from manure fiber with the longest SAA pretreated times was very limited.

For instance, the biogas production after 9 hours of SAA pretreatments was only 8.82% larger than production with 0 hours of SAA pretreatment. In addition, biogas yields were very similar to each other, showing only a minor effect of SAA time on anaerobic digestion using manure fiber.

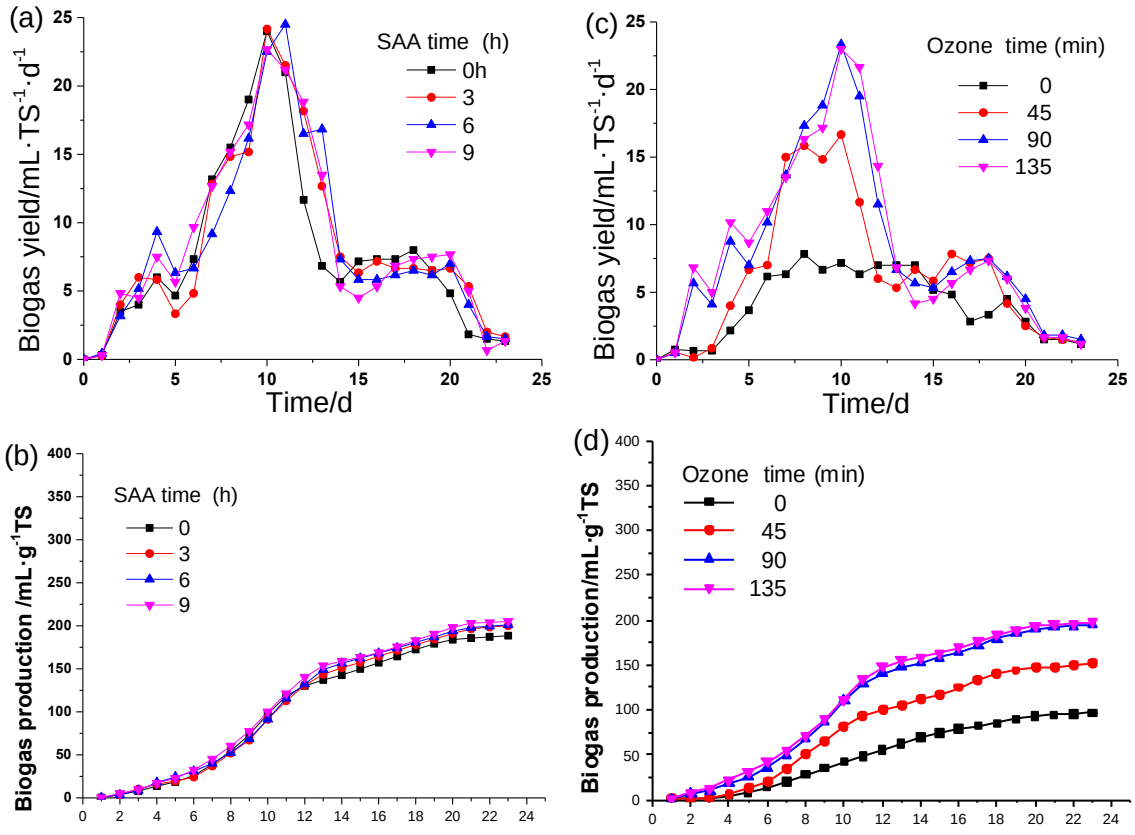

Figure 5.5: Daily biogas yield and cumulative biogas production of manure fiber with different pretreatment :(a) Biogas yield with SAA time, (b) Cumulative biogas production with SAA time, (c) Biogas yield with ozone time, (d) Cumulative biogas production with ozone time. Note that (a)-(b) show results from the SAA experiments with constant ozone time of 90 minutes, and (c)-(d) show results from ozone experiments with constant SAA time of 6 hours.

In the ozone experiments, the influence of the ozone pretreatment time was completely different to what was observed using crop straw. Instead of the small difference observed between production when crop straw was pretreated using different ozone time levels, the biogas production from manure fiber increased greatly—by 24.51%, 44.79% and 45.94%—as the ozone pretreatment time increased to 45, 90, and 135 minutes, respectively. Since the biogas production after 90 and 135 minutes of ozone pretreatment times were similar, an ozone time of 90 minutes would be recommended when OSAA pretreatments are applied to manure fiber. The difference in the response of manure fiber and crop straw to ozone time can be attributed to the different characteristics of the two substrates. This result suggests that great emphasis should be placed on optimizing the OSAA parameters according to the characteristics of the material used as feedstock.

5.3.3 Degradation of lignocellulose via different pretreatment conditions

The variation in lignocellulose content after the two treatment steps—pretreatment and anaerobic digestion—was quite consistent with the trends described above for sugars and biogas yield (Figure 5.6). For example, under the SAA 0-h pretreatment (only pretreated with ozone for 90 minutes), only the relative percentage of lignin decreased after pretreatment, indicating that this

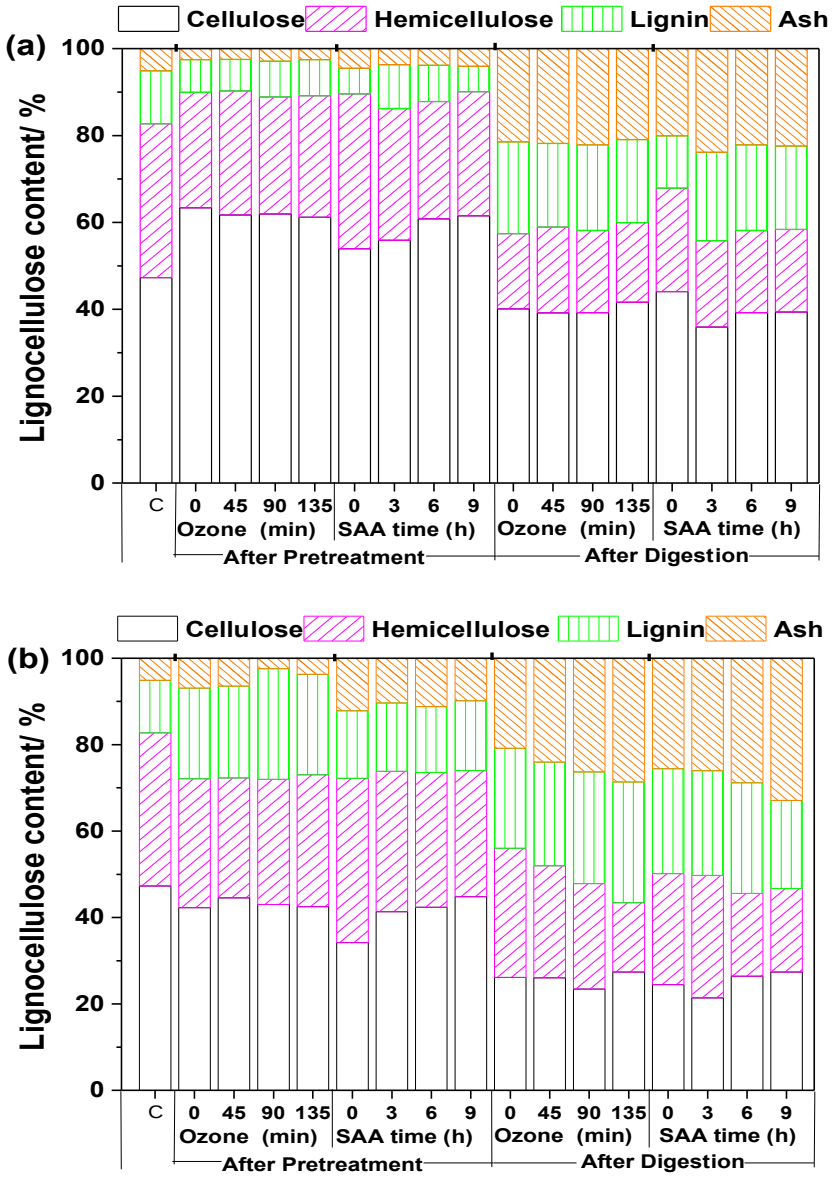

Figure 5.6: Lignocellulose contents after pretreatment and after anaerobic digestion: (a) with crop straw as substrate; and (b) with manure fiber as substrate. The lignocellulose content (%) is shown relative to the sum of cellulose, hemicellulose, lignin and ash.

component was degraded by the ozone pretreatment. This change was also consistent with expected results, as ozone can have a major effect on the solubilization of lignin. On the other hand, after the anaerobic digestion step, the largest decrease occurred in hemicelluloses, which is also in accordance with the expected hemicellulose variation during anaerobic digestion (Figure 5.6).

Reduction in volatile solid (VS) concentrations occurred mainly after anaerobic digestion (Figure 5.7). Volatile solids reduction was highly correlated with biogas production. When crop straw was used as substrate, the maximum VS reduction after digestion was obtained under the SAA 0-h pretreatment (Figure 5.7(a)), which also had the lowest biogas production. When manure fiber was used as substrate, however, the VS reduction decreased as the ozone pretreatment time increased (Figure 5.7(b)), while biogas production increased.

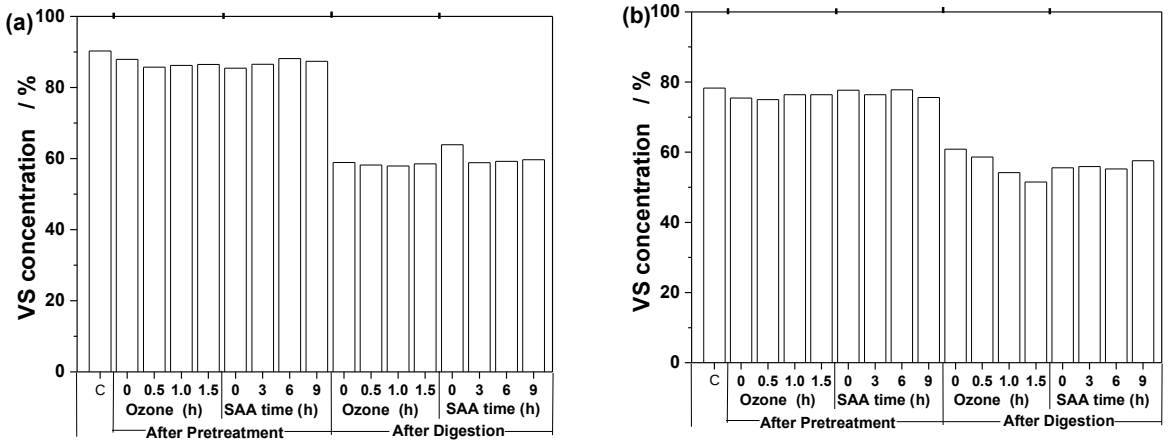

Figure 5.7: Effect of different pretreatments on the volatile solid content before and after fermentation: (a) crop straw, (b) manure fiber.

5.4 Conclusions

The SAA and ozone pretreatment times in the OSAA process were comprehensively investigated in this study, evaluating its performance on crop straw and manure fiber. This project's results enable the design of an OSAA process for agricultural residues that shows improved efficiency and increases methane production during anaerobic digestion. During the enzymatic hydrolysis, the SAA pretreatment time had greater impact on the recovery of fermentable sugars than the ozone pretreatment time. Changes in SAA time from 2 to 10 hours increased the glucose concentration over 50%, compared to the SAA 0-h pretreatment. Meanwhile, the ozone pretreatment time did not show a positive correlation with sugar recovery.

The advantages and synergistic effects of the OSAA pretreatment were confirmed in this study. When crop straw was used as a substrate, pretreatments with SAA for 3 to 9 hours resulted in 214.21-272.81% biogas increase compared to the SAA 0 h pretreatment. Pretreatment with ozone for 45 to 135 minutes, on the other hand, led to 28.77%-39.88% increases in biogas

production. SAA pretreatment time had a major function to play in promoting biogas production from crop straw via the OSAA process.

The effect of SAA and ozone pretreatment time on the anaerobic digestion of manure fiber was completely different from that of crop straw. Manure fiber pretreated by SAA for 3 to 9 hours resulted in limited increases in biogas production—8.82% at the most—while pretreatment with ozone for 45 to 135 minutes caused a 24.51%-45.79% biogas increase. Great emphasis should be placed, therefore, on optimizing the OSAA parameters according to the characteristics of the material used as feedstock.

5.5 References

APHA. 1998. Standard Methods for the Examination of Water and Wastewater. 20th American Public Health Association Meeting.Washington, DC.

Bauer, A., Lizasoain, J., Theuretzbacher, F., Agger, J.W., Rincón, M., Menardo, S., Saylor, M.K., Enguídanos, R., Nielsen, P.J., Potthast, A., Zweckmair, T., Gronauer, A., and Horn, S.J. 2014. Steam explosion pretreatment for enhancing biogas production of late harvested hay. Bioresource Technology 166, 403-410.

Baboukani, S., Vossoughi, B., Alemzadeh, I. 2012. Optimisation of dilute-acid pretreatment conditions for enhancement sugar recovery and enzymatic hydrolysis of wheat straw. Biosystems Engineering 111, 166-174.

Cesaro, A., Belgiorno, V. 2013. Sonolysis and ozonation as pretreatment foranaerobic digestion of solid organic waste. Ultrasonics Sonochemistry 20(3), 931–936.

García-Cubero, M.T., Coca, M., Bolado, S., González-Benito, G. 2010. Chemical oxidation with ozone as pre-treatment of lignocellulosic materials for bioethanol production. Chemical Engineering Transactions 21(1): 1273-1278.

García, A., Alriols, G., Labidi, M. 2014. Evaluation of different lignocellulosic raw materials as potential alternative feedstocks in biorefinery processes. Industrial Crops and Products 53, 102-110.

Gao, A.H., Bule, M.V., Laskar, D.D., Chen, S. 2012. Structural and thermal characterization of wheat straw pretreated with aqueous ammonia soaking. Journal of Agricultural and Food Chemistry 60(35), 8632-8639.

Hendriks, A., Zeeman, G. 2009. Pretreatments to enhance the digestibility of lignocellulosic biomass. Bioresource Technology 100, 10-18.

Kim, T. H., Taylor F., Hicks K.B. 2008. Bioethanol production from barley hull using SAA (soaking in aqueous ammonia) pretreatment. Bioresource Technology 99(13), 5694-5702.

Kim, T.H., Lee, Y.Y. 2007. Pretreatment of corn stover by soaking in aqueous ammonia at moderate temperature. Applied Biochememistry and Biotechnology 137(1-12), 81-92.

Li, D., Liu, S., Mi, L., Li, Z., Yuan, Y., Yan, Z., Liu, X. 2015. Effects of feedstock ratio and organic loading rate on the anaerobic mesophilic co-digestion of rice straw and pig manure. Bioresource Technology 187, 120-127.

Li, X., Kim T., Nghiem N. 2010. Bioethanol production from corn stover using aqueous ammonia pretreatment and two-phase simultaneous saccharification and fermentation (TPSSF). Bioresource Technology 101(15), 5910-5916.

Martinez, A., Speranza, M., Ruiz-Duenas, F.J. 2005. Biodegradation of lignocellulosics: microbial, chemical, and enzymatic aspects of the fungal attack of lignin. International Microbiology 8(3),195-204.

Mcintosh, S., Vancor, T. 2011. Optimisation of dilute alkaline pretreatment for enzymatic saccharification of wheat straw. Biomass and Biotechnology 35(7), 3094-3103.

Saady, N.M.C., Massé, D.I. 2015. Impact of organic loading rate on the performance of psychrophilic dry anaerobic digestion of dairy manure and wheat straw: Long-term operation. Bioresource Technology 182, 50-57.
Sluiter, A., Ruiz, R., Scarlata, C., Sluiter, J., Templeton, D. 2005. Determination of extractives in biomass. Laboratory Analytical Procedure (LAP), 1617.
Sun, Y., Lin, L., Pang, C., Deng, H., Peng, H., Li, J., He, B., Liu, S. 2007. Hydrolysis of cotton fiber cellulose in formic acid. Energy and Fuels 21(4), 2386-2389.
Sun, Y., Cheng, J. 2002. Hydrolysis of lignocellulosic materials for ethanol production: a review. Bioresource Technology 83, 1-11.
Teater, C., Yue, Z.B., MacLellan, J., Liu, Y., Liao, W. 2011. Assessing solid digestate fromanaerobic digestion as feedstock for ethanol production. Bioresource Technology 102, 1856–1862.
Travaini, R., Otero, M.D.M., Coca, M., Da-Silva, R., Bolado, S. 2013. Sugarcane bagasse ozonolysis pretreatment: Effect on enzymatic digestibility and inhibitory compound formation. Bioresource Technology 133(0), 332-339.
Wen, Z.Y., Liao W., Chen, S.L. 2004. Hydrolysis of animal manure lignocellulosics for reducing sugar production. Bioresource Technology 91, 31–39.
Wood, I.P., Elliston, A., Ryden, P., Bancroft, I., Roberts, I.N., Waldron, K.W. 2012. Rapid quantification of reducing sugars in biomass hydrolysates: Improving the speed and precision of the dinitrosalicylic acid assay. Biomass and Bioenergy, 44, 117-121.
Yu, L., Bule, M., Ma, J.W., Zhao, Q., Frear, C., Chen, S. 2014. Enhancing volatile fatty acid (VFA) and bio-methane production from lawn grass with pretreatment. Bioresource Technology 162, 243-249.
Yue, Z., Teater, C., Liu, Y., MacLellan, J., Liao, W. 2010. A sustainable pathway of cellulosic ethanol production integrating anaerobic digestion with biorefining. Biotechnology and Bioengineering 105(6), 1031-1039.
Zhang, G., Yang J., Liu H., Zhang, J. 2009. Sludgeozonation: Disintegration, supernatant changes and mechanisms. Bioresource Technology 100(3), 1505-1509.
Zhou S., Zhang Y., Dong Y. 2012. Pretreatment for biogas production by anaerobic fermentation of mixed corn stover and cow dung. Energy 46(1), 644-648.
Zuo, Z., Tian, S., Chen, Z., Li, J., Yang, X. 2012. Soaking pretreatment of corn stover for bioethanol production followed by anaerobic digestion process. Applied Biochemistry and Biotechnology 167(7), 2088-2102.

6. Production of Microbial Biofertilizer from Wheat Straw

Allan Gao, Rishi Ghoghare, and Shulin Chen

6.1 Background

Efforts to develop processes for converting lignocellulosic agricultural residues—such as wheat straw and corn stover—into a sugar substrate for the production of renewable fuels continue. Not all of the biomass present in a field is available for harvest, however, because a significant portion needs to be returned to the soil to preserve soil quality and prevent erosion. In a future where harvest and use of agricultural residues by biorefineries becomes prevalent, practices and technologies will be needed so that the constant removal of nutrients from the field year after year does not result in the loss of organic carbon from the soil, as well as the loss of nitrogen and phosphorous necessary for crop growth.

The use of a portion of the harvested lignocellulose for production of a microbial biofertilizer may present a partial solution to the problem of residue removal. Microbial biofertilizers are an array of organisms that are nitrogen-fixers or phosphate-solubilizers. Some microbial strains provide added benefits, such as suppressing the growth of harmful microorganisms and releasing micronutrients (Singh et al., 2007). There are many organisms that provide biofertilizer capabilities, including bacteria in the genera *Azospirillum, Azotobacter,* and *Rhizobia* (Hayat et al., 2010). In the past, the production of microbial biofertilizers has used sugars derived from starchy crop residues, including cassava and potato; the use of cane sugar has also been documented (Hayat et al., 2010).

This study proposes to use a local biorefinery consuming agricultural residues such as wheat straw and corn stover to produce microbial biofertilizer. Such biofertilizers have the capacity to release nutrients over time, and are also beneficial in reducing leaching from the soil and in suppressing the growth of harmful microorganisms (Table 6.1). On the other hand, some drawbacks of microbial biofertilizers include a lower nutrient content than conventional chemically-derived fertilizers, and the requirement for ideal soil conditions in order to reach their maximum effectiveness (Table 6.1). These are not mutually exclusive practices, however. The supplementation of chemical fertilizers with small amounts of microbial biofertilizers has the potential to reduce the amount of fertilizers that farmers must purchase and apply to their fields.

This research investigated key steps in the processing of wheat straw to develop a source of sugars to support the growth of a microbial biofertilizer. The specific steps studied were:

1) The use of a low severity, chemical process for pretreating wheat straw, consisting of ozone and soaking aqueous ammonia (OSAA), in order to improve the breakdown of complex carbohydrates in the straw, and resultant release of sugars (enzymatic saccharification).
2) The growth and nitrogen fixation of biofertilizer species based on the sugars that are released after the saccharification process, supplemented with nutrients.

Table 6.1: Advantages and disadvantages of microbial biofertilizer compared to conventional chemically-derived fertilizer.

Advantages	Disadvantages
✓ **Balanced nutrient supply**	✓ Low total nutrient content
✓ **Increased soil organic matter for increased soil stability**	✓ Nutrient release rate is constant, but slow
✓ **Suppress growth of harmful microorganisms, and encourage growth of beneficial organisms and earthworms**	✓ Initial growth slow compared to chemical fertilizer
✓ **Reduction of soil leaching**	✓ Nutrient composition is highly variable depending on biofertilizer growth conditions
✓ **Application of micronutrients**	✓ Pre-existing soil conditions can affect biofertilizer growth and nutrient production

6.2 Concept and methods

6.2.1 Pretreatment and hydrolysis of wheat straw for sugar production

The ozone and soaking aqueous ammonia pretreatment (OSAA) was utilized to pretreat wheat straw. The wheat straw was hammer milled, and sieved through a Taylor screen to ensure a particle size between 42 and 60 mesh.

In the first step of pretreatment, the moisture of the wheat straw particles was adjusted (90% w/w). The particles were then placed into an enclosed stainless steel reactor with a 1 cm bed height, to ensure equal contact time of the entire particle with ozone, and operated in semi-continuous mode as reported in earlier work (Bule et al., 2013). The ozonation reaction was performed with 5.4% ozone concentration (w/w) at a flow rate of 2 L min^{-1} for a period of 10 minutes. Ozone was produced by a L11-L24 Ozone Generator manufactured by Pacific Ozone (California, USA) and ozone concentration at the outlet was determined according to the procedure adopted by Rakness et al. (1996). Final moisture content was not analyzed and samples were dried at 50°C for 24 hours to ensure that the remaining water was evaporated before the subsequent soaking aqueous ammonia (SAA) treatment. The ozone-treated particles were then treated by SAA using ammonium hydroxide solution (JTB-9721-03) with a solid-to-liquid ratio of 1:4 at 50°C with no agitation in a 1000 mL screw cap Pyrex solution bottle (Gao et al., 2012). After completion of the incubation, the wheat straw particles were washed twice thoroughly with distilled water to reach a neutral pH. The pretreated wheat straw obtained was again washed and then dried at 50°C prior to enzymatic saccharification.

Enzymatic saccharification was carried out at a 5% (w/w) solid loading in a citrate buffer at pH 4.8. The enzymes used were Novozymes CTEC 2 (cellulase) and HTEC 2 (hemicellulase), and they were added into the wheat straw at a 0.04 g g^{-1} glucan loading for CTEC and a 0.004 g g^{-1} glucan loading for HTEC. The HTEC loading is small due to prior studies demonstrating that CTEC has a relatively high hemicellulase activity in addition to its cellulase activity. The flasks

containing the wheat straw and enzyme mixture were placed into a rotary shaker for 72 hours at 180 rpm and 50°C.

The sugar content after saccharification was analyzed using a Dionex ICS-3000. In addition, the composition of wheat straw before and after pretreatment was assessed according to the National Renewable Energy Laboratory method for determination of structural carbohydrates and lignin (Sluiter et al., 2010).

6.2.2 Culturing of biofertilizer species and nitrogen assay

Two biofertilizer species were chosen for this task, *Azotobacter vinelandii* and *Azospirillum brasilense*. These two species have been studied extensively and have been shown to be able to grow on a variety of 6-carbon sugars (Mishra et al., 2013; Mohammadi and Sohrabi, 2012). The two species were obtained from ATCC (Manassas, VA) and cultured on ATCC medium 1713 for *Azotobacter* strains and ATCC medium 838 for *Azospirillum* strains.

Both cultures grew well on plates and were transferred to liquid media supplemented with 20 g L^{-1} of sucrose. Two-day starter cultures in 3 mL of broth in a test tube were inserted into 50 mL shake flasks placed at 30°C. Nitrogen content was analyzed using Hach Persulfate Digestion Kits (Hach 2672245).

Interestingly, *A. vinelandii* had a much higher specific growth rate than *A. brasilense*, showing more than three times the cell mass after three days and more than six times the cell mass at five days (Table 6.2). As a result, the growth trials with nitrogen-free Burk and Ashby media, and the nitrogen fixation assays were carried out only on *A. vinelandii*.

Table 6.2: Growth rates of selected biofertilizer species on basic media specified by ATCC, supplemented with 20 g L^{-1} of sucrose.

Strain	***3 day cell mass***	***5 day cell mass***
A. vinelandii	0.236 ± 0.01g	0.744 ± 0.008g
A. brasilense	0.087 ± 0.07g	0.0135 ± 0.002

6.3 Results and discussion

6.3.1 Pretreatment and hydrolysis of wheat straw for sugar production

The OSAA pretreatment of the wheat straw removed a significant amount of lignin from the wheat straw, decreasing the acid insoluble lignin from 20.57% before pretreatment (Table 6.3) to 2.4% after pretreatment (Table 6.4). This was largely due to the ammonolysis of ester bonds and subsequent solubilization of lignin in the basic ammonia effluent (Gao et al., 2012; Kim and Lee, 2007).

Due to the removal of lignin from the biomass, there was mass loss after the pretreatment equal to between 30-35% of the total mass of the wheat straw. Also as a result of the removal of lignin, there was a relative increase in the content of carbohydrate in the pretreated wheat straw, which

increased from about 65% available sugars to 86% available sugars. In the pretreated wheat straw, galactan was not detected. Galactan is one of the primary links between lignin and cellulose in straw (Lawther et al., 1996; Sun et al., 2005). The lack of detection was likely due to the solubilization of galactan into the ammonia effluent.

Table 6.3: Composition of wheat straw (*Triticum aestivum)* prior to pretreatment.

Component	% (w/w)
Glucan	37.08 ± 0.53
Xylan/Mannan	24.22 ± 0.41
Arabinan	2.76 ± 0.04
Galactan	0.63 ± 0.006
Acid Soluble Lignin	2.42 ± 0.18
Acid Insoluble Lignin	20.57 ± 1.83
Ash	8.32 ± 0.23
Total Sugars	**64.69 ± 0.98**

Table 6.4: Composition of wheat straw (*Triticum aestivum)* after 10 minutes of ozone pretreatment and 3 hours of soaking aqueous ammonia pretreatment.

Component	% (w/w)
Glucan	62.07 ± 1.26
Xylan/Mannan	22.85 ± 0.19
Arabinan	1.93 ± 0.03
Galactan	N.D.[1]
Acid Soluble Lignin	4.78 ± 1.25
Acid Insoluble Lignin	3.34 ± 0.41
Ash	2.4 ± 0.05
Total Sugars	**86.85 ± 1.47**

[1] N.D.: not detected.

Based on the available sugar in the pretreated wheat straw, a 43.41 g L^{-1} of total sugar could have been recovered from a 5% (w/w) solid loading. The recovered 37.39 g L^{-1} of sugar represented an 86% sugar yield from the straw (Table 6.5). This sugar was then diluted to a desired concentration of 20 g L^{-1} of glucose. In this study, the concentration of xylose in the obtained sugar was ignored due to the fact that *A. vinelandii* is not known to consume C5 sugars.

Table 6.5: Maximum sugar yield from pretreated wheat straw compared to actual yield after enzymatic saccharification. The diluted concentration represents the concentration of sugar present in wheat straw sugar growth media.

Component	Maximum Yield ($g\ L^{-1}$)	Actual Yield ($g\ L^{-1}$)	Diluted Concentration ($g\ L^{-1}$)
Glucose	31.03	27.12	20.70
Xylose/Mannose	11.42	9.65	8.35
Arabinose	0.96	0.62	0.35
Galactose	N.D.[1]	N.D.	N.D.

[1] N.D.: not detected.

6.3.2 Culturing of biofertilizer species and nitrogen assay

The growth of *A. vinelandii* was significantly better on Ashby media compared to Burk media, with Ashby media reaching about 5.65 g L^{-1} of cell mass compared to 3.55 g L^{-1} of cell mass on the Burk media (Figure 6.1). Similarly, the nitrogen fixation of *A. vinelandii* on Ashby media was higher as well, with 65.5 µg mL^{-1} of nitrogen compared to 38.1 µg mL^{-1} of nitrogen on Burk media (Figure 6.2). The wheat straw sugar supplemented with Burk and Ashby media performed significantly worse compared to control media with sucrose added. This was likely due to the presence of inhibitor compounds, likely soluble aromatic compounds generated during the course of pretreatment. However, the results showed that *A. vinelandii* is able to grow appreciably well on Ashby media supplemented with sugar obtained from wheat straw hydrolysate, resulting in an approximate 28% (w/w) yield of cell mass from sugar.

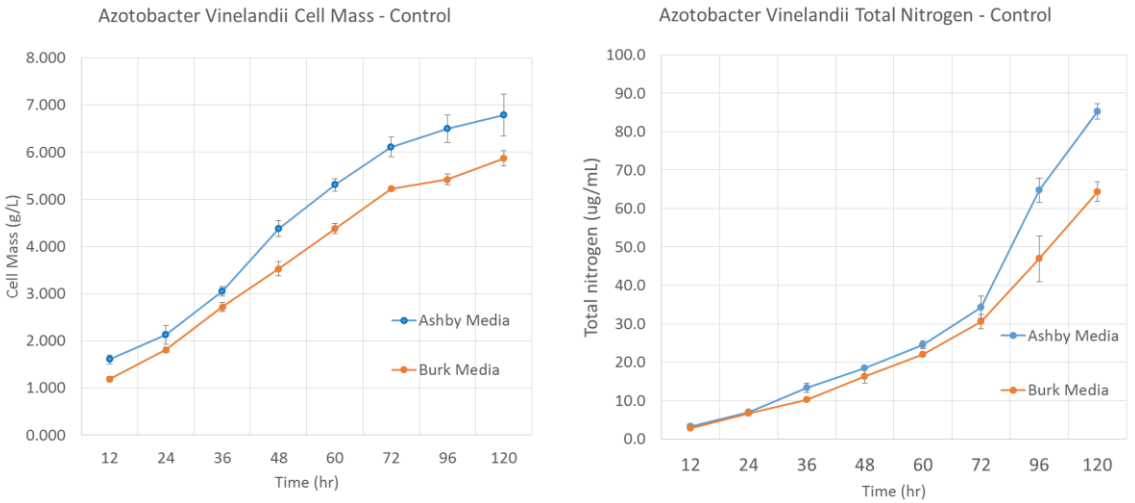

Figure 6.1: Cell mass accumulation and nitrogen fixation of *A. vinelandii* on Burk and Ashby media over a 5-day growth period.

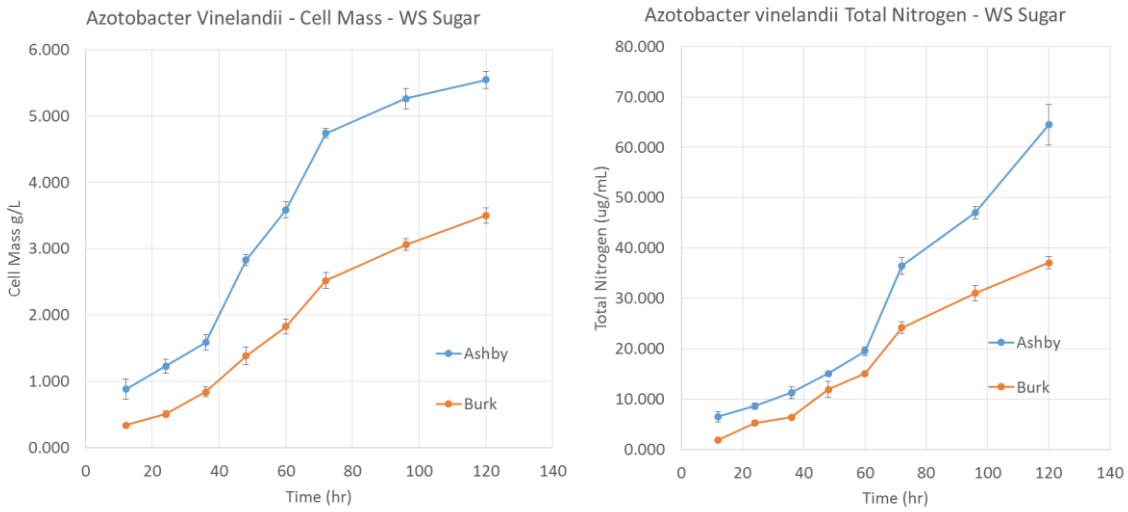

Figure 6.2: Nitrogen content of *A. vinelandii* on Burk and Ashby media over a 5-day growth period.

6.3.3 Preliminary economic analysis and application to farms in Washington

The laboratory scale conditions used for pretreatment and production of microbial biofertilizer were modeled in Aspen Plus v8.6[1] (Aspen Technologies Inc., USA) in order to provide an initial estimate of the operating cost per ton of wheat straw (Table 6.6) and the economic feasibility of such a process.

Table 6.6: Operating cost of each major operation, per ton of wheat straw

Operation	$ per ton wheat straw input
Pretreatment	$32.83
Enzymatic Hydrolysis	$95.56
Biofertilizer Culture	$15.14
Total	$143.53

Based on the model, the mass balance resulted in one ton of wheat straw yielding 294 kg (648 lb) of C6 sugar, which could then be converted into approximately 81.6 kg (180 lb) of biofertilizer, resulting in an operating cost of $1.76 kg^{-1} ($0.80 lb^{-1}, or $1,600 per ton). This is a relatively high cost compared to traditional chemical fertilizer. However, the amount of biofertilizer needed is much lower, with only 6 kg (13.2 lb) of dry cell mass required for effective inoculation of 1 ha (Biari et al., 2008).

In addition to needing lower amounts of biofertilizer, compared to chemical fertilizers, the potential effectiveness of biofertilizer is significant (Table 6.7). Ozturk et al. (2003) found that a loading of biofertilizer with 40 kg of chemical nitrogen fertilizer was able to exceed the growth of plants that were grown with 80 kg of chemical nitrogen fertilizer alone (Table 6.7). In

[1] A detailed model and costing information is not included here for brevity, but is available upon request.

addition, the inoculation of just the biofertilizer *Azospirillum* achieved wheat yields comparable to those obtained with chemical fertilizer applied at 80 kg ha^{-1}. This means that 6 kg of biofertilizer costing $10.56 has the potential to replace 40 kg of ammonia fertilizer with a cost of approximately $29 (based on 2013 price of ammonia: $725 per metric ton).

Table 6.7: Comparative study of wheat yield based on chemical fertilizer use and biofertilizer use (Ozturk et al., 2003).

Inoculum	Wheat Yield (MT ha^{-1})
Control	1.63
Azospirillum	1.95
Bacillus	1.79
40 kg N ha^{-1}	1.83
80 kg N ha^{-1}	1.98
Azospirillum + 40 kg ha^{-1}	2.02
Bacillus + 40 kg ha^{-1}	1.97

6.4 Conclusions

The ozone and soaking aqueous ammonia pretreatment process was demonstrated to be an effective low-temperature and -pressure pretreatment capable of effectively pretreating wheat straw such that 87% of available sugars was released during high-solids enzymatic hydrolysis. In addition, *A. vinelandii* was demonstrated to grow well on Ashby media with wheat straw-derived sugar, producing a 28% (w/w) yield of cell mass on sugar, with 65.65 µg mL^{-1} of fixed nitrogen in the final culture medium. A preliminary economic analysis demonstrated that, if effective, the microbial biofertilizer produced could have the potential to generate significant fertilizer cost-savings for farmers, while improving soil quality and providing an alternative for removing wheat straw from the field.

6.5 References

Biari A., Gholami, A., Rahmani, H. 2008. Growth promotion and enhanced nutrient uptake of maize (*Zea mays* L.) by application of plant growth promoting rhizobacteria in arid region of Iran. Journal of Biological Sciences 8, 1015-1020.

Bule, M.V., Gao, A.H., Hiscox, B., Chen, S. 2013. Structural modification of lignin and characterization of pretreated wheat straw by ozonation. Journal of Agricultural and Food Chemistry 61, 3916-3925.

Gao, A.H., Bule, M.V., Laskar, D.D., Chen, S.L. 2012. Structural and thermal characterization of wheat straw pretreated with aqueous ammonia soaking. Journal of Agricultural and Food Chemistry 60, 8632-8639.

Hayat, R., Ali, S., Amara, U., Khalid, R., Ahmed, I. 2010. Soil beneficial bacteria and their role in plant growth promotion: a review. Annals of Microbiology 60, 579-598.

Kim, H.T., Lee, Y.Y. 2007. Pretreatment of corn stover by soaking in aqueous ammonia at moderate temperatures. Applied Biochemistry and Biotechnology 137(1-12), 81-92.

Lawther, J.M., Sun, R.C., Banks, W.B. 1996. Fractional characterization of wheat straw lignin components by alkaline nitrobenzene oxidation and FT-IR spectroscopy. Journal of Agricultural and Food Chemistry 44, 1241-1247.

Mishra, D., Rajvir, S., Mishra, U., Kumar, S.S. 2013. Role of bio-fertilizer in organic agriculture: a review. Research Journal of Recent Sciences ISSN 2277, 2502.

Mohammadi, K., Sohrabi, Y. 2012. Bacterial biofertilizers for sustainable crop production: A review. Journal of Agricultural and Biological Science 7, 307-316.

Ozturk, A., Caglar, O., Sahin, F. 2003. Yield response of wheat and barley to inoculation of plant growth promoting rhizobacteria at various levels of nitrogen fertilization. Journal of Plant Nutrition and Soil Science 166, 262-266.

Rakness, K., Gordon, G., Langlais, B., Masschelein, W., Matsumoto, N., Richard, Y., Robson, C.M., Somiya, I. 1996. Guideline for measurement of ozone concentration in the process gas from an ozone generator. Ozone: Science and Engineering 18, 209-229.

Singh, R., Behl, R., Jain, P., Narula, N., Singh, K. 2007. Performance and gene effects for root characters and micronutrient uptake in wheat inoculated with arbuscular mycorrhizal fungi and *Azotobacter chroococcum.* Acta Agronomica Hungarica 55, 325-330.

Sluiter, A., Hames, B., Ruiz, R., Scarlata, C., Sluiter, J., Templeton, D., Crocker, D. 2010. Determination of structural carbohydrates and lignin in biomass. NREL Laboratory Analytical Procedure.

Sun, X.F., Xu, F., Sun, R.C., Geng, Z.C., Fowler, P., Baird, M.S. 2005. Characteristics of degraded hemicellulosic polymers obtained from steam exploded wheat straw. Carbohydrate Polymers 60, 15-26.

7. Utilization of Wheat Straw for the Production of Lipids

Tao Zhu, Shuai Zhang, Ali Abghari, and Shulin Chen

7.1 Background

Biodiesel produced from vegetable oils, plant oils, or animal fats by transesterification with alcohols of low molecular weight is an important renewable fuel (Subramaniam et al., 2010). Vegetable oils have been used in motor vehicles since the beginning of the automobile industry. However, conventional biodiesel derived from plant oils or animal fats cannot be produced in large enough volumes to meet growing fuel demand, and also raises concerns about competition with food supplies (Fairley, 2011). As the world population increases and arable land shrinks, the large-scale plantation of oil crops for fuel is not sustainable. In addition, multiple factors such as climate and geography affect the growth and productivity of oil plants. So plant oil cannot fuel the world's increasing demand for energy. Microbial lipids, however, provide an alternative possibility for fueling the world as the next-generation renewable energy source. In addition to their potential as a solution to energy issues, microbial lipids can also be used as precursors or building blocks for many industrial products including polymers, lubricants, pharmaceuticals, foods, and cosmetics, to name a few.

Microbial lipids have similar composition to plant oils and animal fats, and have often been considered more renewable and sustainable (Gao et al., 2013; Subramaniam et al., 2010; Zhang et al., 2011). These lipids have a number of desirable characteristics, including high productivity, short process cycle, easier scalability, as well as their utilization of renewable feedstock. These characteristics make oleaginous microbes a promising platform for economical and sustainable production of advanced biofuels (Gao et al., 2013; Subramaniam et al., 2010). In addition, microorganisms have many advantages over plants for the production of lipids, such as less labor required, less demand for space, and lower restrictions on venue, season and climate. Photosynthetic microorganisms have a 100-fold higher lipid yield per hectare than plants do. Microbial lipids are rich in specific polyunsaturated fatty acids, so are often used in dietary supplements and for infant nutrition (Subramaniam et al., 2010).

Microorganisms as diverse as microalgae, bacillus, and fungi (molds and yeasts) possess the ability to produce and accumulate a large fraction of their dry mass as lipids. Those with lipid content in excess of 20% are classified as 'oleaginous' (Subramaniam et al., 2010). Oleaginous yeasts have a fast growth rate and a high oil content, and their triacylglycerol fraction is similar to that of plant oils. These organisms can grow on a multitude of carbon sources—glucose, xylose, arabinose, mannose, glycerol—, which can also be obtained from agricultural and industrial residues.

Lignocellulosic biomass—such as can be obtained from agricultural residues—is attractive as a carbon source for the production of microbial oils. However, its compositional heterogeneity somewhat complicates its commercial use. Compared to conventional sugars, lignocelluloses

need to be hydrolyzed to obtain fermentable saccharides, usually with a thermo-chemical pretreatment. As a result, pentose and hexose coexist with the dominant glucose and xylose in the lignocellulosic hydrolysate (Xu et al., 2013).

Animal manure represents a large potential bioresource for producing biologically-based chemicals, materials and energy (Wen et al., 2005). One possible approach to the utilization of manure lignocellulose is to hydrolyze the materials into fermentable saccharides, which can then be converted into value-added products or bioenergy, as in the case of the anaerobic digestion (AD) of dairy manure. A typical AD process is limited by the microbes' inability to utilize the manure fiber, due to the lignocellulosic component of the fiber being very resistant to biodegradation (Wen et al., 2005). Previous work from this laboratory showed that AD fiber from manure produced only limited amounts of sugars when subjected to enzymatic hydrolysis. Utilization of this fiber for advanced biofuel production may not, therefore, be a viable option.

Wheat straw is another lignocellulosic material that is an abundant byproduct in many wheat production regions. In 2008 the worldwide wheat production was estimated to be over 650 metric tons, thus about 850 metric tons of wheat straw were produced annually, based on the straw-to-crop ratio of 1.3 (Yu et al., 2011). Moreover, wheat is Washington State's main crop. This state therefore has significant potential for producing lipids using wheat straw as a carbon source.

Combining chemical engineering and microbiology together, the aim of this project was to test the suitability of this locally available and abundant lignocellulosic material—wheat straw—as feedstock for microbial lipid production (Figure 7.1).

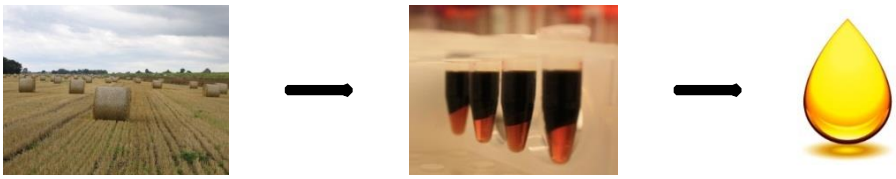

Figure 7.1: Biomass suitability and processibility for fermentation of oleaginous organisms to produce biodiesel.

7.2 Methods

7.2.1 Technical routes

Wheat straw is widely available in the state of Washington. In this project, the wheat straw was treated with three parallel pretreatment methods developed in Washington State University's (WSU) Bioprocessing and Bioproducts Engineering Laboratory. The pretreated samples were then submitted to enzymatic hydrolysis, and the total sugars released were measured. The non-detoxified liquids obtained via hydrolysis of the pretreated samples were then used as carbon sources for single cell oil production by different oleaginous yeasts.

The yeasts usually used for producing lipids are *Rhodotorula glutinis*, *Cryptococcus albidus*, *Lipomyces starkeyi*, and *Candida curvata*. *Cryptococcus curvatus*, however, has shown the highest lipid concentrations in medium on both detoxified and non-detoxified hydrolysates of

lignocellulose, when compared to *R. glutinis*, *Rhodosporidium toruloides*, *L. starkeyi*, and *Yarrowia lipolytica* (Yu et al., 2011). *C. curvatus*, therefore, was expected to be the highest oil producer in this study.

7.2.2 Chemical pretreatments

7.2.2.1 Ozonation pretreatment (Ozone)

Wheat straw was ground to obtain particles ranging from 0.354 to 0.5 mm in size. These wheat straw particles were then used for the ozone pretreatment. Ozone was produced by a L11-L24 Ozone Generator manufactured by Pacific Ozone, CA, USA. The particle samples (3 g) were adjusted for moisture (90% w/w) and placed into an enclosed stainless steel reactor, with a 1 cm bed height to ensure equal contact time between all particles and the ozone. The reactor was operated in a semi-continuous mode. The ozonation reaction was performed under 5.3% ozone concentration (w/w), at a flow rate of 2,000 mL min^{-1} for 10 minutes. The ozone dose was 0.79 g O_3 g^{-1} total solids (TS). These processed samples were used for further investigation.

7.2.2.2 Soaking aqueous ammonia pretreatment (SAA)

The wheat straw particle samples were pretreated by soaking aqueous ammonia (SAA) using 28-30% (w/w) ammonium hydroxide solution (JTB-9721-03), with a solid-to-liquid ratio of 2:10 at 50°C for 24 hours without agitation in a 1,000 mL screw cap Pyrex solution bottle. After completion of the incubation, the particles were washed twice thoroughly with distilled water to reach a neutral pH. The resultant cake was dried at 50°C and used for further investigation.

7.2.2.3 Ozonation and soaking aqueous ammonia pretreatment (OSAA)

Wheat straw samples were pretreated using the above-described ozone pretreatment for 10 minutes, followed by the SAA pretreatment, also described above, for 6 hours. The resulting material was used for further investigation.

7.2.3 Enzymatic hydrolysis of pretreated lignocellulosic materials

The enzymatic hydrolysis of the pretreated wheat straw was carried out at 2.5% (w/v) solid loading in 50 mL working solution in 250 mL 0.05 M citric acid buffer (pH 4.8) containing 1% (v/v) Cellic® CTec2 (Novozymes). The reaction was conducted at 50°C in an orbital shaker for 48 hours. The total sugars released after 48 hours of incubation were then measured.

7.2.4 Determination of sugar content in pretreatment liquid

Glucose, xylose and cellobiose were analyzed using a Dionex ICS-3000 ion chromatography system (Dionex Corp., CA), employing CarboPac TM PA 20 (4 × 50 mm) and CarboPac TM PA 20 (3 × 30 mm) columns as described by Yu et al. (2011), with minor modifications. The gradient profile used for the chromatographic separation was: 80% eluent A (deionized water) with 20% eluent B (50 mM NaOH) at a flow rate of 0.4 mL min^{-1} for 4 minutes, 80% eluent A with 20% eluent B at a flow rate of 0.5 mL min^{-1} for 26 minutes, and 100% eluent C (200 mM NaOH) at a flow rate of 0.5 mL min^{-1} for 30 minutes.

7.2.5 Yeast strains and medium

Three yeasts—*Cryptococcus curvatus ATCC 20509*, *Rhodotorula glutinis ATCC 204091* and *Yarrowia lipolytica ATCC 20460*—were evaluated in this study (Figure 7.2). Each yeast was

grown in the medium containing 3 g L^{-1} of yeast extract, 3 g L^{-1} of malt extract, 5 g L^{-1} peptone, and 10 g L^{-1} xylose. A culture of yeast was first incubated at 30°C and 150 rpm for 24 hours for seed. Seed cultures (10% v/v) were added to the culture medium, which contained 50 mL non-detoxified enzymatic hydrolysate, as well as 0.4 g L^{-1} $MgSO_4$-7▪H_2O, 2 g L^{-1} KH_2PO_4, 0.003 g L^{-1} $MnSO_4$▪H_2O, 0.0001 g L^{-1} $CuSO_4$▪$5H_2O$, and 1.5 g L^{-1} yeast extract. Cultures were maintained at 30°C and 200 rpm in 250 mL flasks unless stated otherwise.

Figure 7.2: Three species of oleaginous yeasts. From left to right: *Cryptococcus curvatus*, *Rhodotorula glutinis* and *Yarrowia lipolytica*.

7.2.6 Cell dry weight measurement

To determine the amount of biomass, the pipette tips and saline water were first sterilized. A 0.5-1 mL cell suspension sample was centrifuged at 9,000 rpm for 3 minutes. The cell pellet was then washed with sterile saline water. The 0.5-1 mL solutions were placed in dried pre-weighed aluminum dishes. The samples were weighed, placed in the oven at 105°C for 16 hours, then weighed again. The final mass was expressed as dry cell weight.

7.2.7 Measuring the fatty acids in lipids

For the fatty acid profile, a Fatty Acid Methyl Esters (FAME) analysis was used. The sample was prepared as follows: 5.3 mL of methanol and 1 mL of tridecanoic acid (0.5 mg mL^{-1} in methanol) were added to each 1.0 mL of yeast culture. The sample was placed in a Vortex for 30 seconds. Then 0.7 mL of 10 KOH in water was added to dissolve the biomass, finishing with esterification for 15 minutes at 85°C. 0.58 mL H_2SO_4 (12 M) was added, and the sample again placed in the Vortex for 1 minute. The samples were then cooled down with tap water. Finally, 2.0 mL H_2O were mixed in, then 2.0 mL hexane were added. The samples were centrifuged at 3/4 1,500 g for 2 minutes, then the top hexane layer was transferred into gas chromatography vials for the FAME analysis.

A Gas Chromatography–Flame Ionization Detector (GC-FID) analysis was carried out on an Agilent 6890N Network gas chromatography system equipped with a flame ionization detector, an Agilent 7683 series autosampler, and an Agilent chemstation. An HP-5 column with 0.25 μm film thickness (30 m × 0.320 mm I.D., USA) was used for separation. Splitless injection was used, and the carrier gas was nitrogen at a flow rate of 2 mL min^{-1}. Nitrogen (25 mL min^{-1}), hydrogen (40 mL min^{-1}) and dry air (400 mL min^{-1}) were used as auxiliary gases for the flame ionization detector. The injector and detector temperatures were 300°C. The oven temperature was held at 150°C for 1 minute and then increased to 320°C at a rate of 28°C min^{-1}. The temperature was held at 320°C for 3 minutes.

The FAME profile was identified using Gas Chromatography–Mass Spectrometry (GC-MS) by the Institute of Biological Chemistry at WSU. An Omegawax 250 Column was used for the separation of FAME.

7.3 Results and discussion

7.3.1 Sugar content after pretreatment and hydrolysis

The sugar content in the samples measured after the different pretreatments and the enzymatic hydrolysis procedure showed that the OSAA pretreatment produced the highest total amount of sugars, as well as the highest amount of each of the three main ones: glucose, xylose and arabinose (Table 7.1).

Table 7.1: The sugar composition of wheat straw after different pretreatments and hydrolysis.

Pretreatment	Glucose ($g\ L^{-1}$)	Xylose ($g\ L^{-1}$)	Arabinose ($g\ L^{-1}$)	Total sugar ($g\ L^{-1}$)
OSAA+Hydrolysis	12.50	9.00	0.70	22.2
SAA+Hydrolysis	6.00	1.88	0.10	7.98
Ozone+Hydrolysis	2.19	3.18	0	5.67

In order to compare the three pretreatments for yeast fermentation, we optimized the three different non-detoxified liquids obtained via hydrolysis to a total sugar content of 20.0 $g\ L^{-1}$ (Table 7.2).

Table 7.2: The sugar composition of pretreated samples optimized for use in the yeast fermentation step.

Pretreatment	Glucose ($g\ L^{-1}$)	Xylose ($g\ L^{-1}$)	Arabinose ($g\ L^{-1}$)	Total sugar ($g\ L^{-1}$)
OSAA+Hydrolysis	11.26	8.11	0.63	20.00
SAA+Hydrolysis	15.03	4.71	0.25	20.00
Ozone+Hydrolysis	7.72	11.22	0	20.00

7.3.2 Conversion of sugars to microbial lipids

The fermentable sugars produced by the enzymatic hydrolysis were converted into microbial lipids via fermentations by the three different yeasts. The total fatty acid content obtained from the different yeasts when wheat straw was pretreated through three different routes ranged from 5% to 42% (Table 7.3). The highest single cell oil contents were obtained using *C. curvatus*, as expected, based on wheat straw pretreated with SAA (Table 7.3).

The OSAA pretreatment may be an efficient approach for the production of sugars from wheat straw. However, once optimized for yeast fermentation, the SAA pretreated samples produced approximately 3- to 5-fold more total fatty acids than the OSAA pretreated samples, depending on the yeast strain used (Table 7.3). The Ozone pretreatment had low microbial biomass

production (Table 7.3), possibly due to the production of some phenolic compounds, such as phenolic acid, which are toxic for cell growth. Therefore only the data from the SAA and OSAA pretreatments are shown.

Table 7.3: Single cell oil from three oleaginous yeasts by SHF, feeding on feedstocks prepared with different pretreatment methods.

	SAA			OSAA			Ozone*
	DCW ($g\ L^{-1}$)	**Total fatty acids ($g\ L^{-1}$)**	**Fatty acid (%)**	**DCW ($g\ L^{-1}$)**	**Total fatty acids ($g\ L^{-1}$)**	**Fatty acid (%)**	**DCW ($g\ L^{-1}$)**
C. curvatus	16.4	6.9	42.08%	12.3	1.4	11.38%	6.5
R. glutinis	15.7	5.08	32.33%	11.3	1.2	10.62%	1.2
Y. lipolytica	12.0	0.98	6.83%	6.0	0.3	5.00%	4.0

* The Ozone pretreatment produced very low biomass, so the total fatty acids were not measured.

The fermentation step results showed that all the three species of yeast simultaneously utilized glucose and xylose (Figure 7.3). Among the three species, *Cryptococcus curvatus* was able to use the xylose the fastest and most completely. However, *C. curvatus* was unable to assimilate glucose when the concentration of glucose was at very low concentrations (0.24-0.64 $g\ L^{-1}$) (Figure 7.3A and B). *R. glutinis* and *Y. lypolitica* also showed fast utilization of xylose (Figure 7.3C to F). However, these two species showed a higher preference for glucose, relative to *C. curvatus*. *R. glutinis* and *Y. lypolitica* also assimilated glucose and arabinose completely (Figure 7.3C to F).

The gas chromatography results showed that *C. curvatus*, *R. glutinis* and *Y. lypolitica* had very similar fatty acid profiles. Most of the lipids present were C16:0, C18:0, C18:1 and C18:2 (Table 7.4).

Table 7.4: Highest single cell oil profiles from SAA.

	Fatty acid Profiles*
Cryptococcus curvatus	$C^{14:0}$,**$C^{16:0}$**,$C^{16:1}$, $C^{17:0}$,$C^{17:1}$,**$C^{18:0}$**, **$C^{18:1}$**, **$C^{18:2}$**, $C^{18:3}$, $C^{20:0}$, $C^{20:1}$, $C^{22:0}$, **$C^{24:0}$**
Rhodotorula glutinis	$C^{14:0}$, **$C^{16:0}$**,$C^{16:1}$, $C^{17:0}$,$C^{17:1}$,**$C^{18:0}$**, **$C^{18:1}$**, **$C^{18:2}$**, **$C^{18:3}$**, $C^{20:0}$, $C^{20:1}$, $C^{22:0}$, $C^{24:0}$
Yarrowia lipolytica	$C^{14:0}$, **$C^{16:0}$**,$C^{16:1}$, $C^{17:0}$,$C^{17:1}$,**$C^{18:0}$**, **$C^{18:1}$**, **$C^{18:2}$**, $C^{18:3}$, $C^{20:0}$, $C^{20:1}$, $C^{22:0}$, **$C^{24:0}$**

* Fatty acids with concentrations greater than 100 $mg\ L^{-1}$ are exhibited in bold.

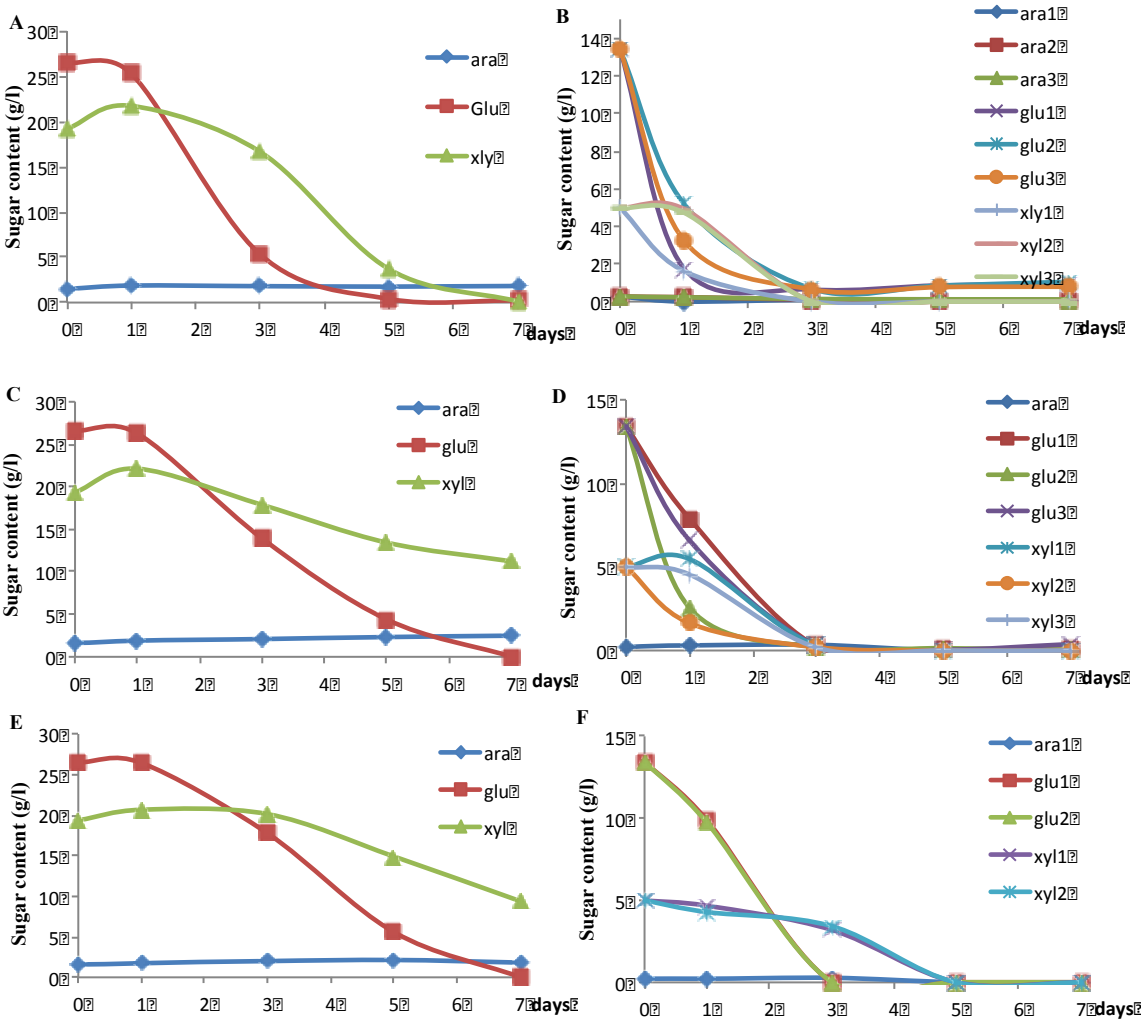

Figure 7.3: Time course of sugar co-fermentation by three oleaginous yeast. *C. curvatus* SAA (A) and OSAA (B); *R. glutinis* SAA (C) and OSAA (D); *Y. lypolitica* SAA (E) and OSAA (F); *ara* represents arabinose, *glu* represents glucose and *xyl* represents xylose.

7.3.3 Advantages of the oleaginous yeast *Cryptococcus curvatus*

The advantages of *C. curvatus* have been described in previous research carried out in this laboratory (for more details see Yu et al., 2011; Zhang et al., 2011). *C. curvatus* exhibits the best tolerance towards inhibitors generated in the pretreatment process, and good profile of lipids accumulation (Figure 7.4). Table 7.5 and Table 7.6 show the growth profiles, lipids accumulation profiles, and fatty acids profiles of different yeasts under non-detoxified and detoxified conditions.

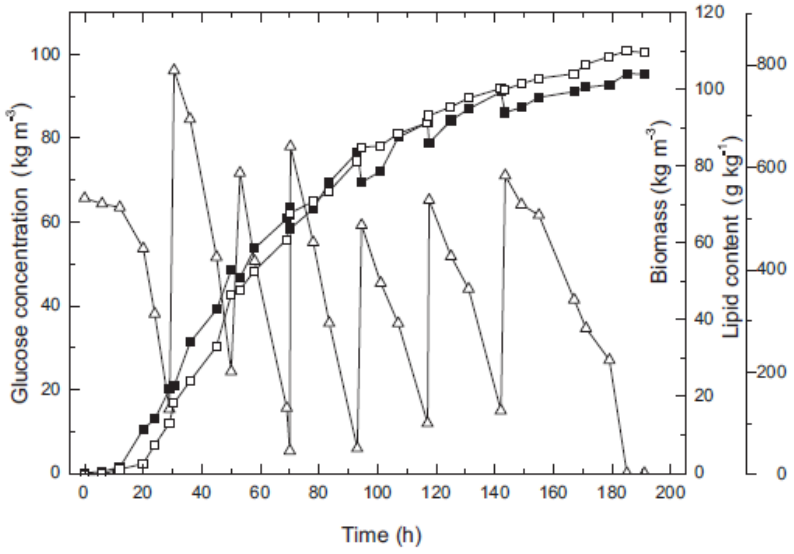

Figure 7.4: Fed-batch fermentation profile of *C. curvatus* O3 in a 30*10^{-3} m^3 fermenter. △: Glucose concentration; ■:Biomass; □: Lipid content (Zhang et al., 2011).

Table 7.5: Effect of non-detoxified liquid hydrolysate (NDLH) and detoxified liquid hydrolysate (DLH) on yeast strain cell growth (dry cell weight—DCW) and lipid accumulation (Yu et al., 2011).

Strain	DCW(g/L)		Lipid content(%, w/w)		Lipid concentration in medium (g/L)	
	NDLH	DLH	NDLH	DLH	NDLH	DLH
Y. lipolytica	7.8 ± 0.7	7.2 ± 0.2	4.6 ± 0.0	4.4 ± 0.3	0.4 ± 0.0	0.3 ± 0.0
C. curvatus	17.2 ± 0.4	15.6 ± 0.0	33.5 ± 0.1	27.1 ± 0.6	5.8 ± 0.1	4.2 ± 0.1
R. glutinis	13.8 ± 0.3	11.8 ± 0.3	25.0 ± 0.6	20.7 ± 0.9	3.5 ± 0.0	2.4 ± 0.2
R. toruloides	N/D	9.9 ± 0.0	N/D	24.6 ± 0.7	N/A	2.4 ± 0.1
L. starkeyi	14.7 ± 0.5	12.7 ± 0.2	31.2 ± 1.3	29.1 ± 0.5	4.6 ± 0.0	3.7 ± 0.0

Experiments were conducted at 28 °C and 200 rpm for 6 days.
N/D: not detected.
N/A: not available.

Table 7.6: Fatty acid profiles of lipids accumulated utilizing non-detoxified liquid hydrolysate (NDLH) and detoxified liquid hydrolysate (DLH) (Yu et al., 2011).

Strain	Relative fatty acid content (%)							
	C16:0		C18:0		C18:1		C18:2	
	NDLH	DLH	NDLH	DLH	NDLH	DLH	NDLH	DLH
Y. lipolytica	6.0 ± 0.8	5.7 ± 1.3	2.0 ± 0.3	0.8 ± 0.1	56.0 ± 3.5	55.3 ± 1.0	19.9 ± 3.5	20.9 ± 0.3
C. curvatus	25.9 ± 0.0	27.0 ± 0.0	15.2 ± 0.2	15.3 ± 0.2	47.7 ± 0.3	45.0 ± 0.0	6.42 ± 0.1	7.3 ± 0.0
R. glutinis	23.5 ± 0.8	22.4 ± 0.3	9.0 ± 0.2	9.3 ± 0.4	43.4 ± 0.3	42.7 ± 0.3	15.4 ± 0.3	17.0 ± 0.6
R. toruloides	N/A	19.8 ± 0.3	N/A	5.9 ± 0.1	N/A	53.4 ± 0.1	N/A	13.5 ± 0.1
L. starkeyi	36.2 ± 0.1	37.1 ± 0.2	4.5 ± 0.0	5.5 ± 0.3	46.3 ± 0.4	45.1 ± 0.0	3.4 ± 0.2	4.9 ± 0.0

In this study, *C. curvatus* still developed a good profile of lipids accumulation (Table 7.3). *Cryptococcus curvatus* provided 16.4 g L^{-1} biomass and 6.9 g L^{-1} lipids, which can reach as high as 42.08% of the dry cell weight. Moreover, this species produced over 50 mg L^{-1} of several kinds of long chain polyunsaturated fatty acids (chains longer than C20) (results not shown), much more unsaturated long chain fatty acids than *Rhodotorula glutinis* or *Yarrowia lipolytica*.

The production of these unsaturated long chain fatty acids suggests that *Cryptococcus curvatus* could have potential as a platform for metabolic engineering.

The results of this project, which used fermentable sugars produced from wheat straw to support microbial lipid production, indicate that *C. curvatus* was a desirable producer of microbial lipids in the context of lignocellulosic sugar fermentation.

7.4 Conclusions

Anaerobic digestion fiber, wheat straw, and other lignocellulosic biomass are desirable feedstock for lipid production, and are widely available in Washington State. Among the three pretreatment methods evaluated, the SAA pretreatment followed by hydrolysis was the most efficient pretreatment method for the single cell oil production by oleaginous yeasts. The OSAA pretreatment may be an efficient approach for the production of sugars from wheat straw, especially xylose. The Ozone pretreatment had low microbial biomass production, possibly due to the production of some phenolic compounds, such as phenolic acid, which are toxic for cell growth. Hence, the non-detoxified liquid obtained from this pretreatments supported only low levels of microbial biomass production, so was not considered further.

Among the yeasts tested for their ability to utilize the lignocellulosic biomass for production of lipids, *Cryptococcus curvatus* was the best producer. *C. curvatus* assimilated xylose very fast, without this assimilation being inhibited by glucose. Moreover, this species was able to fully harvest the xylose, leaving a relatively low amount of glucose unused.

There are multiple advantages to using *Cryptococcus curvatus*, which will make this species a good platform for the production of biofuels from sustainable bioresources in the future, as well as showing potential for metabolic engineering of lipids.

7.5 References

Fairley, P. 2011. Next generation biofuels. Nature 474(7352), S2-S5.

Gao, D., Zeng, J., Zheng, Y., Yu, X., Chen, S. 2013. Microbial lipid production from xylose by Mortierella isabellina. Bioresource Technology 133, 315-321.

Subramaniam, R., Dufreche, S., Zappi, M., Bajpai, R. 2010. Microbial lipids from renewable resources: production and characterization. Journal of Industrial Microbiology and Biotechnology 37(12), 1271-87.

Wen, Z., Liao, W., Chen, S. 2005. Production of cellulase/β-glucosidase by the mixed fungi culture *Trichoderma reesei* and *Aspergillus phoenicis* on dairy manure. Process Biochemistry 40(9), 3087-3094.

Xu, J., Du, W., Zhao, X., Zhang, G., Liu, D. 2013. Microbial oil production from various carbon sources and its use for biodiesel preparation. Biofuels, Bioproducts and Biorefining 7(1), 65-77.

Yu, X., Zheng, Y., Dorgan, K.M., Chen, S. 2011. Oil production by oleaginous yeasts using the hydrolysate from pretreatment of wheat straw with dilute sulfuric acid. Bioresource Technology 102(10), 6134-6140.

Zhang, J., Fang, X., Zhu, X.-L., Li, Y., Xu, H.-P., Zhao, B.-F., Chen, L., Zhang, X.-D. 2011. Microbial lipid production by the oleaginous yeast *Cryptococcus curvatus* O3 grown in fed-batch culture. Biomass and Bioenergy 35(5), 1906-1911.

8. A Comprehensive Techno-Economic Model to Evaluate Different Anaerobic Digestion Options for Various Applications

Liang Yu and Shulin Chen

8.1 Background

Anaerobic digestion (AD) has recently become an increasingly important industrial process. Anaerobic digestion is a green technology involving the generation of methane-rich biogas via the biological degradation of regionally available biomass like agricultural residues and municipal solid wastes and wastewaters. Anaerobic digestion processes have for many years been used to treat and sanitize sewage sludge waste from aerobic wastewater and animal manure, to reduce its odor and volume, and to produce useful biogas. Biogas in turn is a first-generation, renewable biofuel that offers the prospect of replacing fossil fuels in the transportation sector and limiting the net greenhouse gas emissions that contribute to climate change (Magnusson and Alvfors, 2012).

Co-digestion refers to the simultaneous anaerobic digestion of multiple organic residues in one digester. Co-digestion is used to increase methane production from low-yielding or difficult to digest materials. In agriculture, co-digestion is often used to increase the methane production from the anaerobic digestion of manure. Since crop residues have higher total solid:volatile solid ratios (TS:VS) than manure, they often produce more biogas. Especially after pretreatment, the biogas productivity of crop residues can be increased by 20% (Yuan et al., 2015).

Between 1950 and 1980, high production-rate systems were developed and used to process effluents from agricultural and industrial sectors. Processing of effluents that contained toxic and recalcitrant compounds from the pulp and paper, petrochemical, and other chemical industries was later possible as both technology and knowledge pertaining to toxicity and biodegradability improved (Mata-Alvarez et al., 2000). Anaerobic digestion technology has been widely adopted by Germany and Denmark, which have implemented rigorous waste disposal legislation. Since 2000, annual electricity generation from digester projects in the U.S. has increased almost 25-fold, from 14 million kilowatt-hours (kWh) to an estimated 331 million kWh per year (EPA, 2010).

The majority of current agricultural biogas facilities digest chicken, cow, and pig manure, supplemented with co-substrates to increase the content of organic material and the gas yield. Such co-substrates have routinely included harvest residues (e.g. sugar beet leaves and tops), agricultural organic residues (e.g. energy crops), and municipal food and biowaste collected from restaurants and households (Appels et al., 2008; Cakir and Stenstrom, 2005; Chynoweth and Isaacson, 1987) (see Table 8.1 for the typical composition of common AD substrates). Substrate digestibility and biogas production are affected by substrate salinity, loading rate, mineral and volatile fatty acid composition, carbon-to-nitrogen ratio, and pH, as well as reactor temperature

and hydraulic retention time (Krzystek et al., 2001; Novak et al., 2003; Sanchez et al., 2006). Compared to AD systems in rural areas, those in urban settings require higher retention of biomass, smaller reactor volumes, shorter hydraulic retention times, and higher loading rates.

Table 8.1: Typical composition for common substrates used in anaerobic digestion.

Composition	**Dairy manure** (Amon et al., 2006**;** Stafford et al., 1980)	**Food scraps** (Buffiere et al., 2006)	**Swine manure** (Boopathy, 1998**;** Xiu et al., 2010)	**Wheat straw** (Kaparaju et al., 2009)	**Corn Stover** (Humbird et al., 2011**;** Yuan et al., 2015)
Cellulose (mg g^{-1} DM[1])	310	39 – 126	59.7	359.7	388.1
Hemicellulose (mg g^{-1} DM)	120	85 – 295	199 – 281.1	239.5	295.0
Lignin (mg g^{-1} DM)	122 – 190	19 – 96	40 – 124.7	193.3	66 – 112
Crude protein (mg g^{-1} DM)	125 – 297	90 – 208	171 – 217.8	6.5	31 – 40
Lipid (mg g^{-1} DM)	23.8 – 46.4	35 – 81	48.6 – 127.6	1.5	12 – 30
Carbohydrate (mg g^{-1} DM)	125	263 – 609	151.2 – 931.8	853.1	351 – 806

[1] DM: dry matter.

Digestion technology is environmentally beneficial as it captures and combusts the methane (CH_4), a greenhouse gas, produced when these waste products decompose. The technology consists of an airless vessel and heating system to optimize a naturally occurring biological process. The direct result of the process is the production of methane and a reduction in harmful organisms. A metric ton of methane has a global warming capacity twenty-five times greater than an equal amount of carbon dioxide (Bishop and Shumway, 2009). Digestion also reduces the organisms that generate high chemical and biological oxygen demand in dairy manure. Further benefits of digestion technology include electrical production, reduced on-farm odor, and pathogen-free fiber for animal bedding. These benefits make digestion technology potentially desirable for dairy farms and the surrounding communities (Bishop and Shumway, 2009).

While digestion technology has multiple benefits, it has not been widely adopted in the United States (Bishop and Shumway, 2009). The limited adoption of digestion could be due to financial infeasibility or lack of information regarding the financial feasibility of digestion, or both. This project explores the possibility that the key to techno-economic feasibility lies in co-product marketing from multiple integrated processes. The best- documented co-product of anaerobic digestion is electricity (Lazarus and Rudstrom, 2007). In addition to the energy output, potential co-product revenue streams include avoided costs of other farm inputs (e.g., fertilizer purchases), heat exchange, and revenue from services (e.g., accepting food scraps). A series of research

reports have recommended that an integrated framework including multiple conversion routes would be the best approach to developing a sustainable, cost-efficient renewable energy system (Yuan and Chen, 2012).

To comprehensively assess the integration benefits from multiple unit operations, the process integration methodology commonly used in sustainable process systems engineering (PSE) can be used, thereby reducing and focusing the need for expensive experimental research. Process systems engineering is a relatively young field of chemical engineering (about 35 years old), focusing on the design, operation, control and optimization of processes via the systematic aid of computer-based methods (Jacquemin et al., 2012). This field "develops methods and tools that allow industry to meet its needs by tying science to engineering" (Grossmann, 2004), and encompasses a vast range of industries, such as petrochemical, mineral processing, advanced material, food, pharmaceutical and biotechnological.

So far, the field of process systems engineering has been used to support the conceptual design of an integrated biorefinery, and to address to the specific technical barriers in generating optimal design (Kokossis and Yang, 2010). Process systems engineering tools are able to generate alternatives that fulfill optimization objectives such as minimum cost or environmental impact. Established processing pathways available at commercial scales have been extensively analyzed and optimized. Such processes include power and heat generation (Lumley et al., 2014; Pantaleo et al., 2014; Uris et al., 2014), biodiesel production (Brownbridge et al., 2014; Glisic and Orlovic, 2014; Koutinas et al., 2014), and bioethanol production (Littlewood et al., 2013; Meyer et al., 2013; Song et al., 2014).

As for the techno-economic evaluation of lignocellulosic ethanol, the first detailed technical reports found in the literature concerning U.S. cases date back to the mid-1980s. Since 1987, the U.S. National Renewable Energy Laboratory (NREL) has received several technical reports delivered by subcontractors (Aden et al., 2002; Badger Engineers Inc., 1987; Humbird et al., 2011; Wooley et al., 1999). The differences between them are related to the size of the plant, the type of hydrolysis and the mode of electricity supply (Gnansounou and Dauriat, 2010). Flowsheeting and simulation studies certainly dominate the literature, as in the work of Alzate and Toro (2006), who used Aspen Plus (Aspen Technologies Inc., USA) to evaluate process configurations in the production of ethanol from lignocellulosic biomass. Therefore, it is feasible to use the aforementioned process modeling method and technology to assess the integration of anaerobic digestion and related technologies developed at Washington State University (WSU) to broaden the application of AD for co-processing manure and agricultural residues.

This project had three specific objectives, which were to:

(1) Use a process model to develop a novel ammonia recycling technology.
(2) Develop a process model that included pretreatment, AD, biogas purification and nutrient recovery.
(3) Compare the profitability of these technologies when applied using different feedstocks for co-digestion (food scraps, animal manure and agricultural residues).

8.2 General description of the process model

In this project, a holistic process model was developed to integrate pretreatment, AD, and nutrient recovery (Figure 8.1). The corresponding modules were developed for these processes. The feedstocks include lignocellulosic materials (wheat straw, corn stover), food scraps, dairy manure and swine manure. Most of the lignocellulosic materials are fed to pretreatment, while most of degradable organic are fed directly to AD (Figure 8.1). The AD effluent is then fed to nutrient recovery for nitrogen (N) and phosphorous (P) removal. The AD biogas is purified to produce compressed natural gas (CNG, which is greater than 96% CH_4).

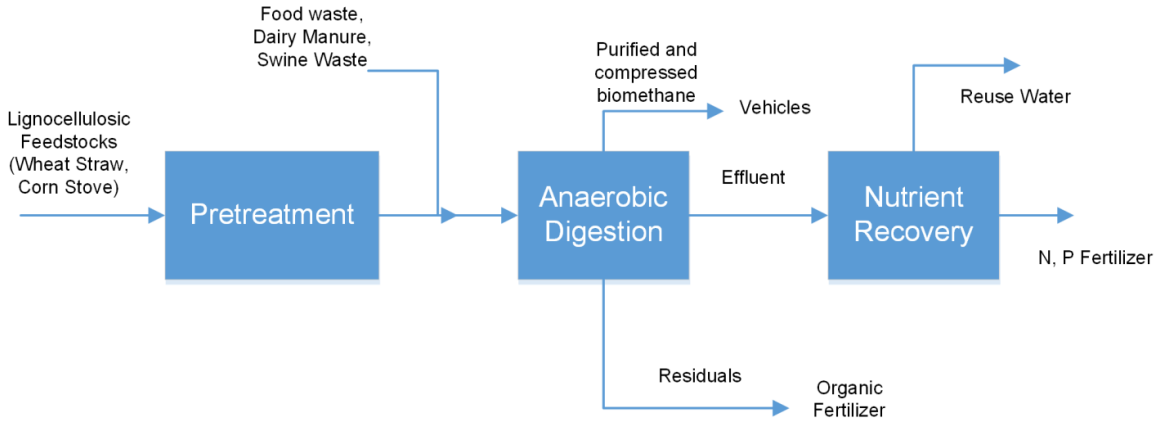

Figure 8.1: A holistic process model that integrates pretreatment, AD, and nutrient recovery.

8.3 Novel ammonia recycling technology

8.3.1 Concept and process model description

The proposed novel technology for recycling ammonia improves upon AIRTRAP technology, using the recovered ammonia for biogas purification and pretreating of crop residues and manure fibers. After the AD of high-N and -P organic residues, such as animal manure and food scraps, the majority of the effluent is sent to an ammonia stripping column where biogas with low CO_2 content is used as the stripping agent to remove ammonia from the effluent under a higher temperature (over 50°C). After stripping, the effluent with low ammonia concentration can be reused as dilution water for high-solids feedstock entering the digester. Separately, the ammonia-bearing biogas and vapor will be sent to a CO_2 and H_2S absorber, where ammonia is absorbed under slightly higher pressure with CO_2 to precipitate into crystalline NH_4HCO_3 at low temperature (under 30°C). The biogas stream is purified by cycling through the CO_2, NH_3, and H_2S absorber several times, before achieving a target level of purity (96%, for example). The crystalline NH_4HCO_3 is sent to the CO_2 regenerator to be heated to a temperature greater than 50°C. This causes the NH_4HCO_3 to decompose into ammonium and carbon dioxide. Additionally, H_2S contained in the stream will also leave the solution. This process allows for

separation of the H_2S and CO_2 into their gaseous forms, while retaining ammonia in the solution in the form of NH_4OH.

The mixture of NH_4OH/NH_4HCO_3 remaining in the solution will then be diluted and used to pretreat the lignocellulosic feedstocks, such as crop residues. The pretreated solids are then fed to the anaerobic digester. The ammonia can be recycled to remove more CO_2 from the biogas by forming NH_4HCO_3. Excess ammonia can also be directed to a separate side stream to react with H_2SO_4 to produce ammonium sulfate fertilizer. In this process, ammonia is used for both pretreatment and biogas purification through reacting with CO_2 to form NH_4HCO_3.

The major difference between this concept and the previously developed AIRTRAP technology is the use of biomethane instead of air to strip ammonia, thus avoiding introducing air as a separate stream. However, a series of experiments need to be conducted to understand the process equilibrium to enhance the efficiency of the ammonia-CO_2 conversion process and the lignocellulose pretreatment process.

Ammonia recycling technology process description: A process model was developed to study the feasibility of the proposed novel technology for recycling ammonia (Figure 8.2). Effluent is fed to the ammonia stripping tower (F-101 in Figure 8.2). The tower temperature is 55°C and the pressure is 0.163 atm. After stripping, the effluent with low ammonia content (S-103 in Figure 8.2) is sent out of the system. High content ammonia and water vapor (S-101 in Figure 8.2) are sent to the CO_2 and H_2S absorber (R-101 in Figure 8.2). The absorber temperature is 30°C and the pressure is 10 atm. In this absorber, the stripped ammonia reacts with CO_2 in the introduced biogas to generate NH_4HCO_3 crystals. The resultant stream (S-102 in Figure 8.2) is sent into the liquid-solid separator (SEP-101 in Figure 8.2). The liquid stream (S-105 in Figure 8.2) is sent to the flash tank (F-102 in Figure 8.2) where the CH_4 (> 96%) (S107 in Figure 8.2) is separated from the water (S-106 in Figure 8.2). The solid stream (S-104 in Figure 8.2) is sent to the heat exchanger (E-101 in Figure 8.2) and then sent to the CO_2 regenerator (R-102 in Figure 8.2). The regenerator temperature is 70°C and the pressure is 1 atm. The resultant stream (S-109 in Figure 8.2) is then sent to the flash tank (F-103 in Figure 8.2) to separate the CO_2 stream (S-110 in Figure 8.2) from the ammonia water (S-113 in Figure 8.2). The gas phase separator (SEP-102 in Figure 8.2) is used to further separate CO_2 (S-111 in Figure 8.2) from the ammonia water (S-112 in Figure 8.2).

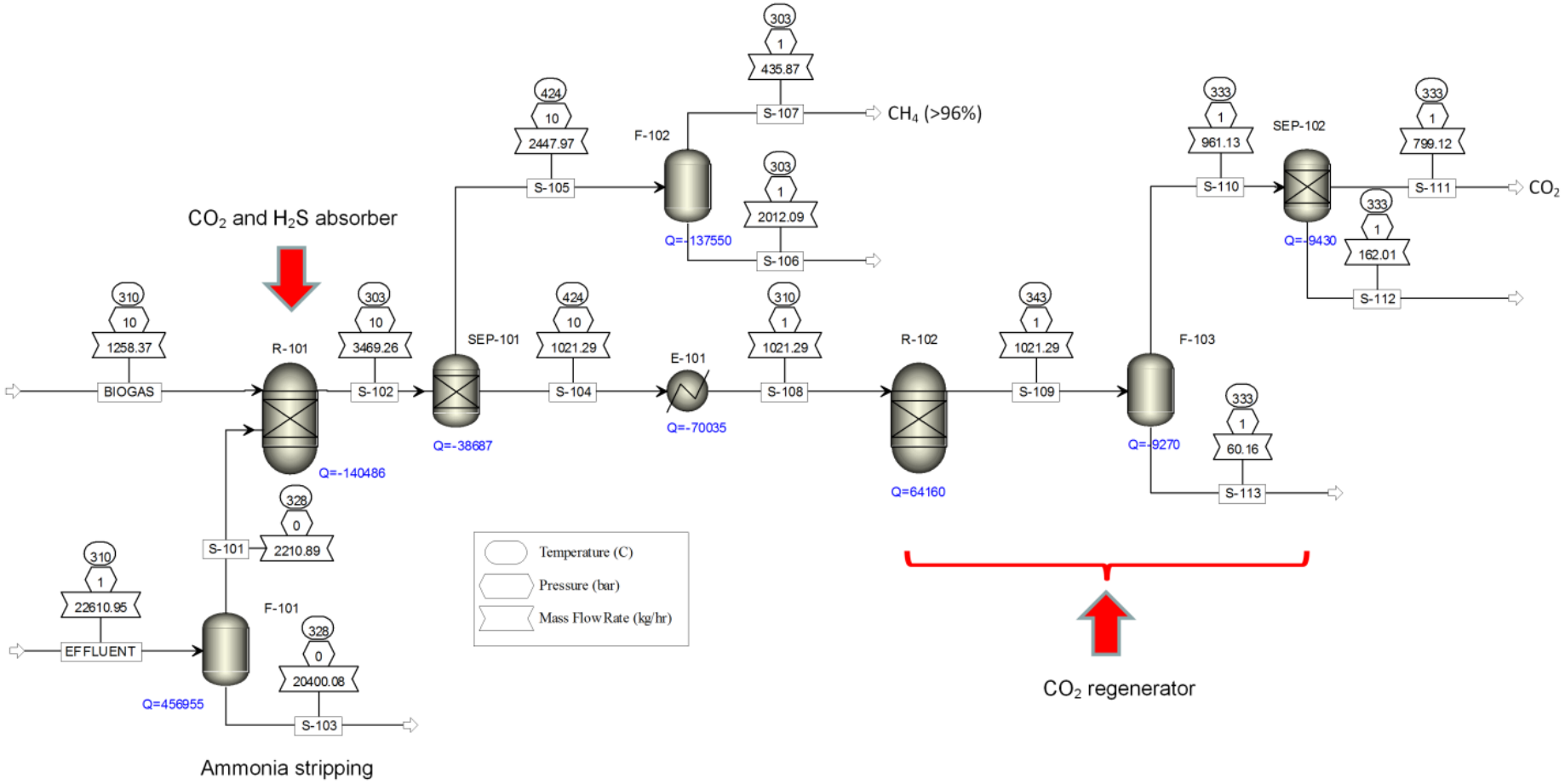

Figure 8.2: Process flow diagram of novel ammonia recycling technology.

8.3.2 Chemical reaction models

To describe the aforementioned ammonia recycling technology, the following reaction models are used in the process model.

(1) Equilibrium reactions:

$$2H_2O \leftrightarrow H_3O^+ + OH^- \quad \text{(R-1)}$$

$$k_{eq,1}=[H_3O^+][OH^-]/[H_2O]^2 \quad (1)$$

$$NH_3 + H_2O \leftrightarrow NH_4^+ + OH^- \quad \text{(R-2)}$$

$$k_{eq,2}=[NH_4^+][OH^-]/([NH_3][H_2O]) \quad (2)$$

$$HCO_3^- + H_2O \leftrightarrow CO_3^{2-} + H_3O^+ \quad \text{(R-3)}$$

$$k_{eq,3}=([CO_3^{2-}][H_3O^+])/([HCO_3^-][H_2O]) \quad (3)$$

$$CO_2 + 2H_2O \leftrightarrow HCO_3^- + H_3O^+ \quad \text{(R-4)}$$

$$k_{eq,4}=[HCO_3^-][H_3O^+]/([CO_2][H_2O]^2) \quad (4)$$

$$NH_3 + HCO_3^- \leftrightarrow NH_2COO^- + H_2O \quad \text{(R-5)}$$

$$k_{eq,5}=[NH_2COO^-][H_2O]/([NH_3][HCO_3^-]) \quad (5)$$

where the equilibrium constants k_{eq} for R-1 to R-5 are computed from Gibbs energies.

(2) Kinetic reactions:

$$CO_2 + OH^- \rightarrow HCO_3^- \quad \text{(R-6)}$$

$$R_6=k[CO_2][OH^-] \quad (6)$$

$$k = k_0 e^{-\frac{E}{RT}} \quad (7)$$

where k is the rate constant of the reaction, the pre-exponential factor is $k_0=4.32\times10^{13,}$ and the activation energy is E=13,249 cal mol^{-1}.

$$HCO_3^- \rightarrow CO_2 + OH^- \quad \text{(R-7)}$$

$$R_7=k[HCO_3^-] \quad (8)$$

where the pre-exponential factor is $k_0=2.38\times10^{17}$ and the activation energy is E=29,451 cal mol^{-1}.

$$NH_3 + CO_2 + H_2O \rightarrow NH_2COO^- + H_3O^+ \quad \text{(R-8)}$$

$$R_8=k[NH_3][CO_2] \quad (9)$$

where the pre-exponential factor is $k_0=1.35\times10^{11}$ and the activation energy is E=11,585 cal mol^{-1}.

$$NH_2COO^- + H_3O^+ \rightarrow NH_3 + CO_2 + H_2O \quad \text{(R-9)}$$

$$R_9=k[NH_2COO^-][H_3O^+] \quad (10)$$

where the pre-exponential factor is $k_0=2.14\times10^{21}$ and the activation energy is E=17,203 cal mol^{-1}.

(3) Salt dissolution reaction:

$$NH_4HCO_3\,(S) \leftrightarrow NH_4^+ + HCO_3^- \quad \text{(R-10)}$$

$$k_{eq,10}=[NH_4^+][HCO_3^-] \quad (11)$$

where the equilibrium constants k_{eq} is computed from Gibbs energies.

8.3.3 Results and analysis

We conducted preliminary mass balance and energy analyses using the ASPEN process (Aspen Plus software, Aspen Technologies Inc., USA) to simulate processing the effluent (542 ton day^{-1}) from an AD facility treating manure from 100,000 pigs. The resulting model output data (provided as the red numbers in Figure 8.3) demonstrated the feasibility of the proposed ammonia recycling technology. The biggest use of energy in this technology was by the

ammonia stripping unit. The heat duty for the CO_2 and H_2S absorber unit was negative, suggesting that no external heat needs to be taken into account. The heat duty for the CO_2 regenerator unit was seven times lower than that for the ammonia stripping unit. The energy consumed by the whole system was approximately 0.15–0.17 kWh per ton of effluent processed. Since the energy-demanding ammonia stripping unit is also a key unit in the AIRTRAP technology, the results show that the proposed ammonia recycling technology would not consume more energy than the AIRTRAP technology commercially available today.

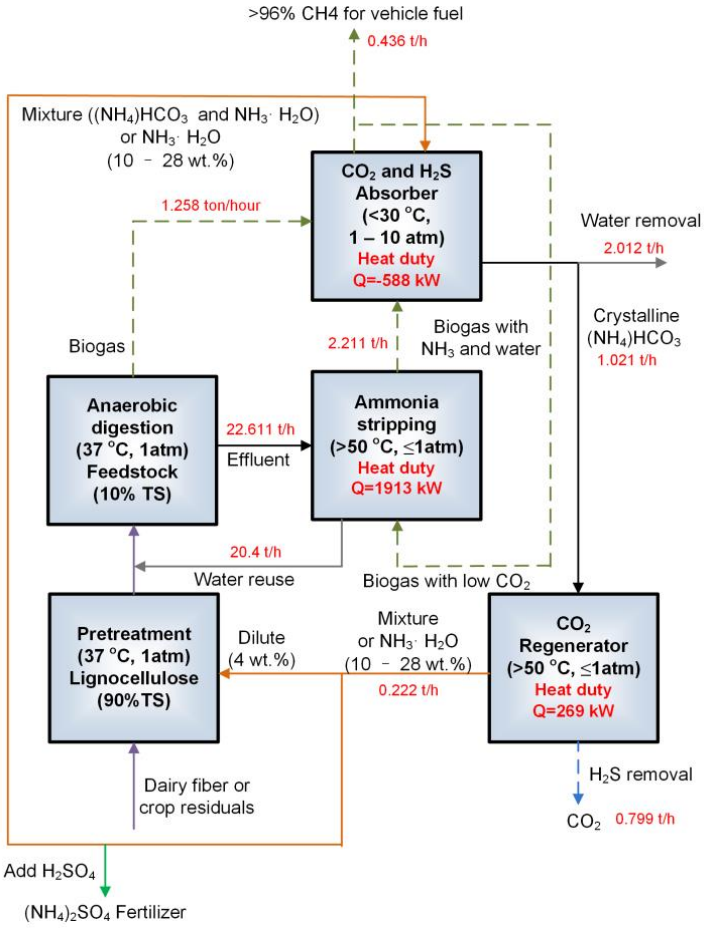

Figure 8.3: Mass balance and energy analysis for the novel ammonia recycling technology.

The proposed ammonia recycling technology therefore provides an option to improve on the currently commercialized AIRTRAP technology, as it provides multiple benefits that can offset the high energy consumption during ammonia stripping:

1) Biogas is purified to produce CNG (CH_4 > 96%). Using ammonia and vapor to capture CO_2 has many advantages. Carbon dioxide absorption operates at lower temperatures. The lower the temperature, the less chance of ammonia evaporating and being discharged into the atmosphere. This process also results in a higher removal efficiency and a greater CO_2 loading capacity (Yeh and Bai, 1999). Ammonia reacts very fast, allowing for a wider operating range. The energy consumption for regeneration is also less than that required by other absorbents such as monoethanolamine, reducing operating costs.

2) Carbon dioxide is released to produce a high purity product (>99.99%). NH_4HCO_3 decomposes above about 36°C into NH_3, CO_2, and water in an endothermic process, and a low enthalpy of dissociation is required to release the CO_2. The solubility of NH_3 (49.6 g g^{-1} water, 20°C) is about 200 times higher than CO_2 (0.17 g g^{-1} water, 20°C), so most of the CO_2 will be released into the gas phase while most of the NH_3 will stay in the liquid phase.

3) Agricultural residues are pretreated with ammonia produced on-site to increase biogas productivity. NH_3 and water vapor stripped from the AD effluent can react with CO_2 to generate crystalline NH_4HCO_3. Theoretically, NH_4HCO_3 crystals can reach 48.6% ammonia concentration via CO_2 removal. However, high energy consumption and cost would be incurred to achieve such concentrations. Most existing pretreatment technologies were developed for bioethanol production, in which a high concentration of ammonia is desirable to obtain more fermentable sugars in the subsequent enzymatic hydrolysis process. However, high ammonia concentrations inhibit the AD process, so a separation process would have to be used to remove the excess ammonia. To avoid such a separation process, low ammonia content should be used to treat the lignocellulosic materials. Yuan et al. (2015) showed that 4% (w/w) ammonia content resulted in the highest biogas production at 37°C, while 6% (w/w) ammonia content caused inhibition. Therefore, to generate ammonia from the effluent, thereby reducing the cost incurred from the purchase of ammonia, a novel pretreatment technology for processing lignocellulosic materials using a combination of NH_4HCO_3 and NH_4OH should be developed to balance biogas productivity with energy consumption.

4) Ammonium sulfate—a fertilizer providing both nitrogen and sulfur—is produced. When the excessive NH_4HCO_3/NH_4OH mixture in the proposed ammonia recycling technology is treated with acid, ammonium sulfate ($(NH_4)_2SO_4$) fertilizer is produced. The value of $(NH_4)_2SO_4$ as a fertilizer is better than that of NH_4HCO_3 (Yeh and Bai, 1999). Although ammonium bicarbonate (NH_4HCO_3) can be directly produced by the reaction of CO_2 and NH_3, there is no significant market in the U.S. for this product (NETL, 2007), due to significant nutrient losses when used as a fertilizer (Yeh and Bai, 1999).

5) About 10% clean water is generated from water vapor, which can be used as livestock drinking water. The other low ammonia effluent can be recycled back to the anaerobic digester without causing inhibition. This technology will significantly reduce the ammonia concentration of the effluent being discharged, which could help dairy farmers comply with current or future ordinances or permit requirements set to avoid environmental impacts.

The process model detailed here showed that the concept of the proposed ammonia recycling technology is technically feasible. To further develop this technology, experiments have to be conducted to refine the necessary information and knowledge for scale-up and commercialization.

8.4 Integration of pretreatment, anaerobic digestion, and nutrient recovery

8.4.1 Process model descriptions

Pretreatment process description: Lignocellulosic materials such as corn stover and wheat straw (S101 in Figure 8.4) are mixed with ammonia in water (4%; S102 in Figure 8.4) (Yang et al., 2014; Yuan et al., 2015). The mixed stream (S103 in Figure 8.4) is fed to a pretreatment reactor (R-101 in Figure 8.4). The reactor temperature is 35±2°C, at atmospheric pressure. After pretreatment, the lignocellulosic materials are sent to the anaerobic digester (Figure 8.5).

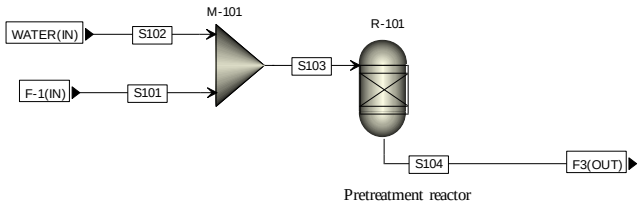

Figure 8.4: Process flow diagram of the pretreatment process.

Anaerobic digestion process description: Food scraps and animal manure (S202 in Figure 8.5) are fed to a mixer (M-201 in Figure 8.5), to mix with the pretreated lignocellulosic materials (S201 in Figure 8.5). These substrates are diluted to 10% total solids using wastewater. The slurry stream (S203 in Figure 8.5) is pumped to a heat exchanger (E-201 in Figure 8.5), and then into an anaerobic digester (R-201 in Figure 8.5). The reactor temperature is 35±2°C, at atmospheric pressure. After anaerobic digestion, the slurry is sent to a buffer tank (FL-202 in Figure 8.5) to separate the biogas. The slurry is continually sent to a solid-liquid separator (SEP-201 in Figure 8.5). After separation of the biogas, the remaining effluent is pumped out of the system and the residuals are also removed. The residuals are used as organic fertilizer. The biogas is sent to a gas purification step (A-201 in Figure 8.5). N-methyl-2-pyrrolidone (NMP) is one of the physical solvent methods commonly used to remove acid gases such as CO_2 and H_2S (Burr and Lyddon, 2008). Higher pressure favors the absorption of CO_2. Thus, the biogas stream (S208 in Figure 8.5) first uses a compressor (C-201 in Figure 8.5) to increase the pressure, and then uses another heat exchanger (E-202 in Figure 8.5) to decrease the temperature. After purification, CH_4 and partial CO_2 removed from the biogas are sent out of the system.

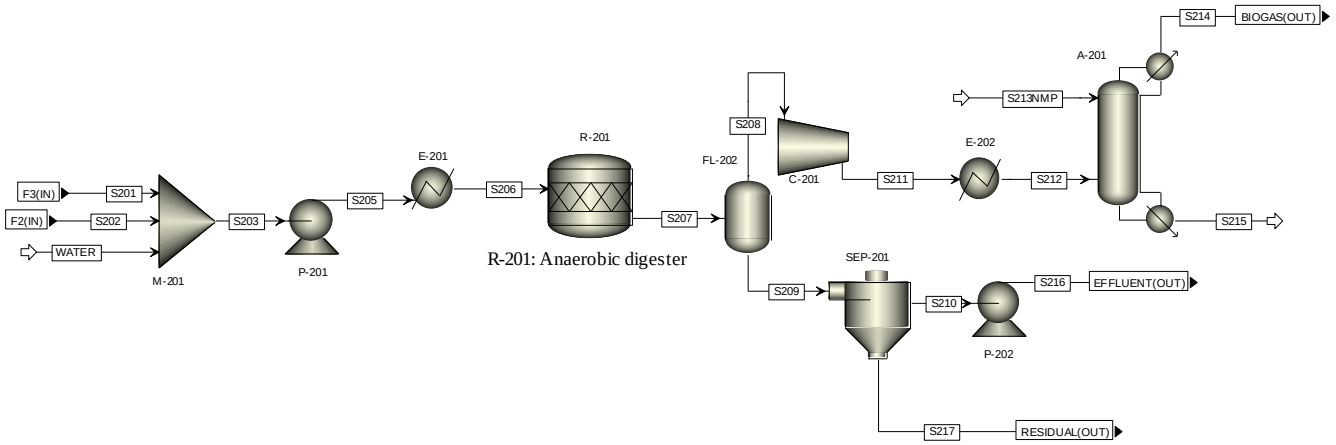

Figure 8.5: Process flow diagram of the AD process.

Nutrient recovery process description: The AD effluent is heated by a heat exchanger (E-401 in Figure 8.6), and then fed into an ammonia stripping tower (A-401 in Figure 8.6). Hot air is used to strip ammonia from the AD effluent. After the stripping process, the top stream (S402 in Figure 8.6) is sent to an N fertilizer reactor. The reactor temperature is 35±2°C, at atmospheric pressure. H_2SO_4 is used to react with the ammonia to form $(NH_4)_2SO_4$, a fertilizer. Liquid ($(NH_4)_2SO_4$ and water, and gas (air), are separated by a flash tank (FL-401 in Figure 8.6). The liquid stream is sent to a dryer (D-401 in Figure 8.6) where water is removed from the $(NH_4)_2SO_4$. The dry N fertilizer is thereby produced. The bottom stream (S406 in Figure 8.6) is fed to a P fertilizer reactor (R-402 in Figure 8.6). The reactor temperature is 35±2°C, at atmospheric pressure. In R-402, $MgSO_4$ is added to precipitate the PO_4^{-3}, which will be used as P fertilizer. The slurry stream (S407 in Figure 8.6) is then separated by SEP-401 to obtain P fertilizer (S409 in Figure 8.6) and wastewater. This wastewater contains little N and P. Thus, it can be reused in the AD without inhibition, and for irrigation without eutrophication.

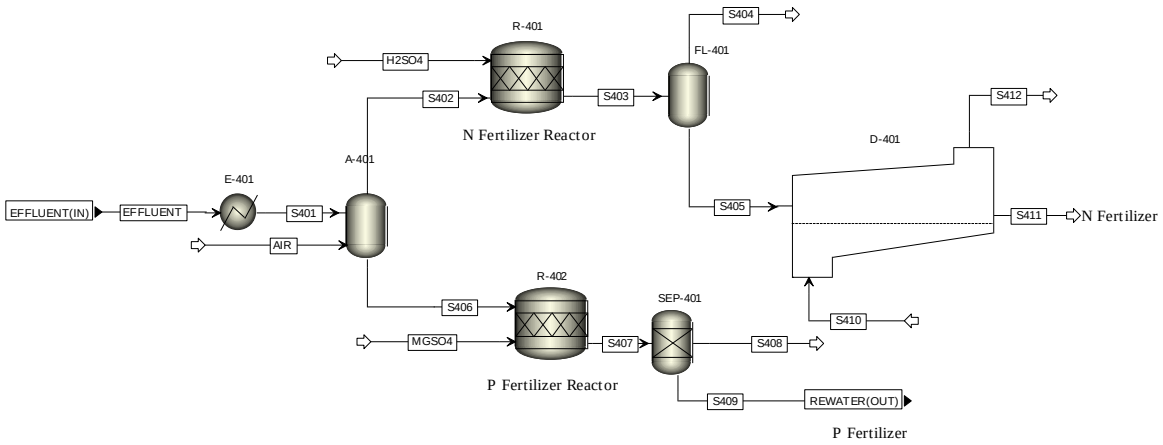

Figure 8.6: Process flow diagram of the nutrient recovery process.

8.5 Techno-economic analysis of anaerobic co-digestion

8.5.1 Profitability of the integrated pretreatment, anaerobic digestion, and nutrient recovery processes

8.5.1.1 Methods

As described above, co-digestion of food scraps, animal manure and lignocellulosic materials was investigated using a holistic process model that integrated pretreatment, AD, and nutrient recovery. The plant size in the above design was 22.5 dry ton day^{-1}. With an expected 8,000 operating hours per year, the annual feedstock requirement is 7,500 dry ton $year^{-1}$. Feedstocks with different total solids (TS) were added to the anaerobic digester. Food scraps, dairy or swine manure were considered to be 30% TS; wastewater was considered to be 1% TS; and lignocellulosic materials (corn stover or wheat straw) were considered to be 90% TS. The biogas yield varied for the different feedstocks (Table 8.2). Ammonia pretreatment conditions were selected to enhance biogas productivity. The corn stover and wheat straw pretreated with 4% ammonia at 70% moisture content showed the highest anaerobic digestibility (Yang et al., 2014; Yuan et al., 2015). Therefore, these conditions were used in the pretreatment process.

Table 8.2: Biogas yield for different substrates.

	Biogas yield (m^3 kg^{-1} TS)	TS[1] (%)	VS[1] (%)	Methane content (%)	Reference
Food scraps	0.561	27.8	24.3	62.6	(Banks et al., 2011)
Dairy manure	0.320	13.8	11.0	65.6	(El-Mashad and Zhang, 2010)
Swine manure	0.305	28.14	22.26	65.9	(Qiao et al., 2011)
Corn stover (Pretreated)	0.398	94.5	88.16	60 – 70	(Yuan et al., 2015)
Wheat straw (Pretreated)	0.304	95.6	85.6	50 – 65	(Yang et al., 2014)

[1] TS: Total solids; VS: volatile solids.

We conducted case studies of the process integration described above using ASPEN Economic Analyzer software (Aspen Technologies Inc., USA), to provide cost estimates for different situations. The process unit operations used were based on existing technologies. The target products included CNG ($0.35 m^{-3}), ammonium sulfate fertilizer ($125 ton^{-1}), phosphate fertilizer ($772 ton^{-1}), and organic fertilizer ($20 ton^{-1}). For food scraps, a tipping fee ($60 ton^{-1}) was also considered. All financial values were adjusted to and reported for the 2012 cost year. The income streams did not include CO_2, carbon credits, and Renewable Identification Numbers (RINs). The cost for purchase, transport and pretreatment of crop residues was $59 ton^{-1} (Humbird et al., 2011). The value of the biogas (>96% CH_4) was based on natural gas prices reported on the U.S. Energy Information Administration's website. The price of organic fertilizer was determined as $20 ton^{-1} (Levis and Barlaz, 2013). The price of ammonium sulfate fertilizer and phosphate fertilizer was based on the Alibaba Group's website. The mass and energy balance outputs from the Aspen models were used to evaluate all capital and operating costs in order to establish an overall cost of the integrated process and the associated profit. All capital

costs for the pretreatment, AD, and nutrient recovery processes were estimated based on vendor quotes from DVO Inc. The desired rate of return was set as 10%.

8.5.1.2 Results and discussion

At the plant capacity modeled in this study, the economic analysis of the co-digestion of dairy manure with corn stover showed that the total investment cannot be paid back (Table 8.3). The discounted cash flow (DCF) technique was used in the comparative appraisal of the investment proposals, where the flow of income varies over time. The internal rate of return (IRR) is the average annual return earned through the life of an investment, and is computed as the discount rate that reduces to zero the net present value (NPV) of a stream of income inflows and outflows. In this case, the IRR (2.58%) was lower than the desired rate of return on investment (10%), thus this case is not a desirable one.

The profitability index (PI), also known as the profit investment ratio (PIR) and value investment ratio (VIR), is the ratio of payoff to investment of a proposed project. It is a useful tool for ranking projects because it allows the user to quantify the amount of value created per unit of investment. The ratio is calculated as follows:

Profitability index = (Present value of future cash flows)/(Initial investment)

Assuming that the cash flow calculated does not include the investment made in the project, a profitability index of 1 indicates a break-even point. In this case, the PI obtained was 0.46, which is lower than 1, suggesting this project cannot make a profit.

Table 8.3: Economic analysis of co-digestion of dairy manure with corn stover.

Input		**Output**	
Dairy manure 30%TS (ton day^{-1})	25	Biogas CNG (m^3 day^{-1})	5,244.39
Wastewater 1%TS (ton day^{-1})	110	Organic Fertilizer (ton day^{-1})	67.76
Corn stover 90%TS (ton day^{-1})	15.5	Phosphate Fertilizer (ton day^{-1})	0.56
Feedstock ($ ton^{-1})	59	Ammonium Sulfate Fertilizer (ton day^{-1})	2.81
Economic analysis			
Total Project Capital Cost ($)			12,560,432
Total Operating Cost ($ $year^{-1}$)			1,383,515
Total Raw Materials Cost ($ $year^{-1}$)			305,489
Total Utilities Cost ($ $year^{-1}$)			138,873
Total Product Sales ($ $year^{-1}$)			1,329,438
Desired Rate of Return (% $year^{-1}$)			10
P.O. Period (year)			**-**
PI (Profitability Index)			**0.46**

8.5.2 Effect of different feedstocks on profitability

8.5.2.1 Methods

This study selected commonly used feedstocks to develop a method for evaluation of co-digestion processes: food scraps, dairy manure, swine manure, corn stover and wheat straw. The profitability index was calculated for the co-digestion of different combinations of feedstocks. The plant capacity was assumed to be 7,500 dry ton per year during these calculations.

8.5.2.2 Results and discussion

At 1.18 the profitability index of food scraps was the highest value among the compared feedstocks (Figure 8.7). Since the profitability index of food scraps was greater than 1, results indicated that it is possible to make a profit from food scraps through the integrated process of pretreatment, anaerobic digestion and nutrient recovery, under the conditions and plant capacity studied here. This profit was dependent not only on the food scraps' high potential to produce methane, but also on the disposal of such scraps bringing in a tipping fee to offset the disadvantage of a high investment.

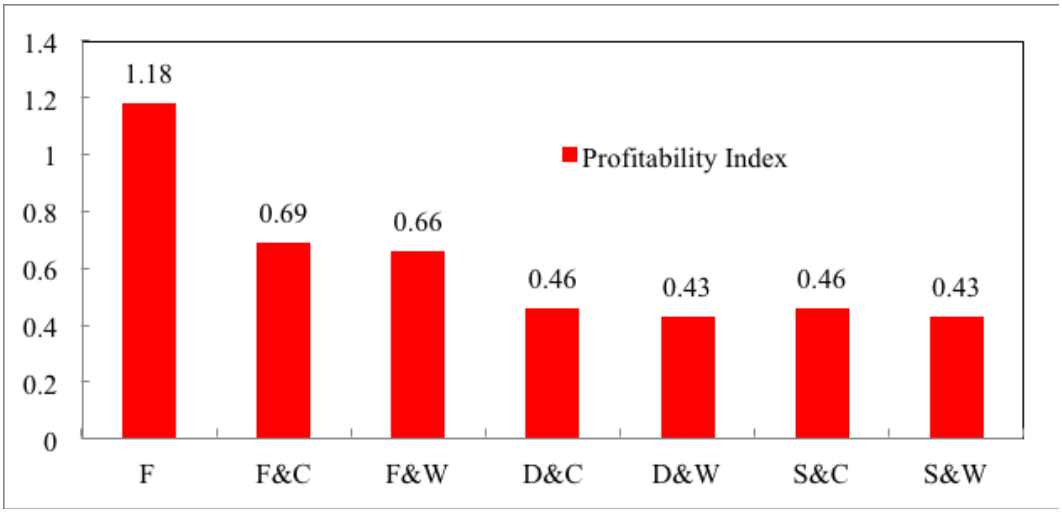

Figure 8.7: Profitability index of the integrated pretreatment, AD, and nutrient recovery process when using different feedstocks. F: food scraps, C: corn stover, W: wheat straw, D: dairy manure, S: swine manure.

Co-digestion of food scraps with crop residues also made a higher profit than co-digestion of animal manure with crop residues. When dairy manure was compared with swine manure, no significant differences ($P>0.05$) in the profitability index were observed among their co-digestion (Figure 8.7), although the biogas yield of dairy manure was a little higher than that of swine manure.

8.5.3 Effect of plant capacity on profitability

8.5.3.1 Methods

To further study the profit potential of the integrated pretreatment, AD, and nutrient recovery processes, the process model was used to scale up plant size. The plant capacity was increased 3-fold. The annual feedstock requirement would therefore be 22,500 dry ton $year^{-1}$.

8.5.3.2 Results and discussion

At this scaled-up capacity, the CNG (>96% CH_4) produced from the co-digestion of dairy manure with corn stover reached 15,733 m^3 day^{-1} (Table 8.4). The corresponding profitability index was 1.06, suggesting that the project can be profitably scaled up. The payback period was 9.91 years at the rate of return of 10% (Table 8.4). Therefore, operation of large-scale anaerobic digestion systems appears to have the advantage of being more economically profitable. Very large scale anaerobic digestion plants—so-called 'centralized anaerobic digestion plants'—have been developed to use feedstock from a variety of sources (Luque et al., 2010).

Table 8.4: Economic analysis of the co-digestion of dairy manure with corn stover after a 3-fold increase in plant capacity.

Input		**Output**	
Dairy manure 30%TS (ton day^{-1})	75	Biogas CNG (m^3 day^{-1})	15,733.2
Wastewater 1%TS (ton day^{-1})	330	Organic Fertilizer (ton day^{-1})	203.29
Corn stover 90%TS (ton day^{-1})	46.5	Phosphate Fertilizer (ton day^{-1})	1.69
Feedstock ($ ton^{-1})	59	Ammonium Sulfate Fertilizer (ton day^{-1})	8.43
		CO_2 (ton day^{-1})	18.30
Economic analysis			
Total Project Capital Cost ($)			21,426,141
Total Operating Cost ($ $year^{-1}$)			2,394,863
Total Raw Materials Cost ($ $year^{-1}$)			916,467
Total Utilities Cost ($ $year^{-1}$)			255,529
Total Product Sales ($ $year^{-1}$)			5,338,955
Desired Rate of Return (% $year^{-1}$)			10
P.O. Period (year)			**9.91**
PI (Profitability Index)			**1.06**

8.6 Conclusions

The processes of pretreatment, anaerobic digestion, and nutrient recovery were integrated using a holistic process model, with the goal of obtaining higher added values from the production chain of these processes. The process model—developed using Aspen Plus software (Aspen Technologies Inc., USA)—computed thermodynamically rigorous mass and energy balances for each unit operation in the conceptual integrated system.

The integrated processes of pretreatment, anaerobic digestion, and nutrient recovery were evaluated by adding different feedstocks. Commonly used feedstocks—food scraps, dairy manure, swine manure, corn stover and wheat straw—were compared using the process model, and a profitability index was calculated for each. The results showed that food scraps had profit potential at a plant capacity of 7,500 dry ton $year^{-1}$, due to higher biogas yield than other feedstocks and to receipt of tipping fees. Co-digestion of other feedstocks would need a larger plant capacity to increase their profit potential. Crop residues have more potential biogas

productivity than animal manure, and the fees for purchase, transportation and pretreatment of crop residues affect the profitability of an integrated process using this feedstock. Therefore, low cost and highly efficient pretreatments are critical to the profitability of anaerobic digestion of crop residues.

Aspen Plus software (Aspen Technologies Inc., USA) was also used to develop the concept of a novel ammonia recycling technology. This technology integrates multiple functions, including nutrient recovery, biogas purification, and pretreatment. The process model shows the feasibility of the proposed technology. Further experiments are needed to increase the understanding and confidence for real industrial application.

8.7 References

Aden, A., Ruth, M., Ibsen, K., Jechura, J., Neeves, K., Sheehan, J., Wallace, B., Montague, L., Slayton, A., Lukas, J. 2002. Lignocellulosic Biomass to Ethanol Process Design and Economics Utilizing Co-Current Dilute Acid Prehydrolysis and Enzymatic Hydrolysis for Corn Stover. National Renewable Energy Laboratory.

Alzate, C.A.C., Toro, O.J.S. 2006. Energy consumption analysis of integrated flowsheets for production of fuel ethanol from lignocellulosic biomass. Energy 31(13), 2447-2459.

Amon, T., Amon, B., Kryvoruchko, V., Bodiroza, V., Potsch, E., Zollitsch, W. 2006. Optimising methane yield from anaerobic digestion of manure: Effects of dairy systems and of glycerine supplementation. International Congress Series 1293(0), 217-220.

Appels, L., Baeyens, J., Degreve, J., Dewil, R. 2008. Principles and potential of the anaerobic digestion of waste-activated sludge. Progress in Energy and Combustion Science 34(6), 755-781.

Badger Engineers Inc. 1987. Economic Feasibility of an Acid-Hydrolysis-based Ethanol Plant. Subcontract Report SERI-STR-231-3142, Badger Engineers, Inc., Cambridge, MA. Prepared under Subcontract ZX-3-03096-2.

Banks, C.J., Chesshire, M., Heaven, S., Arnold, R. 2011. Anaerobic digestion of source-segregated domestic food waste: Performance assessment by mass and energy balance. Bioresource Technology 102(2), 612-620.

Bishop, C.P., Shumway, C.R. 2009. The economics of dairy anaerobic digestion with coproduct marketing. Review of Agricultural Economics 31(3), 394-410.

Boopathy, R. 1998. Biological treatment of swine waste using anaerobic baffled reactors. Bioresource Technology 64(1), 1-6.

Brownbridge, G., Azadi, P., Smallbone, A., Bhave, A., Taylor, B., Kraft, M. 2014. The future viability of algae-derived biodiesel under economic and technical uncertainties. Bioresource Technology 151, 166-173.

Buffiere, P., Loisel, D., Bernet, N., Delgenes, J.P. 2006. Towards new indicators for the prediction of solid waste anaerobic digestion properties. Water Science and Technology 53(8), 233-241.

Burr, B., Lyddon, L. 2008. A Comparison of Physical Solvents for Acid Gas Removal. 87th Annual Gas Processors Association Convention, Grapevine, TX, March. pp. 2–5.

Cakir, F.Y., Stenstrom, M.K. 2005. Greenhouse gas production: A comparison between aerobic and anaerobic wastewater treatment technology. Water Research 39(17), 4197-4203.

Chynoweth, D.P., Isaacson, R. 1987. Anaerobic Digestion of Biomass. Elsevier Applied Science, London and New York.

El-Mashad, H.M., Zhang, R. 2010. Biogas production from co-digestion of dairy manure and food waste. Bioresource Technology 101(11), 4021-4028.

EPA. 2010. U.S. Anaerobic Digester Status Report. Environmental Protection Agency.

Glisic, S.B., Orlovic, A.M. 2014. Review of biodiesel synthesis from waste oil under elevated pressure and temperature: Phase equilibrium, reaction kinetics, process design and techno-economic study. Renewable and Sustainable Energy Reviews 31, 708-725.
Gnansounou, E., Dauriat, A. 2010. Techno-economic analysis of lignocellulosic ethanol: A review. Bioresource Technology 101(13), 4980-4991.
Grossmann, I.E. 2004. Challenges in the new millennium: product discovery and design, enterprise and supply chain optimization, global life cycle assessment. Computers and Chemical Engineering 29(1), 29-39.
Humbird, D., Davis, R., Tao, L., Kinchin, C., Hsu, D., Aden, A., Schoen, P., Lukas, J., Olthof, B., Worley, M., Sexton, D., Dudgeon, D. 2011. Process Design and Economics for Biochemical Conversion of Lignocellulosic Biomass to Ethanol. Technical Report: NREL/TP-5100-47764. National Renewable Energy Laboratory. Contract No. DE-AC36-08GO28308.
Jacquemin, L., Pontalier, P.Y., Sablayrolles, C. 2012. Life cycle assessment (LCA) applied to the process industry: a review. International Journal of Life Cycle Assessment 17(8), 1028-1041.
Kaparaju, P., Serrano, M., Thomsen, A.B., Kongjan, P., Angelidaki, I. 2009. Bioethanol, biohydrogen and biogas production from wheat straw in a biorefinery concept. Bioresource Technology 100(9), 2562-2568.
Kokossis, A.C., Yang, A.D. 2010. On the use of systems technologies and a systematic approach for the synthesis and the design of future biorefineries. Computers and Chemical Engineering 34(9), 1397-1405.
Koutinas, A.A., Chatzifragkou, A., Kopsahelis, N., Papanikolaou, S., Kookos, I.K. 2014. Design and techno-economic evaluation of microbial oil production as a renewable resource for biodiesel and oleochemical production. Fuel 116, 566-577.
Krzystek, L., Ledakowicz, S., Kahle, H.J., Kaczorek, K. 2001. Degradation of household biowaste in reactors. Journal of Biotechnology 92(2), 103-112.
Lazarus, W.F., Rudstrom, M. 2007. The economics of anaerobic digester operation on a Minnesota dairy farm. Applied Economic Perspectives and Policy 29(2), 349-364.
Levis, J.W., Barlaz, M.A. 2013. Composting Process Model Documentation. Project Report, North Carolina State University: Raleigh, NC.
Littlewood, J., Wang, L., Turnbull, C., Murphy, R.J. 2013. Techno-economic potential of bioethanol from bamboo in China. Biotechnology for Biofuels 6(1), 173.
Lumley, N.P.G., Ramey, D.F., Prieto, A.L., Braun, R.J., Cath, T.Y., Porter, J.M. 2014. Techno-economic analysis of wastewater sludge gasification: A decentralized urban perspective. Bioresource Technology 161, 385-394.
Luque, R., Campelo, J., Clark, J. 2010. Handbook of Biofuels Production: Processes and Technologies. Elsevier Science.
Magnusson, Mimmi, Alvfors, P. 2012. Biogas from mechanical pulping industry: Potential improvement for increased biomass vehicle fuels. Proccedings of ECOS 2012: The 25th International Conference on Efficiency, Cost, Optimization, Simulation and Environmental Impact of Energy Systems. Perugia, Italy, June 26-29.
Mata-Alvarez, J., Mace, S., Llabres, P. 2000. Anaerobic digestion of organic solid wastes. An overview of research achievements and perspectives. Bioresource Technology 74(1), 3-16.
Meyer, P.A., Tews, I.J., Magnuson, J.K., Karagiosis, S.A., Jones, S.B. 2013. Techno-economic analysis of corn stover fungal fermentation to ethanol. Applied Energy 111, 657-668.
NETL. 2007. Ammonia-based Process for Multicomponent Removal from Flue Gas. National Energy Technology Laboratory (NETL), USA. Available online at http://www.netl.doe.gov/publications/factsheets/rd/R&D043.pdf.
Novak, J.T., Sadler, M.E., Murthy, S.N. 2003. Mechanisms of floc destruction during anaerobic and aerobic digestion and the effect on conditioning and dewatering of biosolids. Water Research 37(13), 3136-3144.

Pantaleo, A.M., Giarola, S., Bauen, A., Shah, N. 2014. Integration of biomass into urban energy systems for heat and power. Part I: An MILP based spatial optimization methodology. Energy Conversion and Management 83, 347-361.

Qiao, W., Yan, X., Ye, J., Sun, Y., Wang, W., Zhang, Z. 2011. Evaluation of biogas production from different biomass wastes with/without hydrothermal pretreatment. Renewable Energy 36(12), 3313-3318.

Sanchez, J.B., Alonso, J.M.Q., Oviedo, M.D.C. 2006. Use of microbial activity parameters for determination of a biosolid stability index. Bioresource Technology 97(4), 562-568.

Song, H., Dotzauer, E., Thorin, E., Yan, J.Y. 2014. Techno-economic analysis of an integrated biorefinery system for poly-generation of power, heat, pellet and bioethanol. International Journal of Energy Research 38(5), 551-563.

Stafford, D.A., Hawkes, D.L., Horton, R. 1980. Methane production from waste organic matter. CRC Press.

Uris, M., Linares, J.I., Arenas, E. 2014. Techno-economic feasibility assessment of a biomass cogeneration plant based on an Organic Rankine Cycle. Renewable Energy 66, 707-713.

Wooley, R., Ruth, M., Sheehan, J., Ibsen, K., Majdeski, H., Galvez, A. 1999. Lignocellulosic Biomass to Ethanol Process Design and Economics Utilizing Co-Current Dilute Acid Prehydrolysis and Enzymatic Hydrolysis Current and Futuristic Scenarios. National Renewable Energy Laboratory.

Xiu, S., Shahbazi, A., Shirley, V., Cheng, D. 2010. Hydrothermal pyrolysis of swine manure to bio-oil: Effects of operating parameters on products yield and characterization of bio-oil. Journal of Analytical and Applied Pyrolysis 88(1), 73-79.

Yang, D., Pang, Y., Yuan, H., Chen, S., Ma, J., Yu, L., Li, X. 2014. Enhancing biogas production from anaerobically digested wheat straw through ammonia pretreatment. Chinese Journal of Chemical Engineering 22(5), 576-582.

Yeh, A.C., Bai, H. 1999. Comparison of ammonia and monoethanolamine solvents to reduce CO_2 greenhouse gas emissions. Science of The Total Environment 228(2–3), 121-133.

Yuan, H., Li, R., Zhang, Y., Li, X., Liu, C., Meng, Y., Lin, M., Yang, Z. 2015. Anaerobic digestion of ammonia-pretreated corn stover. Biosystems Engineering 129(0), 142-148.

Yuan, Z.H., Chen, B.Z. 2012. Process synthesis for addressing the sustainable energy systems and environmental issues. AIChE Journal 58(11), 3370-3389.